

# SENSORLESS IMPLEMENTATION OF DIRECT TORQUE CONTROLLED INDUCTION MOTOR

## A DISSERTATION

*Submitted in partial fulfillment of the requirements for the award of the degree*

*of*

**MASTER OF TECHNOLOGY**

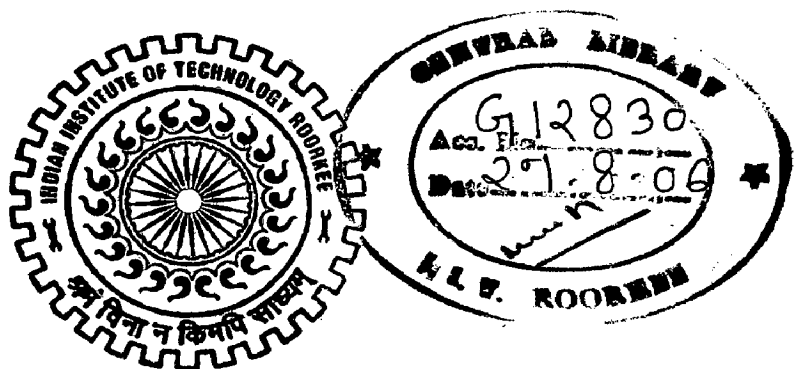
*in*

**ELECTRICAL ENGINEERING**

**(With Specialization in Power Apparatus and Electric Drives)**

*By*

**ASWINI KARTEEK BOMMAREDDY**



DEPARTMENT OF ELECTRICAL ENGINEERING  
INDIAN INSTITUTE OF TECHNOLOGY ROORKEE  
ROORKEE-247 667 (INDIA)

JUNE, 2006

## Candidates Declaration

---

I hereby declare that the work presented in this dissertation entitled "**Sensorless Implementation of Direct Torque Controlled Induction Motor**" submitted in partial fulfillment of the requirement for the award of the Degree of Master of Technology in Electrical Engineering with specialization in **Power Apparatus and Electric Drives**, in the Department of Electrical Engineering, Indian Institute of Technology Roorkee, Roorkee is an authentic record of my own work carried out under the guidance of **Dr. S.P.Singh**, Associate Professor, Department of Electrical Engineering, IIT-Roorkee, Roorkee.

I have not submitted the matter embodied in this report for the award of any other degree or diploma.

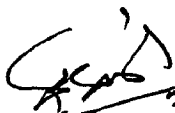
Date: 30 June, 2006

Place: Roorkee

  
(Aswini Karteek Bommareddy)

---

This is to certify that the above statement made by the candidate is true to the best of my knowledge and belief.

  
30/6/06  
(Dr. S.P. Singh)  
Associate Professor  
Department of Electrical Engineering,  
Indian Institute of Technology Roorkee,  
Roorkee-247667,  
Uttaranchal, India

# Acknowledgements

---

I express my deep sense of gratitude and indebtedness to my guide **Dr. S.P.Singh**, Associate Professor, Department of Electrical Engineering, IIT-Roorkee, for his guidance and constructive suggestions for successful completion of the project, with out which this work would not have been possible.

Last but not the least, I thank my parents and friends who provided continuous encouragement and moral support which helped me a lot in completing this work.

  
(Aswini Karteek Bommareddy)

***Abstract:***

In the present work performance of direct torque controlled induction motor drive with three different control strategies is investigated. Induction motor is fed from a voltage source inverter. Torque and flux references are generated from speed error and speed of the motor respectively, flux position is detected. These parameters are used to control the motor drive. The three control strategies implemented are normal direct torque control, hybrid direct torque control, split look-up table. All the control strategies were also simulated without speed sensor, which is known as sensorless control. Transient and steady state performance of each control strategy is investigated under different speed references and load conditions. All the control strategies are simulated using MATLAB SIMULINK software package.

## List of Figures

---

|  |    |
|--|----|
| Fig 2.1(a): Winding diagram 2-pole, 3-phase, Y connected symmetrical Induction Machine.....                                | 9  |
| Fig 2.1(b): Cross-section of 2-pole, 3-phase, Y connected symmetrical Induction Machine.....                               | 9  |
| Fig 2.2 Per phase equivalent circuit for a 3-phase symmetrical motor.....  | 13 |
| Fig 2.3: Transformation for stationary circuits portrayed by trigonometric relationships                                   | 14 |
| Fig 2.4: Transformation for rotating circuits portrayed by trigonometric relationships...                                  | 14 |
| Fig 2.5(a): q component circuit.....   | 16 |
| Fig 2.5(b): d component circuit .....  | 17 |
| Fig 2.5(c): zero component circuit.....  | 17 |
| Fig 2.6(a): q component circuit.....   | 21 |
| Fig 2.6(b): d component circuit .....  | 21 |
| Fig 3.1: Power-circuit configuration of the induction motor drive.....   | 26 |
| Fig 3.2: The inverter output voltage corresponding to switching states.....  | 28 |
| Fig 3.3: Division of sextant for stator flux-linkages identification.....  | 29 |
| Fig 3.4: Effect of switching $V_I$ and $V_{VI}$ on stator-flux phasor.....   | 29 |
| Fig 3.5(a): Voltage vector application when increment in both flux and torque is required .....                            | 34 |
| Fig 3.5(b): Voltage vector application when increment flux and decrement in torque is required .....                       | 34 |
| Fig 3.5(c): Voltage vector application when increment in torque and no change in flux is required .....                    | 35 |
| Fig 3.5(d): Voltage vector application when decrement in torque and no change in flux is required .....                    | 35 |
| Fig 3.6: Block-diagram schematic of the direct torque induction motor drive.....   | 37 |
| Fig 3.7: Block diagram model of direct torque control used for simulation in MATLAB SIMULINK .....                         | 38 |
| Fig 3.8(a): Torque response for step change in speed for direct torque controlled induction motor.....                     | 39 |
| Fig 3.8(b): Speed response for step change in speed for direct torque controlled induction motor .....                     | 40 |
| Fig 3.8(c): Phase current ( $I_{bs}$ ) response for step change in speed for direct torque controlled induction motor..... | 40 |
| Fig 3.8(d): Stator d-q axis flux plot locus for step change in speed for direct torque controlled induction motor.....     | 41 |
| Fig 3.8(e): Stator flux magnitude plot for step change in speed for direct torque controlled induction motor .....         | 41 |
| Fig 3.8(f): Sextant plot for for step change in speed for direct torque controlled induction motor .....                   | 42 |
| Fig 3.9(a): Torque response for step change in load torque for direct torque controlled induction motor.....               | 43 |

|  |    |
|--|----|
| Fig 3.9(b): Speed response for step change in load torque for direct torque controlled induction motor.....                                  | 43 |
| Fig 3.9(c): Phase current ( $I_{bs}$ ) response for step change in load torque for direct torque controlled induction motor.....             | 44 |
| Fig 3.9(d): Stator d-q axis flux locus for step change in load torque for direct torque controlled induction motor.....                      | 44 |
| Fig 3.9(e): Stator flux magnitude for step change in load torque for direct torque controlled induction motor.....                           | 45 |
| Fig 3.9(f): Sextant plot for step change in load torque for direct torque controlled induction motor.....                                    | 45 |
| Fig 4.1: Speed estimation by direct synthesis from state equations   |    |
| Fig 4.2: Block-diagram schematic of the sensorless direct torque induction motor drive .....   | 49 |
| Fig 4.2: Block-diagram schematic of the sensorless direct torque induction motor.....  | 50 |
| Fig 4.3: Block diagram model of sensorless direct torque control used for simulation in MATLAB SIMULINK .....                                | 51 |
| Fig 4.4(a): Torque response for step change in speed for sensorless direct torque controlled induction motor.....                            | 52 |
| Fig 4.4(b): Speed response for step change in speed for sensorless direct torque controlled induction motor.....                             | 52 |
| Fig 4.4(c): Phase current ( $I_{bs}$ ) response for step change in speed for sensorless direct torque controlled induction motor .....       | 53 |
| Fig 4.4(d): Stator d-q axis flux locus for step change in speed for sensorless direct torque controlled induction motor.....                 | 53 |
| Fig 4.4(e): Stator flux magnitude for step change in speed for sensorless direct torque controlled induction motor.....                      | 54 |
| Fig 4.4(f): Sextant plot for step change in speed for sensorless direct torque controlled induction motor.....                               | 54 |
| Fig 4.5(a): Torque response for step change in load torque for sensorless direct torque controlled induction motor.....                      | 55 |
| Fig 4.5(b): Speed response for step change in load torque for sensorless direct torque controlled induction motor.....                       | 56 |
| Fig 4.5(c): Phase current ( $I_{bs}$ ) response for step change in load torque for sensorless direct torque controlled induction motor ..... | 56 |
| Fig 4.5(d): Stator d-q axis flux locus for step change in load torque for sensorless direct torque controlled induction motor .....          | 57 |
| Fig 4.5(e): Stator flux magnitude for step change in load torque for sensorless direct torque controlled induction motor .....               | 57 |
| Fig 4.5(f): Sextant plot for step change in load torque for sensorless direct torque controlled induction motor.....                         | 58 |
| Fig 5.1: Block diagram of fuzzy controller.....  | 60 |
| Fig 5.2: Block diagram of hybrid controller .....  | 61 |
| Fig 5.3(a): Stator flux vector just entered sextant<1> and increment in torque and flux is required. ....                                    | 62 |
| Fig 5.3(b): Stator flux vector is about to leave sextant<1> and decrement in torque and increment in flux is required. ....                  | 62 |
| Fig 5.4: Segmentation of sextants.....   | 63 |

|  |    |
|--|----|
| Fig 5.5: Block-diagram schematic of the split look-up table direct torque induction motor drive .....  | 65 |
| Fig 5.6: Block diagram model of hybrid direct torque control used for simulation in MATLAB SIMULINK .....  | 67 |
| Fig 5.7: Block diagram model of sensorless hybrid direct torque control used for simulation in MATLAB SIMULINK .....                               | 68 |
| Fig 5.8(a): Torque response plot for step change in speed for hybrid direct torque controlled induction motor.....                                 | 66 |
| Fig 5.8(b): Speed response plot for step change in speed for hybrid direct torque controlled induction motor.....                                  | 69 |
| Fig 5.8(c): Phase current ( $I_{bs}$ ) response plot for step change in speed for hybrid direct torque controlled induction motor .....            | 69 |
| Fig 5.8(d): Stator d-q axis flux locus plot for step change in speed for hybrid direct torque controlled induction motor.....                      | 70 |
| Fig 5.8(e): Stator flux magnitude plot for step change in speed for hybrid direct torque controlled induction motor.....                           | 70 |
| Fig 5.8(f): Sextant plot for step change in speed for hybrid direct torque controlled induction motor.....   | 71 |
| Fig 5.9(a): Torque response plot for step change in speed for sensorless hybrid direct torque controlled induction motor .....                     | 71 |
| Fig 5.9(b): Speed response plot for step change in speed for sensorless hybrid direct torque controlled induction motor .....                      | 72 |
| Fig 5.9(c): Phase current ( $I_{bs}$ ) response plot for step change in speed for sensorless hybrid direct torque controlled induction motor ..... | 72 |
| Fig 5.9(d): Stator d-q axis flux locus plot for step change in speed for sensorless hybrid direct torque controlled induction motor .....          | 73 |
| Fig 5.9(e): Stator flux magnitude plot for step change in speed for sensorless hybrid direct torque controlled induction motor .....               | 73 |
| Fig 5.9(f): Sextant plot for step change in speed for sensorless hybrid direct torque controlled induction motor.....                              | 74 |
| Fig 5.10(a): Torque response plot for step change in load torque for hybrid direct torque controlled induction motor.....                          | 75 |
| Fig 5.10(b): Speed response plot for step change in load torque for hybrid direct torque controlled induction motor.....                           | 75 |
| Fig 5.10(c): Phase current ( $I_{bs}$ ) response plot for step change in load torque for hybrid direct torque controlled induction motor .....     | 76 |
| Fig 5.10(d): Stator d-q axis flux plot locus plot for step change in load torque for hybrid direct torque controlled induction motor .....         | 76 |
| Fig 5.10(e): Stator flux magnitude plot for step change in load torque for hybrid direct torque controlled induction motor .....                   | 77 |
| Fig 5.10(f): Sextant plot for step change in load torque for hybrid direct torque controlled induction motor.....                                  | 77 |
| Fig 5.11(a): Torque response plot for step change in load torque for sensorless hybrid direct torque controlled induction motor .....              | 78 |
| Fig 5.11(b): Speed response plot for step change in load torque for sensorless hybrid direct torque controlled induction motor .....               | 78 |

|  |    |
|--|----|
| Fig 5.11(c): Phase current ( $I_{bs}$ ) response plot for step change in load torque for sensorless hybrid direct torque controlled induction motor .....        | 79 |
| Fig 5.11(d): Stator d-q axis flux locus plot for step change in load torque for sensorless hybrid direct torque controlled induction motor .....                 | 79 |
| Fig 5.11(e): Stator flux magnitude plot for step change in load torque for sensorless hybrid direct torque controlled induction motor .....                      | 80 |
| Fig 5.11(f): Sextant plot for step change in load torque for sensorless hybrid direct torque controlled induction motor .....                                    | 80 |
| Fig 5.12: Block diagram model of split look-up table direct torque control used for simulation in MATLAB SIMULINK .....  | 82 |
| Fig 5.13: Block diagram model of sensorless split look-up table direct torque control used for simulation in MATLAB SIMULINK .....                               | 83 |
| Fig 5.14(a): Torque response plot for step change in speed for split look-up table direct torque controlled induction motor .....                                | 81 |
| Fig 5.14(b): Speed response plot for step change in speed for split look-up table direct torque controlled induction motor .....                                 | 84 |
| Fig 5.14(c): Phase current ( $I_{bs}$ ) response plot for step change in speed for split look-up table direct torque controlled induction motor .....            | 84 |
| Fig 5.14(d): Stator d-q axis flux locus plot for step change in speed for split look-up table direct torque controlled induction motor .....                     | 85 |
| Fig 5.14(e): Stator flux magnitude plot for step change in speed for split look-up table direct torque controlled induction motor .....                          | 85 |
| Fig 5.14(f): Sextant plot for step change in speed for split look-up table direct torque controlled induction motor .....  | 86 |
| Fig 5.15(a): Torque response plot for step change in speed for sensorless split look-up table direct torque controlled induction motor .....                     | 86 |
| Fig 5.15(b): Speed response plot for step change in speed for sensorless split look-up table direct torque controlled induction motor .....                      | 87 |
| Fig 5.15(c): Phase current ( $I_{bs}$ ) response plot for step change in speed for sensorless split look-up table direct torque controlled induction motor ..... | 87 |
| Fig 5.15(d): Stator d-q axis flux locus plot for step change in speed for sensorless split look-up table direct torque controlled induction motor .....          | 88 |
| Fig 5.15(e): Stator flux magnitude plot for step change in speed for sensorless split look-up table direct torque controlled induction motor .....               | 88 |
| Fig 5.15(f): Sextant plot for step change in speed for sensorless split look-up table direct torque controlled induction motor .....                             | 89 |
| Fig 5.16(a): Torque response plot for step change in load torque for split look-up table direct torque controlled induction motor .....                          | 90 |
| Fig 5.16(b): Speed response plot for step change in load torque for split look-up table direct torque controlled induction motor .....                           | 90 |
| Fig 5.16(c): Phase current ( $I_{bs}$ ) response plot for step change in load torque for split look-up table direct torque controlled induction motor .....      | 91 |
| Fig 5.16(d): Stator d-q axis flux locus plot for step change in load torque for split look-up table direct torque controlled induction motor .....               | 91 |
| Fig 5.16(e): Stator flux magnitude plot for step change in load torque for split look-up table direct torque controlled induction motor .....                    | 92 |



|  |    |
|--|----|
| Fig 5.16(f): Sextant plot for step change in load torque for split look-up table direct torque controlled induction motor .....  | 92 |
| Fig 5.17(a): Torque response plot for step change in load torque for sensorless split look-up table direct torque controlled induction motor.....                      | 93 |
| Fig 5.17(b): Speed response plot for step change in load torque for sensorless split look-up table direct torque controlled induction motor.....                       | 93 |
| Fig 5.17(c): Phase current ( $I_{bs}$ ) response plot for step change in load torque for sensorless split look-up table direct torque controlled induction motor ..... | 94 |
| Fig 5.17(d): Stator d-q axis flux locus plot <i>for</i> step change in load torque for sensorless split look-up table direct torque controlled induction motor .....   | 94 |
| Fig 5.17(e): Stator flux magnitude plot for step change in load torque for sensorless split look-up table direct torque controlled induction motor .....               | 95 |
| Fig 5.17(f): Sextant plot for step change in load torque for sensorless split look-up table direct torque controlled induction motor .....                             | 95 |

# List of Tables

---

|   |    |
|---|----|
| Table 3.1(a): switching states of inverter phase leg $a$ .....                                      | 26 |
| Table 3.1(b): switching states of inverter phase leg $b$ .....                                      | 26 |
| Table 3.1(c): switching states of inverter phase leg $c$ .....                                      | 27 |
| Table 3.2: Inverter switching states and machine voltages.....                                      | 27 |
| Table 3.3: Hysteresis comparator window for stator flux.....  | 30 |
| Table 3.4: Hysteresis comparator window for torque.....   | 31 |
| Table 3.5: Switching states for possible $S_\lambda$ , $S_T$ , and $S_\theta$ .....                 | 32 |
| Table 3.6: Flux-phasor sextant logic ( $S_\theta$ ) .....   | 33 |
| Table 5.1(a): Switching states for possible $S_\lambda$ , $S_T$ , and $S_\theta$ in segment 1 ..... | 64 |
| Table 5.1(b): Switching states for possible $S_\lambda$ , $S_T$ , and $S_\theta$ in segment 2 ..... | 64 |
| Table 5.1(c): Switching states for possible $S_\lambda$ , $S_T$ , and $S_\theta$ in segment 3 ..... | 65 |

# ***Table of Contents***

---

|  |              |
|--|--------------|
| <b>Candidates Declaration .....</b>                                      | <b>I</b>     |
| <b>Acknowledgements .....</b>  | <b>II</b>    |
| <b>Abstract.....</b>   | <b>III</b>   |
| <b>List of Figures .....</b>   | <b>IV</b>    |
| <b>List of Tables .....</b>  | <b>IX</b>    |
| <b>Table of Contents.....</b>  | <b>X</b>     |
| <b>Chapter - I: Introduction.....</b>                                    | <b>1-7</b>   |
| 1.1 Historical review.....   | 1            |
| 1.2 Scalar control .....   | 2            |
| 1.3 Vector control .....   | 3            |
| 1.4 Direct torque control (DTC) .....                                    | 3            |
| 1.5 Literature review.....   | 4            |
| 1.6 Organization of the work .....                                       | 7            |
| <b>Chapter - II: Mathematical Modeling of Induction Machine .....</b>    | <b>8-23</b>  |
| 2.1 Introduction.....  | 8            |
| 2.2 Voltage equations of induction machine in machine variables .....    | 8            |
| 2.3 D-Q model of Induction motor .....                                   | 13           |
| 2.4 Machine in arbitrary reference frame variables .....                 | 15           |
| 2.5 Machine equations in stationary reference frame .....                | 18           |
| 2.6 Per unit system.....   | 21           |
| <b>Chapter - III: Basic Theory of Direct Torque Controlled Induction</b> |              |
| <b>Motor.....</b>  | <b>24-45</b> |
| 3.1 Introduction.....  | 24           |
| 3.2 Switching states of inverter.....                                    | 25           |
| 3.3 Flux control.....  | 28           |
| 3.4 Torque control.....  | 30           |

|  |    |
|--|----|
| 3.5 Illustration of look-up table .....    | 33 |
| 3.6 Implementation .....                   | 36 |
| 3.7 Results.....                           | 37 |
| 3.7.1 Step change in speed reference ..... | 39 |
| 3.7.2 Step change in load torque.....      | 42 |

**Chapter - IV: Sensorless Direct Torque Control of Induction Motor**

|   |   |
|---|---|
| .....   | <b>46-58</b>                                      |
| 4.1 Introduction.....                           | <i>Normal + sensorless + CPE controller</i><br>46 |
| 4.2 Speed Estimation methods.....               | <b>Error! Bookmark not defined.</b> 6             |
| 4.3 Direct synthesis from state equations ..... | 47  |
| 4.4 Results.....                                | 50  |
| 4.4.2 Step change in load torque.....           | 50  |
| 4.4.1 Step change in speed reference.....       | 55  |

**Chapter - V: Improved Implementation Strategies for Direct Torque Control of Induction Motor.....59-95**

|  |  |
|--|--|
| 5.1 Introduction.....                                | 59   |
| 5.2 Hybrid direct torque control.....                | <i>Normal DTC + CPE + Fuzzy</i><br>59          |
| 5.3 Split look-up table direct torque control.....   | <i>Normal + PI (Split look up table)</i><br>61 |
| 5.4 Results.....                                     | 66   |
| 5.4.1 Hybrid direct torque control.....              | 66   |
| 5.4.1.1 Step change in speed reference.....          | 66   |
| 5.4.1.2 Step change in load torque.....              | 74   |
| 5.4.2 Split look-up table direct torque control..... | 81   |
| 5.4.2.1 Step change in speed reference.....          | 81   |
| 5.4.2.2 Step change in load torque.....              | 89   |

**Chapter - VI: Conclusions and Future Scope.....96-97**

|                        |    |
|------------------------|----|
| 6.1 Conclusions.....   | 96 |
| 6.2 Future Scope ..... | 97 |

**References .....98-99**

**Appendix : Machine Parameters.....100**

## Introduction

---

### 1.1 Historical review:

The history of electrical motors goes back to 1821, when Michael Faraday discovered the electromagnetic rotation and built the first primitive D.C. motor. In 1833 Tesla invented the A.C asynchronous motor. Currently main types of electric motors are still the same, DC, AC asynchronous and synchronous, all based on Oersted, Faraday and Tesla's theories developed and discovered more than a hundred years ago [9].

Since its invention, the asynchronous motor (Induction motor) has become the most widespread electrical motor in use today. At present, 67% of all the electrical energy generated is converted to mechanical energy for utilization. This fact is due to its advantages such as, not requiring any electrical connection between stationary and rotating parts of the motor. Therefore, they do not need any mechanical commutator (brushes), leading to fact that they are maintenance free motors. Induction motors also have low weight and inertia, high efficiency and a high overload capability. Therefore, they are cheaper and more robust, and less prone to any failure at high speeds. Furthermore, the motor can work in explosive environments because no sparks are produced. Taking into account all advantages outlined above, induction motors must be considered the perfect electrical to mechanical energy converter. However, mechanical energy is more than often require at variable speeds, where the speed control system is not a trivial mater.

Induction motor operates at nearly synchronous speed ( $n_s=120*f/P$ ,  $f$  – frequency,  $p$  – number of poles of motor), hence to obtain variable speeds, frequency of supply or number of poles of machine should be varied. With change in number of poles of the motor technique speed can be varied only in discrete steps with more number of windings of machine brought out. Hence, this method can't be used for infinitely variable speeds. In case of wound rotor induction machine, speed can be varied by changing resistance in rotor circuit, but this method eliminates advantages of induction motor and also causes poor performance due to additional losses. Effective method to produce an infinitely

variable induction motor speed drive is to supply the motor with three phase voltage of variable frequency and variable amplitude. A variable voltage is required because the motor impedance reduces at low frequencies and consequently the current has to be limited by means of reducing the supply voltages [22].

Before the days of power electronics DC motors are used for infinitely variable speed drives with good performance existed. These drives had covered wide power range in four quadrants. Moreover, they had good efficiency, and with suitable control with good dynamic response. However, its main drawback was the compulsory requirement of brushes [22].

Due to enormous advances made in semiconductor technology more speed control strategies for induction motor were developed due to following two broadly classified conditions:

- The decreasing cost and improved performance in power electronic switching devices.
- The possibility of implementing complex algorithms in new microprocessors.

However, one precondition had to be made, which was the development of suitable methods to control the speed of induction motors, because in contrast to its mechanical simplicity their complexity regarding their mathematical structure (multivariable and non-linear) is not a trivial matter. It is in this field, that considerable research effort is devoted. The aim is being to find even simpler methods of speed control for induction machines. One method, which is popular at the moment, is Direct Torque Control.

Historically, several general controllers have been developed:

## **1.2 Scalar control:**

Despite the fact that “Voltage - Frequency” (V/F) is the simplest controller; it is the most widespread, being in the majority of the industrial application. It is known as scalar control and acts by imposing a constant relation between voltage and frequency. The structure is very simple and it is normally used without speed feedback. However, this controller doesn't achieve a good accuracy in both speed and torque response, mainly

due to the fact that the stator flux and torque are not directly controlled. Even though, as long as the parameters are identified, the accuracy in the speed can be 2% (except in a very low speed), and the dynamic response can be approximately around 50ms [3, 19].

### **1.3 Vector control:**

In these types of controllers, there are control loops for controlling both the torque and the flux [4]. The most wide spread controllers of this type are the ones that use vector transform such as Park's transformation. Its accuracy can reach values such as 0.5% regarding the speed and 2% regarding the torque, even when at stand still. The main disadvantages are the huge computational capability and the compulsory good identification of the motor parameters.

### **1.4 Direct Torque Control (DTC):**

Direct Torque Control (DTC) has emerged over the last decade to become one possible alternative to the well-known Vector Control of Induction Machine. Its main characteristic is the good performance, obtaining results as good as classical vector control but with several advantages based on its simpler structure and control diagram.

DTC is said to be one of the future ways of controlling the induction machine in four quadrants [1]. In DTC it is possible to control directly the stator flux and the torque by selecting the appropriate inverter state. This method still requires further research in order to improve the motor's performance, as well as achieve a better behavior regarding environmental compatibility (Electro Magnetic Interference and energy ), that is desired nowadays for all industrial applications.

Main features of DTC are as follows:

- Direct control of flux and torque.
- Indirect control of stator currents and voltages.
- Approximately sinusoidal stator fluxes and stator currents.
- High dynamic performance even at stand still.
- Stator flux vector and torque estimation is required.

The main advantages of DTC are:

- Absence of co-ordinate transformation.
- Absence of voltage modulator block, as well as other controllers such as PID for motor flux and torque.
- Minimal torque response time, even better than the vector controllers.

However, some disadvantages are also present such as:

- Possible problems during starting.
- Requirements of torque and flux estimators, implying the consequent parameters identification.
- Inherent torque and stator flux ripple.

### **1.5 Literature review:**

[1] "Direct Torque Control of Induction Motors" I.Ludtke, Dr. M.G. Jayne, University of Glamorgan: This paper gives introduction to basic theory of direct torque control of induction motor.

[2] Domenico Casadei, Francesco Profumo, Giovanni Serra, Angelo Tani, "FOC and DTC: Two Viable Schemes for Induction Motors Torque Control", IEEE Trans. On Power Electronics, Vol 17, No.5, September 2002: This paper presents detailed comparison between field oriented control and direct torque control. Two schemes are evaluated in terms of torque and current ripple.

[3] "High Performance Motion Control of AC Motors Drives" Gerd Terorde, Ronnie Belmans: This paper presents rotor-flux-oriented type vector control. This paper discusses how amplitude of the rotor flux linkages is maintained at a fixed value, and only modifies a torque-producing component in order to control the torque of the ac machine.

[4] Bimal K. Bose; "Modern Power Electronics and AC Drives", Pearson Education Inc., 2002 (Book) This presents basic theory of direct torque control. Speed estimation methods are also discussed.

[5] Petar R. Matic, Branko D. Blanusa, Slobodan N. Vukosavic. "A Novel Direct Torque and Flux Control Algorithm for the Induction Motor Drive": This paper presents an



algorithm which provides decoupled control of the torque and flux with constant inverter switching frequency and a minimum torque and flux ripple.

[6] Nik Rumzi Nik Idris , Abdul Halim Mohd Yatim. “Modeling of a New Torque Controller for Direct Torque Control of Induction Machines”: This paper presents a new direct torque control for induction motor which proposes an alternative for three level hysteresis torque controller.

[7] Mihai Comanescu. “Flux and Speed Estimation Techniques for Sensorless Control of Induction Motors” A dissertation report: In this work different speed estimators for induction motor were presented.

[8] “Methods for Speed Sensorless Control of AC Drives”, Joachim Holtz, University of Wuppertal-Germany: This paper presents signal flow graphs, which give an description of the physical and mathematical systems used in sensorless drive control.

[9] N.R.N. Idris, “Improved direct torque control of induction machines”, PhD Thesis, University Technology Malaysia, 2000.

[10] Joachim Holtz, “Sensorless Control of Induction Motor Drives”, Proceedings of the IEEE, Vol. 90, No. 8, Aug 2002: This gives more details on signal flow graphs for systems used in sensorless drive control.

[11] Salmon Chavez Velazquez, Ruben Alejos Palomares, Alfredo Nava Segura. University of the Americas, Puebla. “Speed Estimation for an Induction Motor using Extended Kalman Filter”: In this paper discretized extended kalman filter is presented.

[12] yen-Shin Lai, Juo-Chiun Lin. “New Hybrid Fuzzy Controller for Direct Torque Control Induction Motor Drives”. IEEE Transaction on Power Electronics, Vol. 18. No. 5, Sept 2003: This paper presents a hybrid fuzzy controller which is used for direct torque control. Different types of fuzzy controllers were presented.

[13] Lus Romeral, Antoni Arias, Emiliano Aldabas, Marcel G. Jayne. “Novel Direct Torque Control(DTC) Scheme with Fuzzy Adaptive Torque-ripple Reduction”. IEEE Transaction on Industrial Electronics, Vol. 50, No. 3, June 2003: In this paper constant switching frequency based fuzzy logic controller for direct torque control is discussed. This method introduces zero voltage vectors between two non zero voltage vectors.

- [14] "A Comparison of Direct Torque Control Methodologies for Induction Motor", P. Marino, M.D'Incecco and Visciano: In this paper different direct torque control strategies like classical DTC, DSVM-DTC and SVM DTC were discussed.
- [15] "Design of Fuzzy Controllers", Jan Jantzen: This paper presents an introduction to fuzzy controller design, describes in detail design choices related to fuzzy controller.
- [16] Fatiha Zidani, Rachid Nait Said, "Direct Torque Control of Indction Motor with Fuzzy Minimization Torque Ripple", Journal of Electrical Engineering, Vol. 56, No. 7-8, 2005: In this paper hysteresis band with variable amplitude based on fuzzy logic controller is presented.
- [17] "Fuzzy Logic Direct Torque Control", A. Arias, J.L. Romeral, E. Aldabas, M.G. Jayne: This paper presents a direct torque control scheme with two fuzzy logic controllers, in which one of them used for calculating duty ration and other to calculate change in duty ratio. This scheme also has constant switching frequency feature.
- [18] "Direct Torque Control of Induction Motors using Fuzzy Variable Switching Sectors", Ji-Su Ryu, In-Sic Yoon, Kee-Sang Lee and Soon-Chan Hong: This paper presents a fuzzy variable switching sector scheme, which shifts sector boundaries at low speeds to prevent flux drooping. This paper also describes fuzzy switching frequency regulator for lowering the switching frequency at low speeds.
- [19] Pawel Z. Grabowski, Marian P. Kazmierkowski, Bimal K. Bose and Frede Blaabjerg, "A Simple Direct-Torque Neuro-Fuzzy Control of PWM-Inverter-Fed Induction Motor Drive", IEEE Transactions on Industrial Electronics, Vol. 47, No. 4, August 2000: This paper presents a neuro-fuzzy control scheme for pulse width modulation inverter fed induction motor drive. Theoretical principle and tuning procedures for neuro-fuzzy control is presented.
- [20] R.Krishnan, "Electric Motor Drives - Modeling, Analysis and Control" Pearson Education (Singapore) Pte. Ltd., Indian Branch, Delhi, 2003(Book): This gives theory of direct torque control and also gives theory of motor parameter sensitivity.
- [21] Ion Boldea, S.A. Nasar, "Electric drives", CRC Press, Taylor and Francis Group, 2006 print(Book): This book presents theory of sensorless direct torque control and discusses speed estimation technique.  
edition.2003(Book).

[22] Mohan, Undeland , Robbins. "Power Electronics". John Wiley & Sons Third : This discusses about induction motor drives.

[23] Paul C. Krause, Oleg Wasynczuk, Scott D. Sudhoff, "Analysis of Electric Machinery and Drive Systems", Wiley Interscience 2004(Book): This provides mathematical modeling of induction machines.

### **1.6 Organization of the work:**

In the present work, performance of direct torque controlled induction motor is estimated by using various control strategies by simulation in MATLAB SIMULINK.

Chapter 1: This chapter gives brief description about historical review of electrical motors, speed control strategies of induction motor. Literature review and work of organization are also presented in this chapter.

Chapter 2: Mathematical modeling of induction machine is presented in this chapter.

Chapter 3: This chapter gives basic theory of direct torque control used for speed control of induction motor. Results obtained are also presented.

Chapter 4: Sensorless direct torque control is presented in this chapter. Results for sensorless implementation are presented.

Chapter 5: This chapter presents Hybrid direct torque control and split look-up table direct torque control strategies. Results for both control strategies with and without speed sensors are also given in this chapter.

Chapter 6: Results obtained in simulation has been compared, conclusions and future scope of the work are presented.

# **Mathematical Modeling of Induction Machine**

---

### **2.1 Introduction:**

This chapter presents the development of generalized equations describing the behavior of the squirrel-cage induction motor drive based on the coupled circuit approach. The system has been analyzed in stationary reference frame. With the help of d-q transformation of variables, basic equations for induction motor, is developed in per unit system [23]. The mathematical model developed has been used in present study for analysis purpose of the drive under direct torque controlled motor drive.

The steps involved in determining the mathematical model of an electrical rotating machine are:

1. Various phases of winding of the machine are identified as coils having certain resistance, self-induction and mutual induction. The equations are written for balance voltages. The equation contain

- a) Ohmic drop in resistance of coil.
- b) Self induction voltage in the coil
- c) Voltage induced in the coil due to mutual coupling
- d) Voltage induced due to rotation

2. Since there is relative motion between stator and rotor, coil inductances are assumed as functions of rotor position. Thus, the linear transformation is derived to convert the impedance matrix to certain coefficient.

### **2.2 Voltage equations of induction machine in machine variables:**

In the following mathematical modeling following assumptions were made:

1. The motor magnetic circuit is considered linear and saturation is neglected.
2. Friction, windage, stray and core losses were not considered.

The winding arrangement for a cross-section of a 2-pole, 3-phase, Y-connected, symmetrical induction machine is shown in fig 2.1. The stator windings are identical, sinusoidally distributed windings, displaced  $120^\circ$ , with  $N_s$  equivalent turns and resistance  $r_s$ . Rotor will also be considered as there identical sinusoidally distributed windings, displaced  $120^\circ$ , with  $N_r$  equivalent turns and resistance  $r_r$ . The positive direction of the magnetic axis of each winding is shown in fig 2.1.

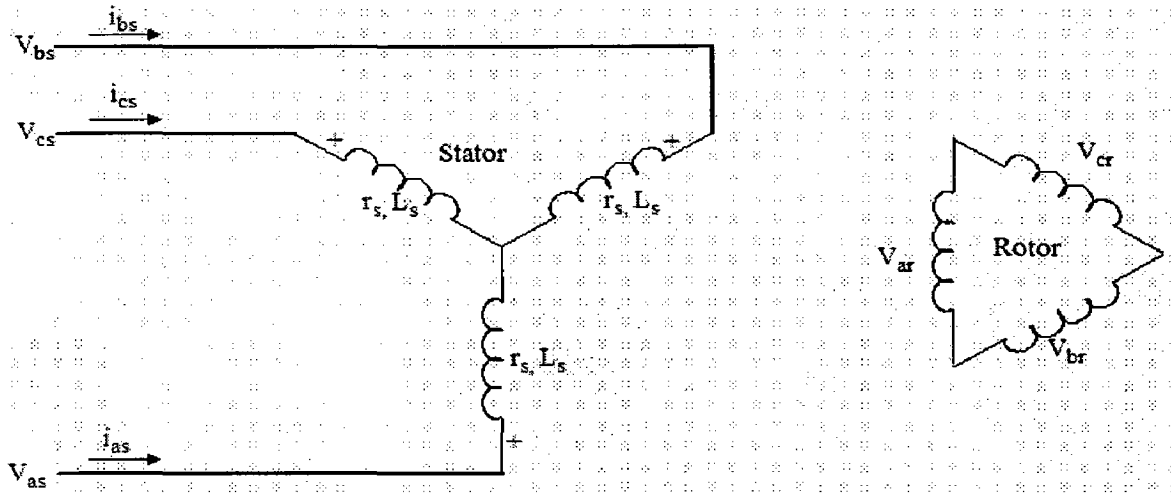


**Fig 2.1(a):** Winding diagram 2-pole, 3-phase, Y connected symmetrical Induction Machine

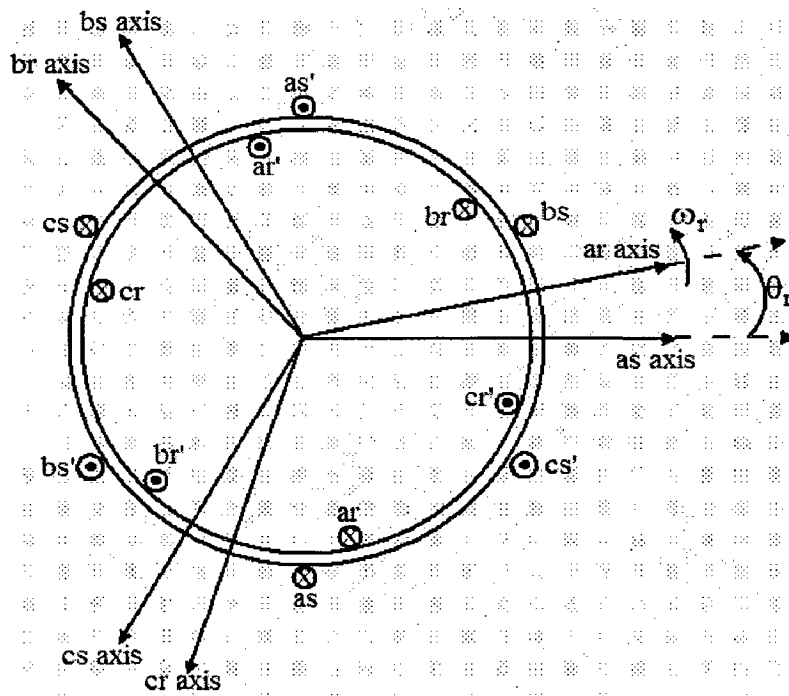


**Fig 2.1(b):** Cross-section of 2-pole, 3-phase, Y connected symmetrical Induction Machine

The voltage equations in machine variables may be expressed as

$$V_{abc s} = r_s i_{abc s} + p \lambda_{abc s} \quad \dots\dots\dots (2.1)$$

$$V_{abc r} = r_r i_{abc r} + p \lambda_{abc r} \quad \dots\dots\dots (2.2)$$

Where

$$(f_{abc s})^T = [f_{as} \ f_{bs} \ f_{cs}] \quad \dots\dots\dots (2.3)$$

$$(f_{abc r})^T = [f_{ar} \ f_{br} \ f_{cr}] \quad \dots\dots\dots (2.4)$$

In the above equations the s subscript denotes variables and parameters associated with stator circuits, and r subscript denoted that of rotor. Both  $r_s$  and  $r_r$  are diagonal matrices, each with equal nonzero elements. For a magnetically linear system, the flux linkages may be expressed as

$$\begin{bmatrix} \lambda_{abc s} \\ \lambda_{abc r} \end{bmatrix} = \begin{bmatrix} L_s & L_{sr} \\ (L_{sr})^T & L_r \end{bmatrix} \begin{bmatrix} i_{abc s} \\ i_{abc r} \end{bmatrix} \quad \dots\dots\dots (2.5)$$

The winding inductances are derived as

$$L_s = \begin{bmatrix} L_{ls} + L_{ms} & -\frac{1}{2} L_{ms} & -\frac{1}{2} L_{ms} \\ -\frac{1}{2} L_{ms} & L_{ls} + L_{ms} & -\frac{1}{2} L_{ms} \\ -\frac{1}{2} L_{ms} & -\frac{1}{2} L_{ms} & L_{ls} + L_{ms} \end{bmatrix} \quad \dots\dots\dots (2.6)$$

$$L_r = \begin{bmatrix} L_{lr} + L_{mr} & -\frac{1}{2} L_{mr} & -\frac{1}{2} L_{mr} \\ -\frac{1}{2} L_{mr} & L_{lr} + L_{mr} & -\frac{1}{2} L_{mr} \\ -\frac{1}{2} L_{mr} & -\frac{1}{2} L_{mr} & L_{lr} + L_{mr} \end{bmatrix} \quad \dots\dots\dots (2.7)$$

$$L_{sr} = L_{sr} \begin{bmatrix} \cos \theta_r & \cos(\theta_r + \frac{2\pi}{3}) & \cos(\theta_r - \frac{2\pi}{3}) \\ \cos(\theta_r - \frac{2\pi}{3}) & \cos(\theta_r) & \cos(\theta_r + \frac{2\pi}{3}) \\ \cos(\theta_r + \frac{2\pi}{3}) & \cos(\theta_r - \frac{2\pi}{3}) & \cos(\theta_r) \end{bmatrix} \dots\dots\dots (2.8)$$

In the above inductance equations  $L_{ls}$  and  $L_{ms}$  are, respectively, the leakage and magnetic inductances of the stator windings;  $L_{lr}$  and  $L_{mr}$  are for the rotor windings. The inductance  $L_{sr}$  is the amplitude of the mutual inductances between stator and rotor windings.

When expressing the voltage equations in machine variable form, it is convenient to refer all rotor variables to the stator windings by appropriate turns ratios:

$$i'_{abc} = \frac{N_r}{N_s} i_{abc} \dots\dots\dots (2.9)$$

$$v'_{abc} = \frac{N_s}{N_r} v_{abc} \dots\dots\dots (2.10)$$

$$\lambda'_{abc} = \frac{N_s}{N_r} \lambda_{abc} \dots\dots\dots (2.11)$$

The magnetizing and mutual inductances are associated with the same magnetic flux path; therefore  $L_{ms}$ ,  $L_{mr}$  and  $L_{sr}$  are related as

$$L_{ms} = \frac{N_s}{N_r} L_{sr} \dots\dots\dots (2.12)$$

Thus we define

$$L'_{ms} = \frac{N_s}{N_r} L_{sr} \begin{bmatrix} \cos \theta_r & \cos(\theta_r + \frac{2\pi}{3}) & \cos(\theta_r - \frac{2\pi}{3}) \\ \cos(\theta_r - \frac{2\pi}{3}) & \cos(\theta_r) & \cos(\theta_r + \frac{2\pi}{3}) \\ \cos(\theta_r + \frac{2\pi}{3}) & \cos(\theta_r - \frac{2\pi}{3}) & \cos(\theta_r) \end{bmatrix} \dots\dots\dots (2.13)$$

$L_{mr}$  may be expressed as

$$L_{mr} = \left( \frac{N_r}{N_s} \right)^2 L_{ms} \dots\dots\dots (2.14)$$

And if

$$L'_r = \left( \frac{N_s}{N_r} \right)^2 L_r \dots\dots\dots (2.15)$$

Then from (2.7)

$$L'_r = \begin{bmatrix} L'_{lr} + L_{ms} & -\frac{1}{2}L_{ms} & -\frac{1}{2}L_{ms} \\ -\frac{1}{2}L_{ms} & L'_{lr} + L_{ms} & -\frac{1}{2}L_{ms} \\ -\frac{1}{2}L_{ms} & -\frac{1}{2}L_{ms} & L'_{lr} + L_{ms} \end{bmatrix} \dots\dots\dots (2.16)$$

where

$$L'_{lr} = \left( \frac{N_s}{N_r} \right)^2 L_{lr} \dots\dots\dots (2.17)$$

The flux linkages can now be expressed as

$$\begin{bmatrix} \lambda_{abc} \\ \lambda'_{abc} \end{bmatrix} = \begin{bmatrix} L_s & L'_{sr} \\ (L'_{sr})^T & L'_r \end{bmatrix} \begin{bmatrix} i_{abc} \\ i'_{abc} \end{bmatrix} \dots\dots\dots (2.18)$$

The voltage equations expressed in terms of machine variables referred to the stator windings can now be written as

$$\begin{bmatrix} v_{abc} \\ v'_{abc} \end{bmatrix} = \begin{bmatrix} r_s + pL_s & pL'_{sr} \\ p(L'_{sr})^T & r'_r + pL'_r \end{bmatrix} \begin{bmatrix} i_{abc} \\ i'_{abc} \end{bmatrix} \dots\dots\dots (2.19)$$

where

$$r'_r = \left( \frac{N_s}{N_r} \right)^2 r_r \dots\dots\dots (2.20)$$



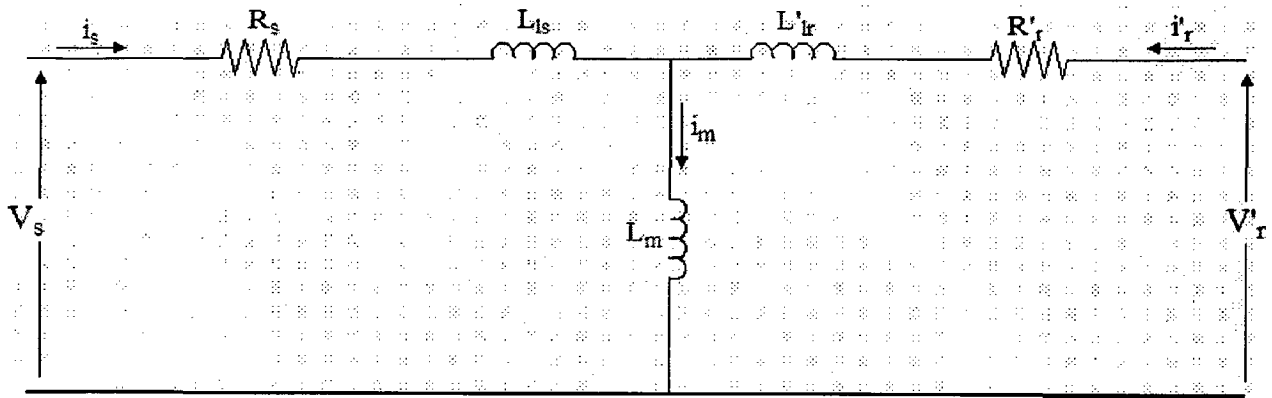


**Fig 2.2** Per phase equivalent circuit for a 3-phase symmetrical motor

Per phase equivalent circuit for a three phase symmetrical motor is shown in fig 2.2.

Torque and rotor speed in machine variables are related by

$$T_e = J \left( \frac{2}{P} \right) p \omega_r + T_L \quad \dots \dots \dots (2.21)$$

Where  $J$  is the inertia of the rotor and in some cases the connected load. The first term on the right-hand side is the inertial torque. In equation (2.21) the units of  $J$  are kilogram.meter<sup>2</sup> (kg.m<sup>2</sup>) or joules.second<sup>2</sup> (J.s<sup>2</sup>). The load torque  $T_L$  is positive for a torque load on the shaft of the induction machine.

### 2.3 D-Q model of Induction motor:

Solving induction machine equations in machine variables is complicated as it involves time varying quantities. This problem can be overcome by converting three winding induction machine into an equivalent two winding machine. This model is known as d-q model; in this model the two windings are mutually decoupled. The two axes direct (d) and quadrature (q) are electrically 90° apart, thus simplifying the machine equations. This mathematical model can be used for all theoretical analysis and simulation purposes. Induction machine equations in machine variables can be converted to d-q model which can be rotating at any speed known as arbitrary reference frame. Commonly used reference frames are synchronous, rotor and stationary reference frames.

Synchronous reference frame converts all variables to dc quantities which can be manipulated easily. Conversion to stationary reference frame avoids the use of trigonometric operation for co-ordinate transformations.

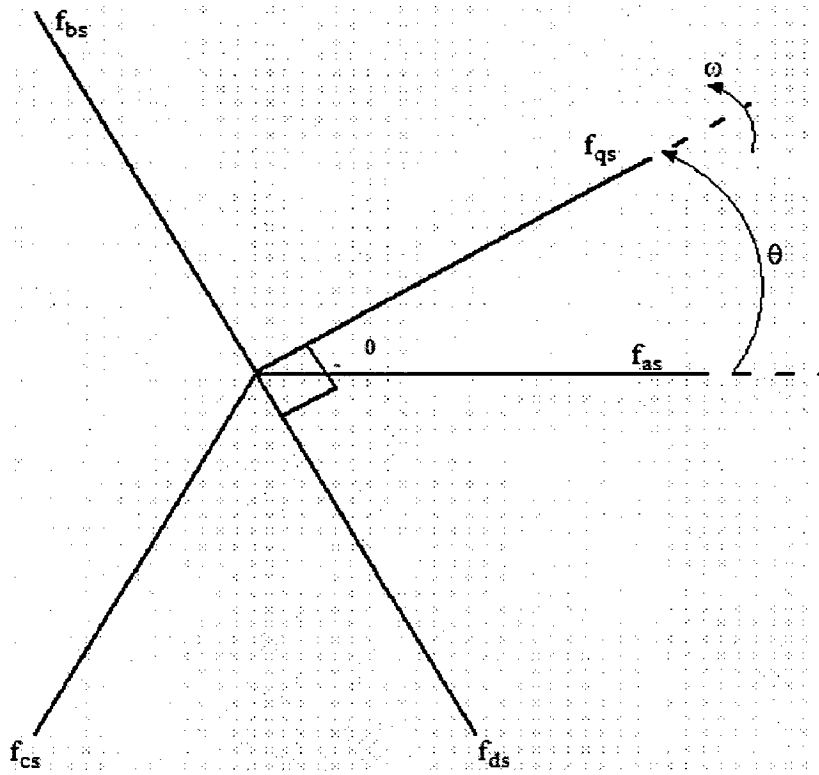


**Fig 2.3:** Transformation for stationary circuits portrayed by trigonometric relationships

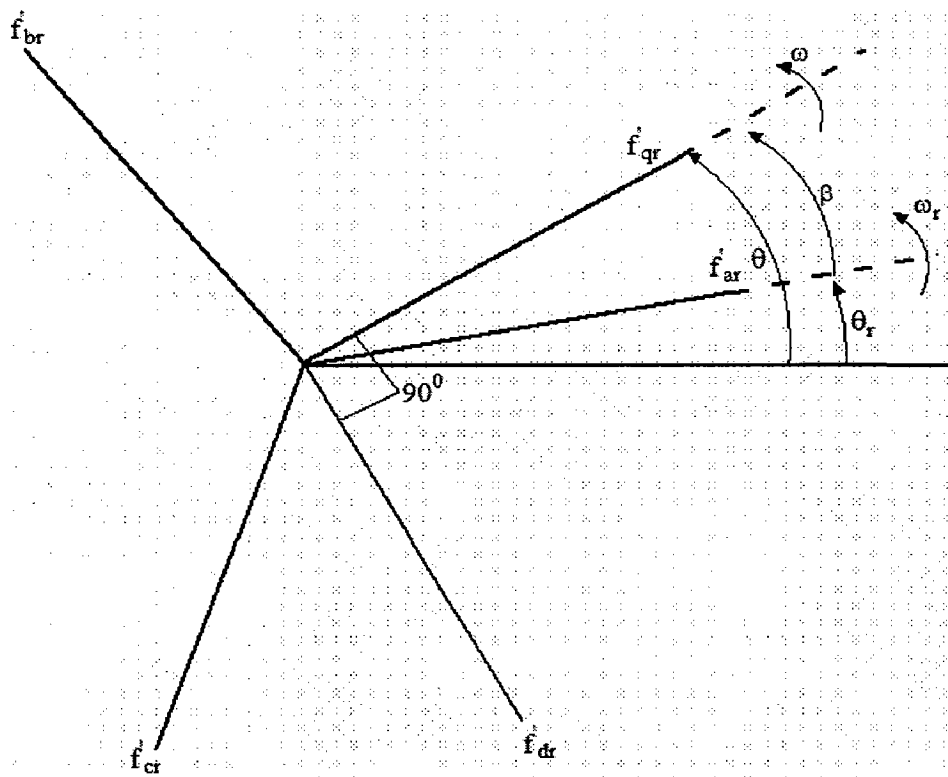


**Fig 2.4:** Transformation for rotating circuits portrayed by trigonometric relationships

## 2.4 Machine in arbitrary reference frame variables:

Voltage equations in the arbitrary reference frame are

$$v_{qdos} = r_s i_{qdos} + \omega \lambda_{dqs} + p \lambda_{qdos} \quad \dots\dots\dots (2.22)$$

$$v'_{qdor} = r'_r i'_{qdor} + (\omega - \omega_r) \lambda'_{dqs} + p \lambda'_{qdos} \quad \dots\dots\dots (2.23)$$

Where

$$(\lambda_{dqs})^T = [\lambda_{ds} \quad -\lambda_{qs} \quad 0] \quad \dots\dots\dots (2.24)$$

$$(\lambda'_{dqr})^T = [\lambda'_{dr} \quad -\lambda'_{qr} \quad 0] \quad \dots\dots\dots (2.25)$$

The set of equations is complete when expressions for the flux linkages are determined. The flux linkage equations for a magnetically linear system are:

$$\begin{bmatrix} \lambda_{qdos} \\ \lambda'_{qdor} \end{bmatrix} = \begin{bmatrix} K_s L_s (K_s)^{-1} & K_s L'_{sr} (K_r)^{-1} \\ K_r (L'_{sr})^T (K_s)^{-1} & K_r L'_r (K_r)^{-1} \end{bmatrix} \begin{bmatrix} i_{qdos} \\ i'_{qdor} \end{bmatrix} \quad \dots\dots\dots (2.26)$$

Transformation matrix  $K_s$ , for transformation of stationary circuit to arbitrary reference frame is:

$$K_s = \frac{2}{3} \begin{bmatrix} \cos \theta & \cos(\theta - \frac{2\pi}{3}) & \cos(\theta + \frac{2\pi}{3}) \\ \sin(\theta) & \cos(\theta - \frac{2\pi}{3}) & \cos(\theta - \frac{2\pi}{3}) \\ \frac{1}{2} & \frac{1}{2} & \frac{1}{2} \end{bmatrix} \quad \dots\dots\dots (2.27)$$

Transformation matrix  $K_r$ , for transformation of rotating circuit to arbitrary reference frame is:

$$K_r = \frac{2}{3} \begin{bmatrix} \cos \beta & \cos(\beta - \frac{2\pi}{3}) & \cos(\beta + \frac{2\pi}{3}) \\ \sin(\beta) & \cos(\beta - \frac{2\pi}{3}) & \cos(\beta - \frac{2\pi}{3}) \\ \frac{1}{2} & \frac{1}{2} & \frac{1}{2} \end{bmatrix} \quad \dots\dots\dots (2.28)$$

$$\beta = \theta - \theta_r$$

Voltage equations written in arbitrary reference frame are:

$$v_{qs} = r_s i_{qs} + \omega \lambda_{ds} + p \lambda_{qs} \dots\dots\dots (2.29)$$

$$v_{ds} = r_s i_{ds} - \omega \lambda_{qs} + p \lambda_{ds} \dots\dots\dots (2.30)$$

$$v_{0s} = r_s i_{0s} + p \lambda_{0s} \dots\dots\dots (2.31)$$

$$v'_{qr} = r'_r i'_{qr} + (\omega - \omega_r) \lambda'_{dr} + p \lambda'_{qr} \dots\dots\dots (2.32)$$

$$v'_{dr} = r'_r i'_{dr} - (\omega - \omega_r) \lambda'_{qr} + p \lambda'_{dr} \dots\dots\dots (2.33)$$

$$v'_{0r} = r'_r i'_{0r} + p \lambda'_{0r} \dots\dots\dots (2.34)$$

Simplifying flux equation and expanding it gives

$$\lambda_{qs} = L_{ls} i_{qs} + L_M (i_{qs} + i'_{qr}) \dots\dots\dots (2.35)$$

$$\lambda_{ds} = L_{ls} i_{ds} + L_M (i_{ds} + i'_{dr}) \dots\dots\dots (2.36)$$

$$\lambda_{0s} = L_{ls} i_{0s} \dots\dots\dots (2.37)$$

$$\lambda'_{qr} = L'_{lr} i'_{qr} + L_M (i_{qs} + i'_{qr}) \dots\dots\dots (2.38)$$

$$\lambda'_{dr} = L'_{lr} i'_{dr} + L_M (i_{ds} + i'_{dr}) \dots\dots\dots (2.39)$$

$$\lambda'_{0r} = L'_{lr} i'_{0r} \dots\dots\dots (2.40)$$

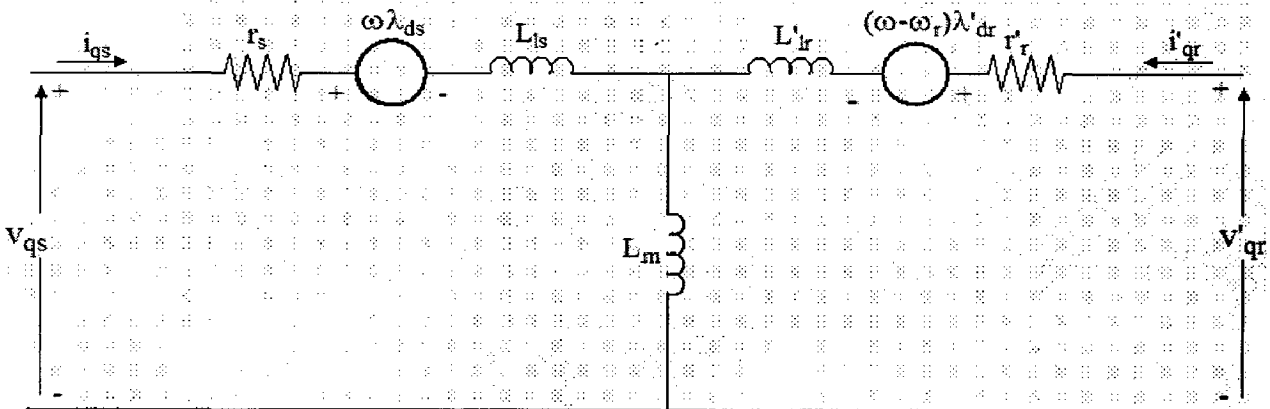


Fig 2.5(a): q component circuit

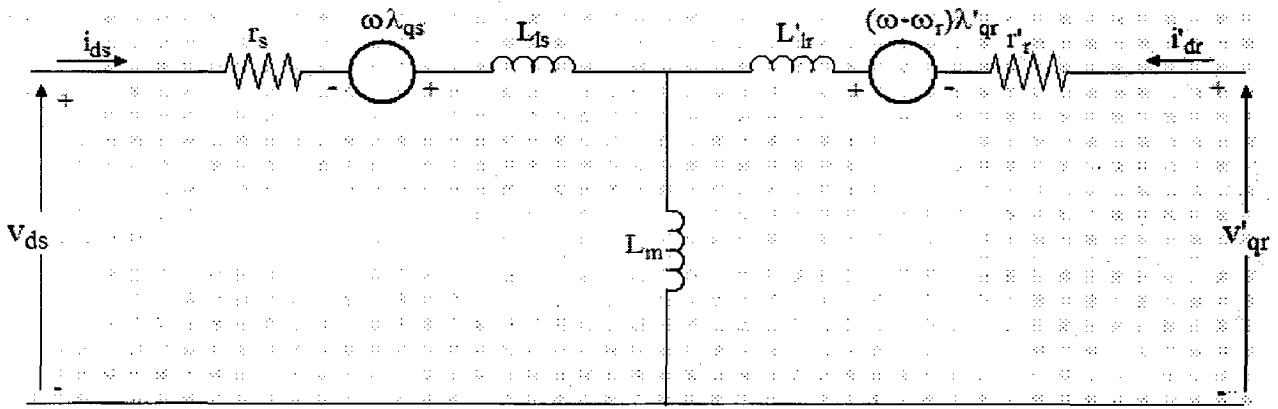


Fig 2.5(b): d component circuit

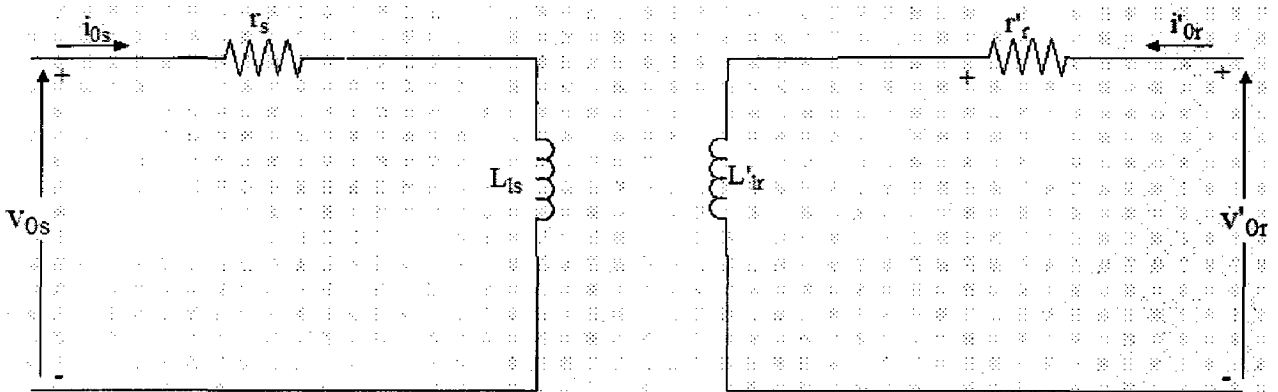


Fig 2.5(c): zero component circuit

Fig 2.5: Arbitrary reference-frame equivalent circuits for a 3-phase, symmetrical induction machine

The voltage and flux linkage equations (2.29) to (2.40) suggests equivalent circuit shown in fig 2.5

In general machine and power system parameters are always given in ohms or percent or per unit of base impedance, it is convenient to express the voltage and flux linkage equations in terms of reactances rather than inductances. Hence equations (2.29) to (2.34) are expressed as:

$$v_{qs} = r_s i_{qs} + \frac{\omega}{\omega_b} \psi_{ds} + \frac{p}{\omega_b} \psi_{qs} \quad \dots \dots \dots (2.41)$$

$$v_{ds} = r_s i_{ds} - \frac{\omega}{\omega_b} \psi_{qs} + \frac{p}{\omega_b} \psi_{ds} \quad \dots \dots \dots (2.42)$$

$$v_{0s} = r_s i_{0s} + \frac{p}{\omega_b} \psi_{0s} \quad \dots \dots \dots (2.43)$$

$$v'_{qr} = r'_r i'_{qr} + \frac{(\omega - \omega_r)}{\omega_b} \psi'_{dr} + \frac{p}{\omega_b} \psi'_{qr} \quad \dots\dots\dots (2.44)$$

$$v'_{dr} = r'_r i'_{dr} - \frac{(\omega - \omega_r)}{\omega_b} \psi'_{qr} + \frac{p}{\omega_b} \psi'_{dr} \quad \dots\dots\dots (2.45)$$

$$v'_{0r} = r'_r i'_{0r} + \frac{p}{\omega_b} \psi'_{0r} \quad \dots\dots\dots (2.46)$$

Where  $\omega_b$  is the base electrical angular velocity used to calculate the inductive reactances. Flux linkages (2.35) to (2.40) become flux linkages per second with the units of volts:

$$\psi_{qs} = X_{ls} i_{qs} + X_M (i_{qs} + i'_{qr}) \quad \dots\dots\dots (2.47)$$

$$\psi_{ds} = X_{ls} i_{ds} + X_M (i_{ds} + i'_{dr}) \quad \dots\dots\dots (2.48)$$

$$\psi_{0s} = X_{ls} i_{0s} \quad \dots\dots\dots (2.49)$$

$$\psi'_{qr} = X'_{lr} i'_{qr} + X_M (i_{qs} + i'_{qr}) \quad \dots\dots\dots (2.50)$$

$$\psi'_{dr} = X'_{lr} i'_{dr} + X_M (i_{ds} + i'_{dr}) \quad \dots\dots\dots (2.51)$$

$$\psi'_{0r} = X'_{lr} i'_{0r} \quad \dots\dots\dots (2.52)$$

Electromagnetic torque of machine in arbitrary reference frame is given by

$$T_e = \left(\frac{3}{2}\right) \left(\frac{P}{2}\right) \left(\lambda_{ds} i_{qs} - \lambda_{qs} i_{ds}\right) \quad \dots\dots\dots (2.53)$$

This can also be written in terms of flux linkages per second and currents as:

$$T_e = \left(\frac{3}{2}\right) \left(\frac{P}{2}\right) \left(\frac{1}{\omega_b}\right) \left(\psi'_{qr} i'_{dr} - \psi'_{dr} i'_{qr}\right) \quad \dots\dots\dots (2.54)$$

### 2.5 Machine equations in stationary reference frame:

For direct torque control of induction motor machine equations in stationary reference frame are chosen as it doesn't require any trigonometric transformations. Machine equations in stationary reference frame can be obtained by substituting  $\omega = 0$  in arbitrary reference frame equations developed in the previous section equations from

(2.41) to (2.46). As squirrel cage induction motor is considered rotor circuit will be short circuited therefore.  $v'_{qr} = 0$  and  $v'_{dr} = 0$ . Zero sequence components are not taken into account as neutral is not connected to ground.

For simulation purpose equations are written using integration rather than using them in derivative form. The equations convenient for simulating the symmetrical induction machine in the stationary frame may be established by first solving the flux linkage equations of flux linkage per second equations for the currents. Thus, from equations (2.47) to (2.52) and writing in stationary reference frame:

$$i_{qs} = \frac{1}{X_{ls}} (\psi_{qs} - \psi_{mq}) \quad \dots\dots\dots (2.55)$$

$$i_{ds} = \frac{1}{X_{ls}} (\psi_{ds} - \psi_{md}) \quad \dots\dots\dots (2.56)$$

$$i'_{qr} = \frac{1}{X'_{lr}} (\psi'_{qr} - \psi_{mq}) \quad \dots\dots\dots (2.57)$$

$$i'_{dr} = \frac{1}{X'_{lr}} (\psi'_{dr} - \psi_{md}) \quad \dots\dots\dots (2.58)$$

Where  $\psi_{mq}$  and  $\psi_{md}$ , which are useful when representing saturation, are defined as

$$\psi_{mq} = X_M (i_{qs} + i'_{qr}) \quad \dots\dots\dots (2.59)$$

$$\psi_{md} = X_M (i_{ds} + i'_{dr}) \quad \dots\dots\dots (2.60)$$

If equations (2.55) to (2.58) are used to eliminate the currents in (2.59) and (2.60) as well as in the voltage equations in stationary reference frame and if the resulting voltage equations are solved for flux linkages per second, following integral equations can be obtained:

$$\psi_{qs} = \frac{\omega_b}{p} \left[ v_{qs} + \frac{r_s}{X_{ls}} (\psi_{mq} - \psi_{qs}) \right] \quad \dots\dots\dots (2.61)$$

$$\psi_{ds} = \frac{\omega_b}{p} \left[ v_{ds} + \frac{r_s}{X_{ls}} (\psi_{md} - \psi_{ds}) \right] \dots\dots\dots (2.62)$$

$$\psi'_{qr} = \frac{\omega_b}{p} \left[ v'_{qr} + \frac{\omega_r}{\omega_b} \psi'_{dr} + \frac{r'_r}{X'_{lr}} (\psi_{mq} - \psi'_{qr}) \right] \dots\dots\dots (2.63)$$

$$\psi'_{dr} = \frac{\omega_b}{p} \left[ v'_{dr} - \frac{\omega_r}{\omega_b} \psi'_{qr} + \frac{r'_r}{X'_{lr}} (\psi_{md} - \psi'_{dr}) \right] \dots\dots\dots (2.64)$$

Equations (2.59) and (2.60) can be expressed as

$$\psi_{mq} = X_{aq} \left( \frac{\psi_{qs}}{X_{ls}} + \frac{\psi'_{qr}}{X'_{lr}} \right) \dots\dots\dots (2.65)$$

$$\psi_{md} = X_{ad} \left( \frac{\psi_{ds}}{X_{ls}} + \frac{\psi'_{dr}}{X'_{lr}} \right) \dots\dots\dots (2.66)$$

In which

$$X_{aq} = X_{ad} = \left( \frac{1}{X_M} + \frac{1}{X_{ls}} + \frac{1}{X'_{lr}} \right)^{-1} \dots\dots\dots (2.67)$$

In the computer simulation equations (2.61) to (2.64) are used to solve for the flux linkages per second and equations (2.55) to (2.60) are used to obtain the currents from the flux linkages per second. Electromagnetic torque is expressed from equation (2.53) in per unit as:

$$T_e = \psi_{ds} i_{qs} - \psi_{qs} i_{ds} \dots\dots\dots (2.68)$$

This is positive for motor action and negative for generator action. Rotor speed can be written as

$$\omega_r = \left( \frac{\omega_b}{2Hp} \right) (T_e - T_L) \dots\dots\dots (2.69)$$

Often per unit rotor speed  $\omega_r / \omega_b$  is used rather than  $\omega_r$ , because it is conveniently incorporated into the integral flux linkage equations.

Equivalent circuit in stationary reference frame will be as shown in Fig 2.6.



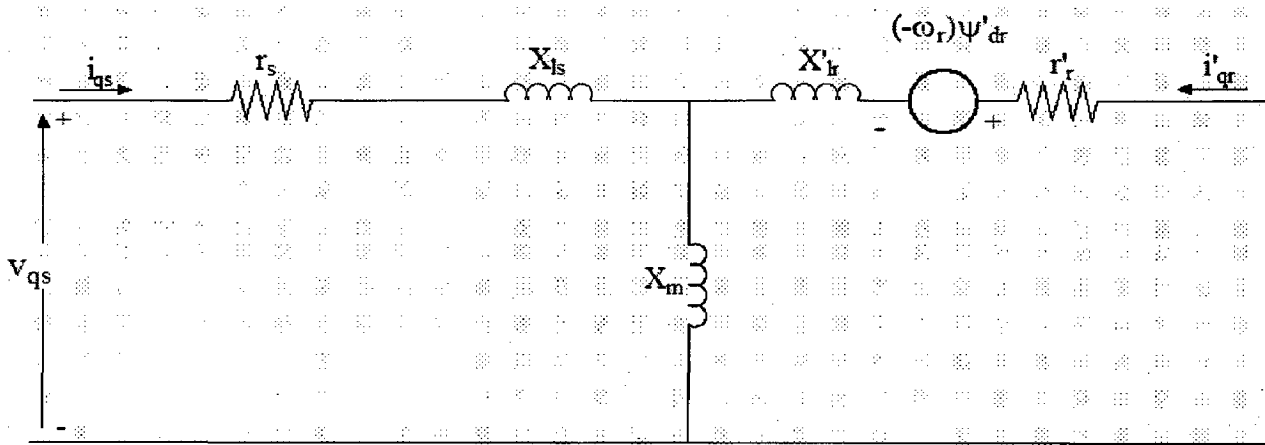


**Fig 2.6(a): q component circuit**

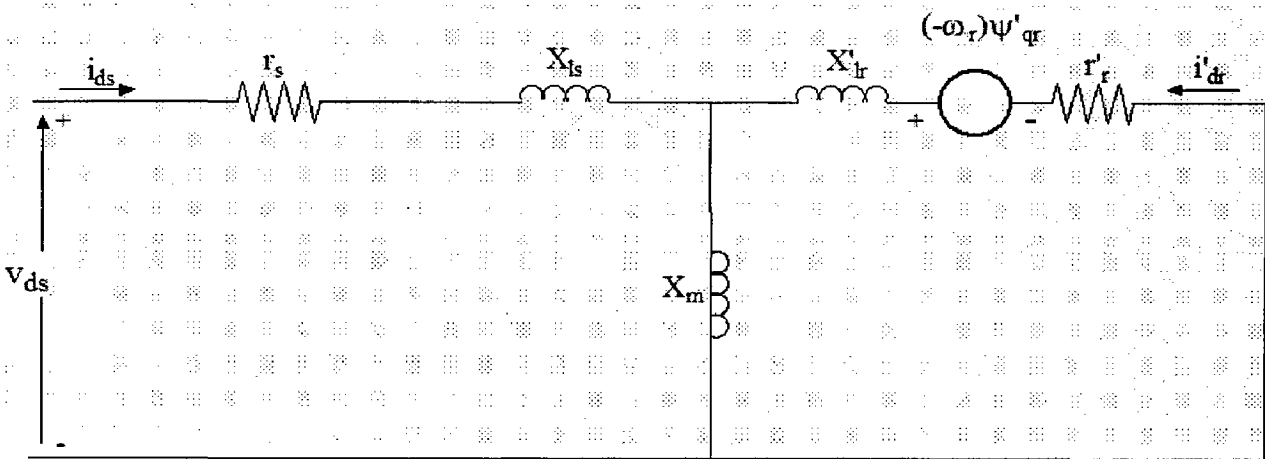


**Fig 2.6(b): d component circuit**

**Fig 2.6:** Stationary reference-frame equivalent circuits for a 3-phase, symmetrical induction machine

### 2.6 Per unit system:

It is convenient to express machine parameters and variables as per unit quantities. Base power and base voltage are selected, and all parameters and variables are normalized using these base quantities. When the machine is being considered separately, the base power is generally selected as the horsepower rating of the machine in volt-amperes (i.e. horsepower times 746). If, on the other hand, the machine is a part of a power system and if it is desirable to convert the entire system to per unit quantities, then only one power base (VA base) is selected which would most likely be different from the rating of any machine in the system.

In general the rms value of the rated phase voltage is selected as base voltage for *abc* variables and peak value as base value for the *abc* variables. That is,  $V_{B(abc)}$  is the rms voltage selected as base voltage for the *abc* variables then  $V_{B(qd0)} = \sqrt{2}V_{B(abc)}$ .

The base power is expressed as

$$P_B = 3V_{B(abc)}I_{B(abc)} \dots\dots\dots (2.70)$$

Or

$$P_B = \frac{3}{2}V_{B(qd0)}I_{B(qd0)} \dots\dots\dots (2.71)$$

where  $I_{B(abc)}$  and  $I_{B(qd0)}$  are base current in *abc* and *abc* variables.

Therefore, as base voltages and base power are selected, base current can be from (2.70) or (2.71). Base impedance can be calculated as:

$$Z_B = \frac{V_{B(abc)}}{I_{B(abc)}} = \frac{3V_{B(abc)}^2}{P_B} \dots\dots\dots (2.72)$$

Or

$$Z_B = \frac{V_{B(qd0)}}{I_{B(qd0)}} = \left(\frac{3}{2}\right) \frac{V_{B(qd0)}^2}{P_B} \dots\dots\dots (2.73)$$

Base torque is expressed as

$$T_B = \frac{P_B}{(2/p)\omega_b} \dots\dots\dots (2.74)$$

Where  $\omega_b$  corresponds to rated or base frequency of the machine. Torque equation (2.54) in per units can be expressed as:

$$T_e = \psi'_{qr} i'_{dr} - \psi'_{dr} i'_{qr} \dots\dots\dots (2.75)$$

The torque balance equation (2.21) can be written in per unit system as:

$$T_e = 2Hp \frac{\omega_r}{\omega_b} + T_L \dots\dots\dots (2.76)$$

Where  $T_L$  is per unit load torque,  $T_e$  is machine per unit electromagnetic torque,  $H$  is inertia constant of machine expressed in seconds given by:

$$H = \left(\frac{1}{2}\right) \left(\frac{2}{P}\right) \frac{J\omega_b}{T_B} = \left(\frac{1}{2}\right) \left(\frac{2}{P}\right)^2 \frac{J\omega_b^2}{P_B} \dots\dots\dots (2.77)$$

Mathematical model of induction machine developed in per unit in the above sections is used to study direct torque controlled induction motor in steady and transient states.

# **Basic Theory of Direct Torque Controlled Induction Motor**

---

## **3.1 Introduction:**

DTC uses feedback control of torque and stator flux, which are computed from the measured stator voltages and currents [4, 20]. The method uses a stator reference model of the induction motor for its implementation, thereby avoiding the trigonometric operations in the coordinate transformations of the synchronous reference frames. This is one of the key advantages of the control scheme. The scheme uses stator flux-linkage control, which enables the flux weakening operation of the motor to be straightforward compared to rotor flux weakening. The stator flux is directly proportional to the induced emf, whereas the rotor flux does not have the same relationship. This reduces the dependence of the scheme on many motor parameters, thus making it a robust scheme in the flux weakening region. The scheme depends only on stator resistance, and on no other parameters. For its flux and torque control, this control scheme requires the position of the flux phasor, which is difficult to obtain at low and zero speeds from measured voltages and currents by using a torque processor. At such low speeds, these signals are very small, making scaling and accuracy problematic; also, the stator-resistance variations introduce significant errors in the flux-phasor computation. Invariably the low-speed operation suffers with this scheme without stator-resistance compensation.

The implementation of the scheme requires flux linkages and torque computations, plus generation of switching states through a feedback control of the torque and flux directly without inner current loops.

The stator  $q$  and  $d$  axes flux linkages are

$$\lambda_{qs} = \int (V_{qs} - r_s i_{qs}) dt \quad \dots\dots\dots (3.1)$$

$$\lambda_{ds} = \int (V_{ds} - r_s i_{ds}) dt \quad \dots\dots\dots (3.2)$$

Where the direct and quadrature axis components are obtained from the  $abc$  variables by using the transformation,

$$i_{qs} = i_{as} \quad \dots\dots\dots (3.3)$$

$$i_{ds} = (1/\sqrt{3})(i_{cs} - i_{bs}) \quad \dots\dots\dots (3.4)$$

This transformation is applicable for voltages and flux linkages as well. To obtain uniformly rotating stator flux, note that the motor voltages have to be varied uniformly without steps. This imposes a requirement of continuously variable stator voltages with infinite steps, which is not usually met by the inverter because it has only finite switching states.

**3.2 Switching states of inverter:**

Consider the inverter shown in fig 3.1. The terminal voltage *a* with respect to negative of the dc supply is considered, and *V<sub>a</sub>* is determined by a set of switches, *S<sub>a</sub>*, consisting of *T<sub>1</sub>* and *T<sub>4</sub>*, and their antiparallel diodes are off, *V<sub>a</sub>* is indeterminate. Such a situation is not encountered in practice and hence, not considered. The switching of *S<sub>b</sub>* and *S<sub>c</sub>* sets for line *b* and *c* can be similarly derived. The total number of switching states possible with *S<sub>a</sub>*, *S<sub>b</sub>* and *S<sub>c</sub>* is eight, they are elaborated in Table 3.1 by using the following relationships:

$$\left. \begin{aligned} V_{ab} &= V_a - V_b \\ V_{bc} &= V_b - V_c \\ V_{ca} &= V_c - V_a \end{aligned} \right\} \dots\dots\dots (3.5)$$

And machine phase voltages for a balanced system are

$$\left. \begin{aligned} V_{as} &= \frac{1}{3}(V_{ab} - V_{ca}) \\ V_{bs} &= \frac{1}{3}(V_{bc} - V_{ab}) \\ V_{cs} &= \frac{1}{3}(V_{ca} - V_{bc}) \end{aligned} \right\} \dots\dots\dots (3.6)$$

And  $q$  and  $d$  axes voltages are given by

$$\left. \begin{aligned} V_{qs} &= V_{as} \\ V_{ds} &= \frac{1}{\sqrt{3}}(V_{cs} - V_{bs}) = \frac{1}{\sqrt{3}}V_{cb} \end{aligned} \right\} \dots\dots\dots (3.7)$$

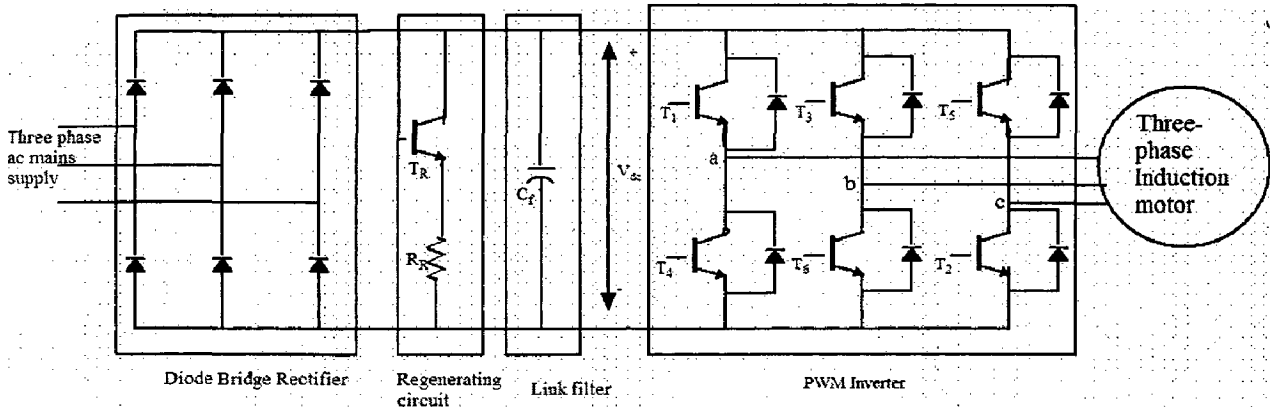


**Fig 3.1:** Power-circuit configuration of the induction motor drive

The stator  $q$  and  $d$  voltages for each state are shown in fig 3.2. The limited states of the inverter create distinct discrete movement of the stator-voltage phasor,  $V_s$  consisting of the resultant of  $V_{qs}$  and  $V_{ds}$ . An almost continuous and uniform flux phasor can be obtained with these discrete voltages states, due to their integration over time as seen from equations (3.1) and (3.2).

|       |       |       |          |
|-------|-------|-------|----------|
| $T_1$ | $T_4$ | $S_a$ | $V_a$    |
| On    | Off   | 1     | $V_{dc}$ |
| Off   | On    | 0     | 0        |

**Table 3.1(a):** switching states of inverter phase leg  $a$

|       |       |       |          |
|-------|-------|-------|----------|
| $T_3$ | $T_6$ | $S_b$ | $V_b$    |
| On    | Off   | 1     | $V_{dc}$ |
| Off   | On    | 0     | 0        |

**Table 3.1(b):** switching states of inverter phase leg  $b$

|       |       |       |          |
|-------|-------|-------|----------|
| $T_5$ | $T_2$ | $S_c$ | $V_c$    |
| On    | Off   | 1     | $V_{dc}$ |
| Off   | On    | 0     | 0        |

**Table 3.1(c):** switching states of inverter phase leg  $c$

| States      | $S_a$ | $S_b$ | $S_c$ | $V_a$    | $V_b$    | $V_c$    | $V_{ab}$   | $V_{bc}$   | $V_{ca}$   | $V_{as}$      | $V_{bs}$      | $V_{cs}$      | $V_{qs}$      | $V_{ds}$            |
|-------------|-------|-------|-------|----------|----------|----------|------------|------------|------------|---------------|---------------|---------------|---------------|---------------------|
| <b>I</b>    | 1     | 0     | 0     | $V_{dc}$ | 0        | 0        | $V_{dc}$   | 0          | - $V_{dc}$ | $2V_{dc}/3$   | $-V_{dc}/3$   | $-V_{dc}/3$   | $2V_{dc}/3$   | 0                   |
| <b>II</b>   | 1     | 0     | 1     | $V_{dc}$ | 0        | $V_{dc}$ | $V_{dc}$   | - $V_{dc}$ | 0          | $V_{dc}/3$    | - $2V_{dc}/3$ | $V_{dc}/3$    | $V_{dc}/3$    | $V_{dc}/\sqrt{3}$   |
| <b>III</b>  | 0     | 0     | 1     | 0        | 0        | $V_{dc}$ | 0          | - $V_{dc}$ | $V_{dc}$   | $-V_{dc}/3$   | $-V_{dc}/3$   | $2V_{dc}/3$   | $-V_{dc}/3$   | $V_{dc}/\sqrt{3}$   |
| <b>IV</b>   | 0     | 1     | 1     | 0        | $V_{dc}$ | $V_{dc}$ | - $V_{dc}$ | 0          | $V_{dc}$   | - $2V_{dc}/3$ | $V_{dc}/3$    | $V_{dc}/3$    | - $2V_{dc}/3$ | 0                   |
| <b>V</b>    | 0     | 1     | 0     | 0        | $V_{dc}$ | 0        | - $V_{dc}$ | $V_{dc}$   | 0          | $-V_{dc}/3$   | $2V_{dc}/3$   | $-V_{dc}/3$   | $-V_{dc}/3$   | - $V_{dc}/\sqrt{3}$ |
| <b>VI</b>   | 1     | 1     | 0     | $V_{dc}$ | $V_{dc}$ | 0        | 0          | $V_{dc}$   | - $V_{dc}$ | $V_{dc}/3$    | $V_{dc}/3$    | - $2V_{dc}/3$ | $-V_{dc}/3$   | - $V_{dc}/\sqrt{3}$ |
| <b>VII</b>  | 0     | 0     | 0     | 0        | 0        | 0        | 0          | 0          | 0          | 0             | 0             | 0             | 0             | 0                   |
| <b>VIII</b> | 1     | 1     | 1     | $V_{dc}$ | $V_{dc}$ | $V_{dc}$ | 0          | 0          | 0          | 0             | 0             | 0             | 0             | 0                   |

**Table 3.2:** Inverter switching states and machine voltages

For speed control of the motor, torque and flux references are generated from speed error and speed of the motor respectively. These references are compared with calculated torque and flux values of the motor to generate torque and flux errors. These errors are given to hysteresis controllers to generate torque and flux commands. Position of the stator flux phasor is used to find in which sextant it was present. From these three variables namely torque command, flux command sextant of stator flux phasor, voltage vector to be switched is decided from the look-up table. This method of controlling the input voltages to the machine has the advantages of, (i) not using pulse-width modulation carrier-frequency signals, (ii) higher fundamental voltages compared to sine-triangle PWM, based controllers, (iii) lower voltage and current ripples.

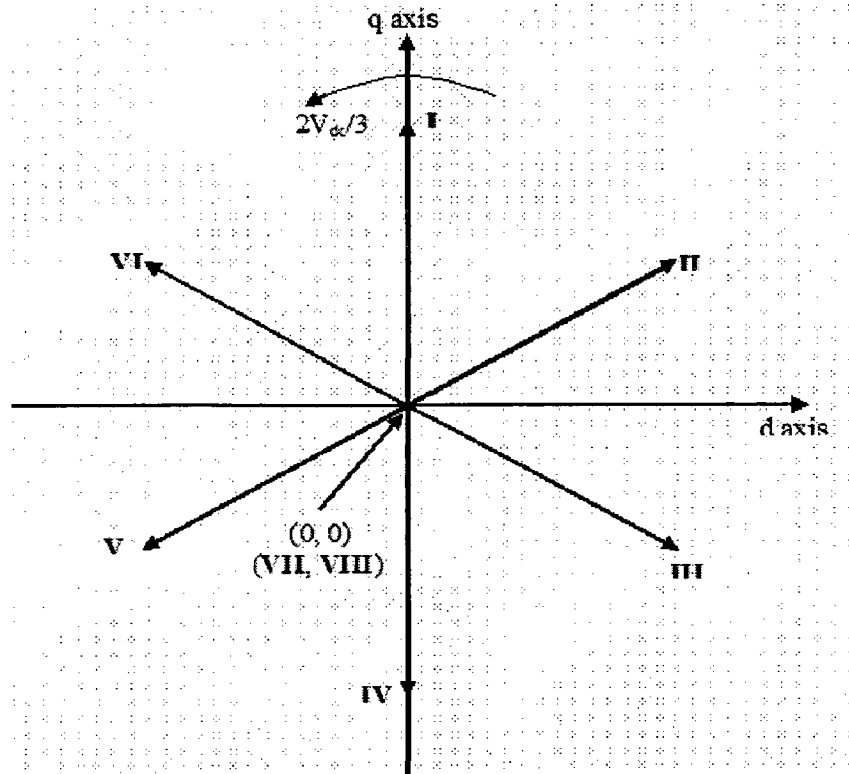


**Fig 3.2:** The inverter output voltage corresponding to switching states

### 3.3 Flux control:

A uniform rotating stator flux is desirable, and it is present in one of the sextants (in the phasor diagram shown in fig 3.3) at any time. The stator-flux phasor has a magnitude of  $\lambda_s$ , with an instantaneous position of  $\theta_{fs}$ . The corresponding  $d$  and  $q$  axes components are  $\lambda_{ds}$  and  $\lambda_{qs}$ , respectively. Assuming that a feedback of stator flux is available, its place in the sextant is identified from its position. Then the influencing voltage phasor is identified by giving a  $90^\circ$  phase shift. For example, if the stator-flux phasor is in sextant<2>, the right influencing voltage phasor has to be either VI or I. Voltage phasor I is  $90^\circ - \theta_{fs}$  and VI is  $150^\circ - \theta_{fs}$  from the flux phasor. One of these two sets increase  $\lambda_s$ , the other decreases  $\lambda_s$ . This is found from the following explanation obtained from fig 3.4.



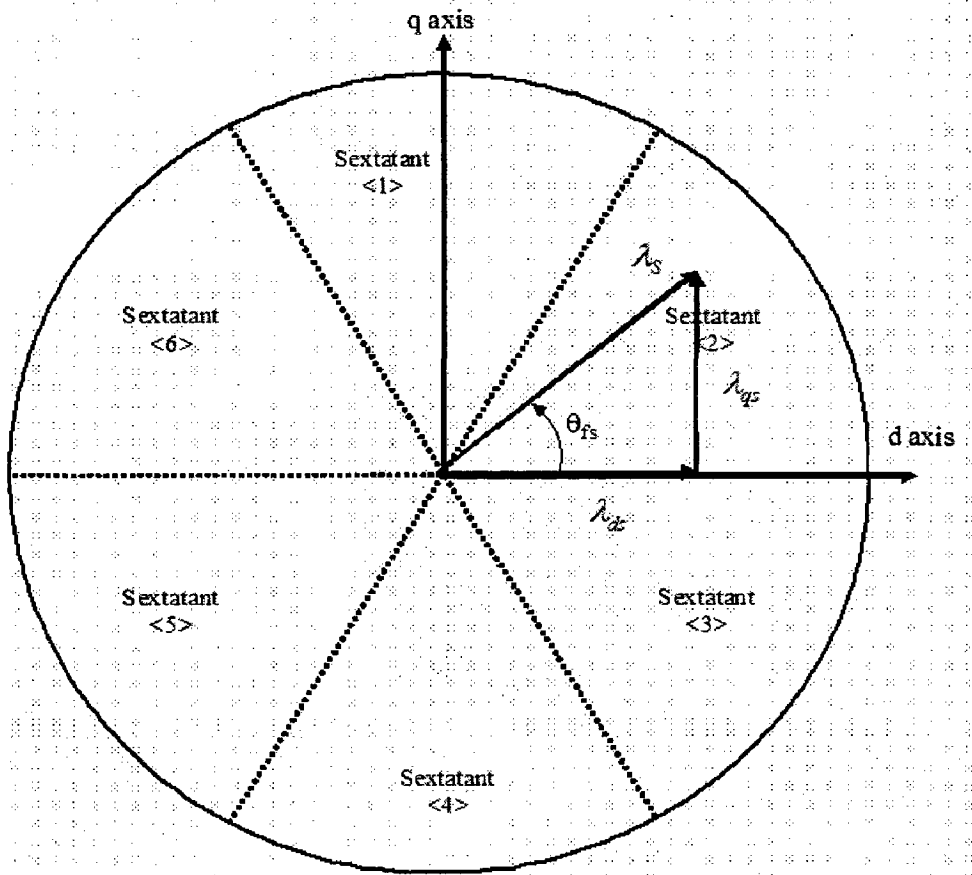


**Fig 3.3:** Division of sextant for stator flux-linkages identification

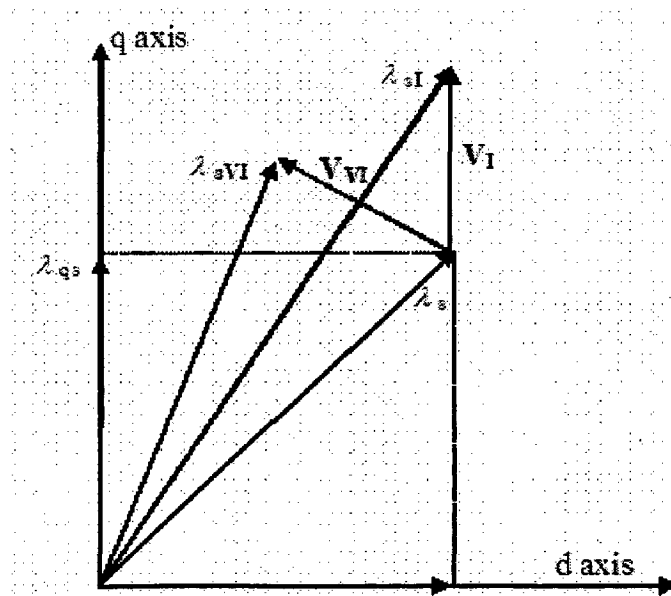


**Fig 3.4:** Effect of switching  $V_I$  and  $V_{VI}$  on stator-flux phasor

Consider the effect of switching voltage phasor **I**,  $V_I$ , and voltage phasor **VI**,  $V_{VI}$ . As seen from the phasor diagram, in the case of **I**, the flux phasor increases in magnitude from  $\lambda_s$ , to  $\lambda_{sI}$ ; in the case of voltage phasor **VI**, it decreases to  $\lambda_{sVI}$ . This implies that the closer voltage-phasor increases the flux and the farther voltage-phasor decreases the flux, but note that both of them advance the flux phasor in position. Similarly for all other sextants, the switching logic is developed. A flux error,  $\lambda_{er}$ , thus determines which voltage phasor has to be called, and this flux error is converted to digital signal with a window comparator with a hysteresis of  $\delta\lambda_s$  (let it be  $S\lambda$ ), as given in the Table 3.3:

| Condition                     | $S\lambda$ |
|-------------------------------|------------|
| $\lambda_{er} > \lambda_s$    | +1         |
| $\lambda_{er} \leq \lambda_s$ | 0          |

**Table 3.3:** Hysteresis comparator window for stator flux

### 3.4 Torque control:

Over and above the flux control, the control of electromagnetic torque is required for high-performance of the drive. It is achieved as follows.

Torque control is exercised by comparison of the reference torque to the torque measured from the stator flux linkages and stator currents as

$$T_e = \left(\frac{3}{2}\right)\left(\frac{P}{2}\right)(\lambda_{ds}^i i_{qs} - \lambda_{qs}^i i_{ds}) \dots\dots\dots (3.8)$$

The error torque is processed through a window comparator with three level hysteresis to produce digital output,  $S_T$ , as given in the Table 3.4.  $T_e^*$  is reference torque generated from speed error.

Interpretation of  $S_T$  is as follows: when it is +1 amount to increasing the voltage phasor, 0 means to keep it at zero, -1 requires retarding the voltage phasor behind the flux phasor to provide regeneration. Combining the flux error output  $S_\lambda$ , the torque error

| Condition                                  | $S_T$ |
|--|-------|
| $(T_e^* - T_e) > \delta T_e$               | +1    |
| $-\delta T_e < (T_e^* - T_e) < \delta T_e$ | 0     |
| $(T_e^* - T_e) < -\delta T_e$              | -1    |

**Table 3.4:** Hysteresis comparator window for torque

output  $S_T$ , and the sextant of the flux phasor  $S_\theta$ , a switching table can be realized to obtain the switching states of the inverter; it is given in Table 3.5. The algorithm for  $S_\theta$  is shown in Table 3.6.

Consider the first column corresponding to  $S_\theta = \langle 1 \rangle$  (sextant 1). The following states of the inverter are indicated in parenthesis; they correspond to  $S_a$ ,  $S_b$  and  $S_c$ . The flux error signal indicates 1, which means the flux is less than its request value and therefore the flux phasor has to be increased. At the same time, torque error is positive, asking for an increase. Merging these two with position of the flux phasor  $\langle 1 \rangle$ , the voltage phasor **I** and **VI** satisfy the requirements only if the flux is within the first  $30^\circ$  of the sextant  $\langle 1 \rangle$ . In the second  $30^\circ$ , note that the voltage phasor **I** will increase the flux-phasor magnitude but will retard it in phase, which will tend to decrease torque. This will result in a reduction of the stator frequency and reversal of the direction of torque. The control requires the advancement of the flux phasor in the same direction (i.e. counterclockwise in this discussion); that could be satisfied only by voltage phasor **VI** in this  $30^\circ$ . Voltage phasor **VI** is the only one satisfying the uniform requirements throughout the sextant  $\langle 1 \rangle$ , so the voltage phasor **VI** is chosen for  $S_T$  and  $S_\lambda$  equal to +1 with the flux phasor in sextant  $\langle 1 \rangle$ . When the torque error is zero, the only logical choice

is to apply zero line voltages; because the previous state had two +1 states, it is easy to achieve zero line voltages by choosing the switching state **VIII** with all ones. If the torque error becomes negative with  $S_T = -1$ , the machine has to regenerate, with a simultaneous increase in flux phasor due to  $S_\lambda = +1$ ; hence, the voltage phasor is retarded close to flux phasor, and, hence, switching state **II** (1, 0, 1) is selected.

| Sextant( $S_\theta$ ) |       |                        |                        |                        |                        |                        |                        |
|-----------------------|-------|------------------------|------------------------|------------------------|------------------------|------------------------|------------------------|
| $S_\lambda$           | $S_T$ | <1>                    | <2>                    | <3>                    | <4>                    | <5>                    | <6>                    |
| +1                    | +1    | <b>VI</b><br>(1,1,0)   | <b>I</b><br>(1,0,0)    | <b>II</b><br>(1,0,1)   | <b>III</b><br>(0,0,1)  | <b>IV</b><br>(0,1,1)   | <b>V</b><br>(0,1,0)    |
| +1                    | 0     | <b>VIII</b><br>(1,1,1) | <b>VII</b><br>(0,0,0)  | <b>VIII</b><br>(1,1,1) | <b>VII</b><br>(0,0,0)  | <b>VIII</b><br>(1,1,1) | <b>VII</b><br>(0,0,0)  |
| +1                    | -1    | <b>II</b><br>(1,0,1)   | <b>III</b><br>(0,0,1)  | <b>IV</b><br>(0,1,1)   | <b>V</b><br>(0,1,0)    | <b>VI</b><br>(1,1,0)   | <b>I</b><br>(1,0,0)    |
| 0                     | +1    | <b>V</b><br>(0,1,0)    | <b>VI</b><br>(1,1,0)   | <b>I</b><br>(1,0,0)    | <b>II</b><br>(1,0,1)   | <b>III</b><br>(0,0,1)  | <b>IV</b><br>(0,1,1)   |
| 0                     | 0     | <b>VII</b><br>(0,0,0)  | <b>VIII</b><br>(1,1,1) | <b>VII</b><br>(0,0,0)  | <b>VIII</b><br>(1,1,1) | <b>VII</b><br>(0,0,0)  | <b>VIII</b><br>(1,1,1) |
| 0                     | -1    | <b>III</b><br>(0,0,1)  | <b>IV</b><br>(0,1,1)   | <b>V</b><br>(0,1,0)    | <b>VI</b><br>(1,1,0)   | <b>I</b><br>(1,0,0)    | <b>II</b><br>(1,0,1)   |

**Table 3.5:** Switching states for possible  $S_\lambda$ ,  $S_T$ , and  $S_\theta$

| $\theta_{fs}$                       | Sextant |
|-------------------------------------|---------|
| $\pi/3 < \theta_{fs} \leq 2\pi/3$   | <1>     |
| $0 < \theta_{fs} \leq \pi/3$        | <2>     |
| $-\pi/3 < \theta_{fs} \leq 0$       | <3>     |
| $-2\pi/3 < \theta_{fs} \leq -\pi/3$ | <4>     |
| $-\pi < \theta_{fs} \leq -2\pi/3$   | <5>     |
| $2\pi/3 < \theta_{fs} \leq \pi$     | <6>     |

**Table 3.6:** Flux-phasor sextant logic ( $S_\theta$ )

If  $S_\lambda = 0$  (i.e. the flux phasor has exceeded its request by the hysteresis window amount,  $\delta \lambda_s$ ), then it has to be decreased to match its request value by choosing a voltage phasor away from flux phasor, i.e., **V**. This accelerates the flux phasor and increasing the slip speed, resulting also in an increase of electromagnetic torque, thus satisfying  $S_T = +1$  demand. When  $S_T = 0$ , reach zero line-voltage states by going to **VII**, because **V** contained two zero states in it. If  $S_T = -1$ , then regenerative, increasing the negative torque but decreasing the flux phasor, this is achieved by retarding the voltage phasor behind the flux phasor, but far away from it, and hence **III** is chosen. Note that it has two zeros in it, and, therefore, transition from **VII** to **III** requires a change of only one switch signal.

### 3.5 Illustration of look-up table:

Let flux vector be present in sextant <1> there will be 6 possible conditions based on flux and torque commands as given in table 3.5. All these are illustrated in the fig 3.5. Let  $\lambda_s$  is the initial position of stator flux and  $\lambda_{sf}$  is the stator flux position after the application of selected voltage vector.

**Case 1:** Increment in flux and Increment in torque i.e.  $S_\lambda = +1$  and  $S_T = +1$  voltage vector **VI**(110) is applied.

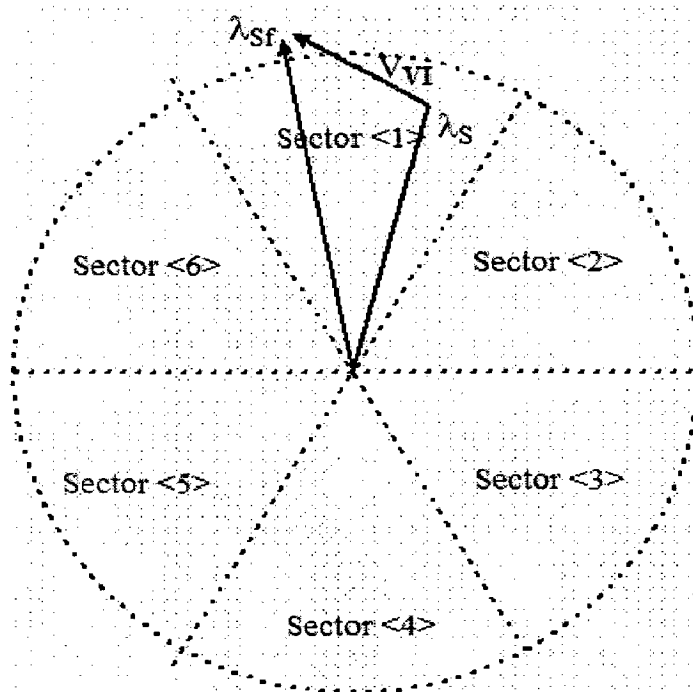


**Fig 3.5(a):** Voltage vector application when increment in both flux and torque is required  
**Case 2:** Increment in flux and Decrement in torque i.e.  $S_\lambda = 1$  and  $S_T = -1$  voltage vector  $\text{II}(101)$  is applied.

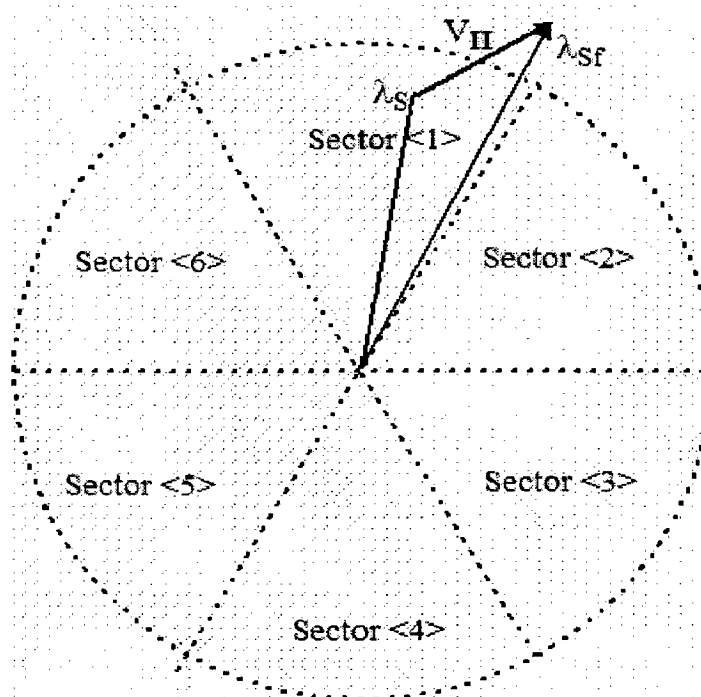


**Fig 3.5(b):** Voltage vector application when increment flux and decrement in torque is required

**Case 3:** No change in flux and Increment in torque i.e.  $S_\lambda = 0$  and  $S_T = 1$  voltage vector  $V(010)$  is applied.

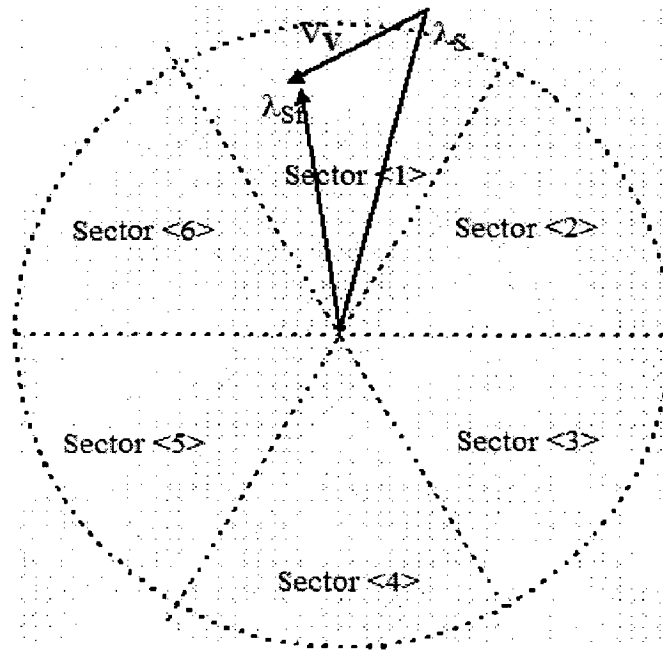


**Fig 3.5(c):** Voltage vector application when increment in torque and no change in flux is required

**Case 4:** No change in flux and Decrement in torque i.e.  $S_\lambda = 0$  and  $S_T = -1$  voltage vector  $V(001)$  is applied.

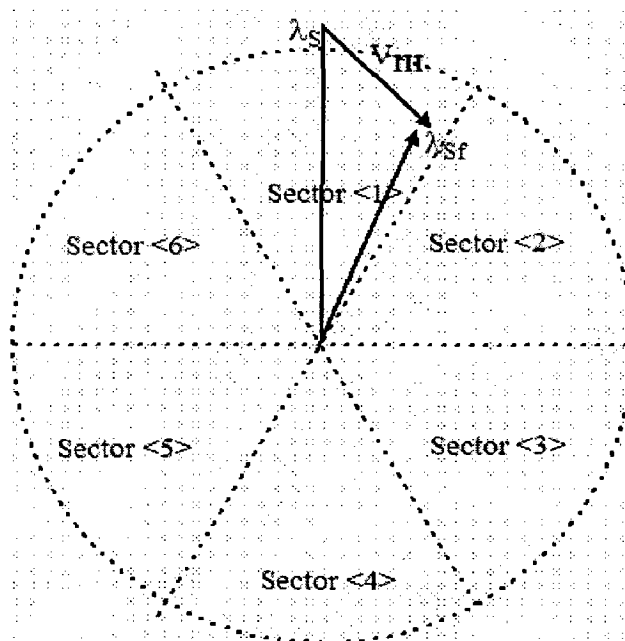


**Fig 3.5(d):** Voltage vector application when decrement in torque and no change in flux is required

**Case 5 and Case 6:** In these two cases i.e. when no change in torque is required and weather increment or no change is required one of zero voltage vectors  $V_{VII}$  or  $V_{VIII}$  is selected.

From the above illustrations following observations can be made for selection of voltage vector.

1. If increment in torque and increment in flux is required then (n-1) voltage vector is selected.
2. If increment in torque and no change in flux then (n-2) voltage vector is selected.
3. If decrement in torque and increment in flux is required then (n+1) voltage vector is selected.
4. If decrement in torque and no change in flux then (n+2) voltage vector is selected.
5. If no change in torque is required irrespective of flux command either of zero vectors [  $V_{VII}(000)$ ,  $V_{VIII}(111)$  ] is chosen.

### **3.6 Implementation:**

The drive scheme is realized as shown in fig 3.6.

Further, to reduce the voltage transducers, the information of line and phase voltages could be obtained from a single dc-link voltage transducer and the gate drive signals. Similarly, the phase currents can be reconstructed from a single dc-link current transducer are required, both of which are electrical; it does not require moving parts, thus making this control scheme robust and reliable. Further, the cost of the drive-system control is very low compared to that of position-sensor-based vector-controlled induction motor drives.



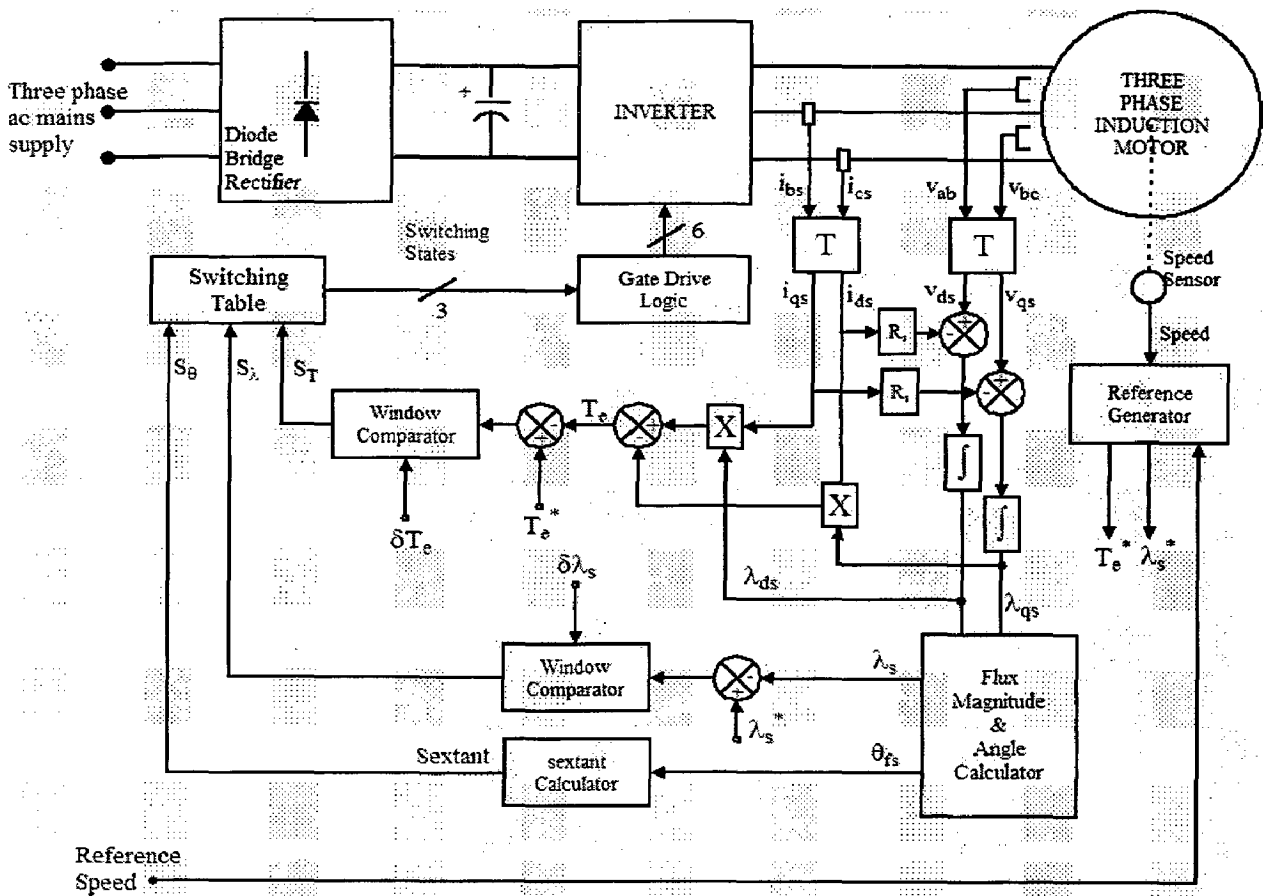


**Fig 3.6:** Block-diagram schematic of the direct torque induction motor drive

### 3.7 Results:

Direct torque control of induction motor presented here is implemented in MATLAB SIMULINK software package. At every instant switching of inverter is decided from flux and torque command, which are generated from flux and torque hysteresis controllers. Fig 3.7 shows the block diagram of simulated drive in MATLAB SIMULINK.

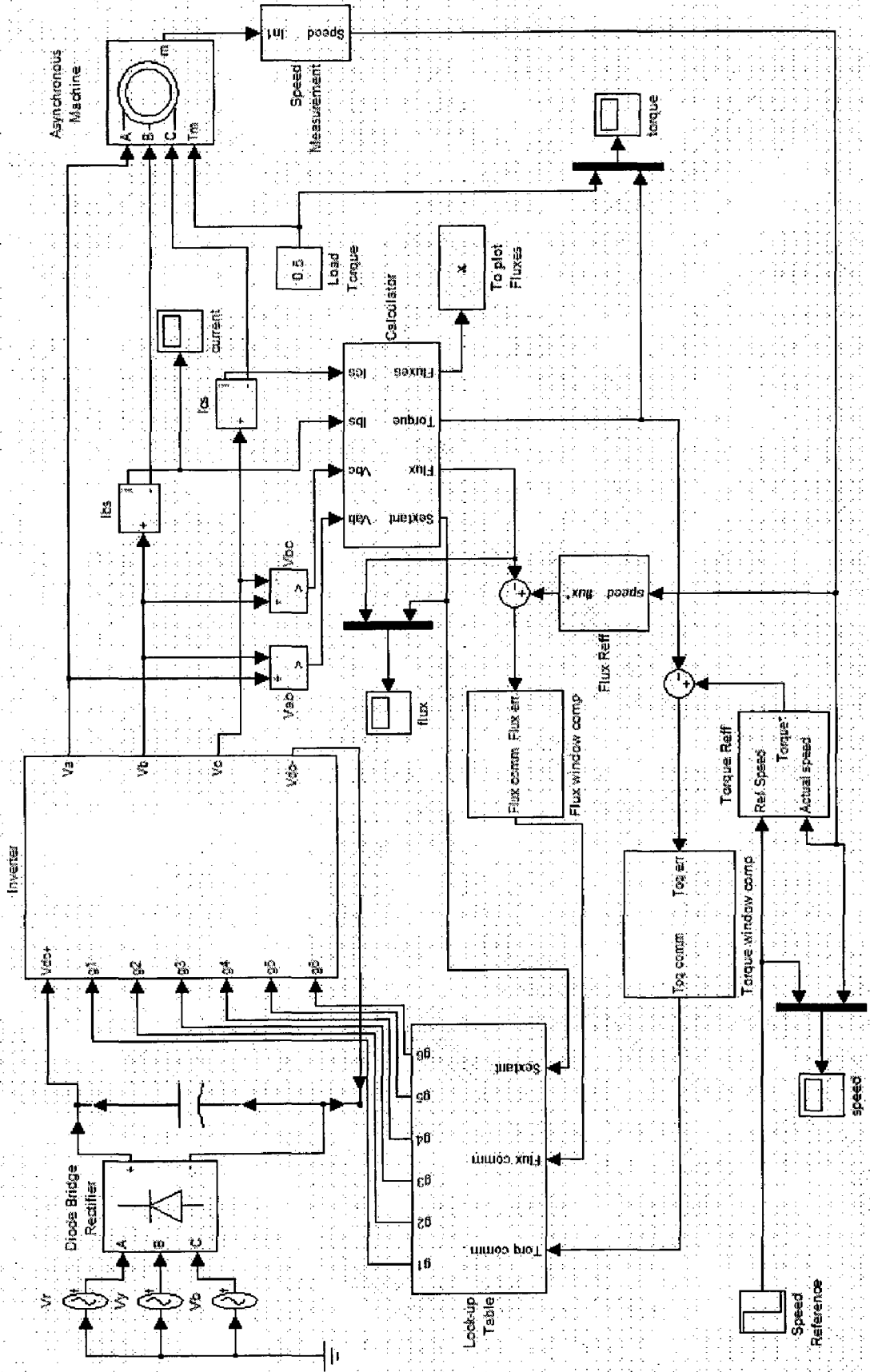
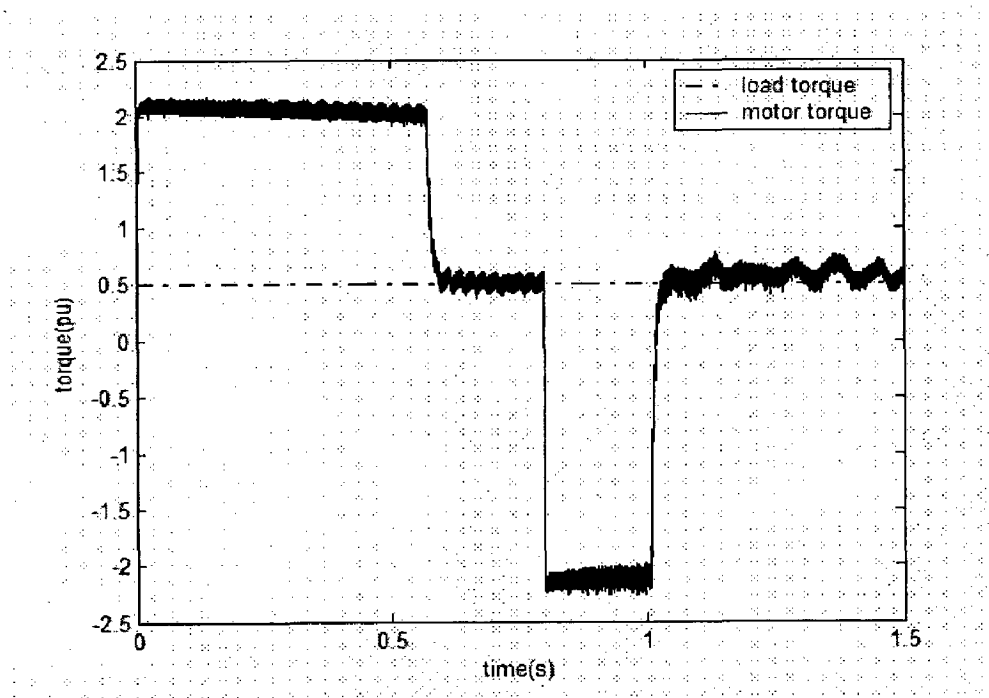


Fig 3.7: Block diagram model of direct torque control used for simulation in MATLAB SIMULINK

The performance of direct torque controlled induction motor drive fed from voltage source inverter is investigated under different load conditions and speed references. Closed loop operation is performed to control speed of induction motor by measuring its speed using a speed sensor. Performance of the induction motor drive controlled using direct torque control under two conditions is presented here.

### 3.7.1 Step change in speed reference:

In this case speed reference is changed from 0.8pu to 0.25pu at 0.8 sec with load torque at 0.5pu. Results are plotted and are shown in fig 3.8.



**Fig 3.8(a):** Torque response for step change in speed for direct torque controlled induction motor

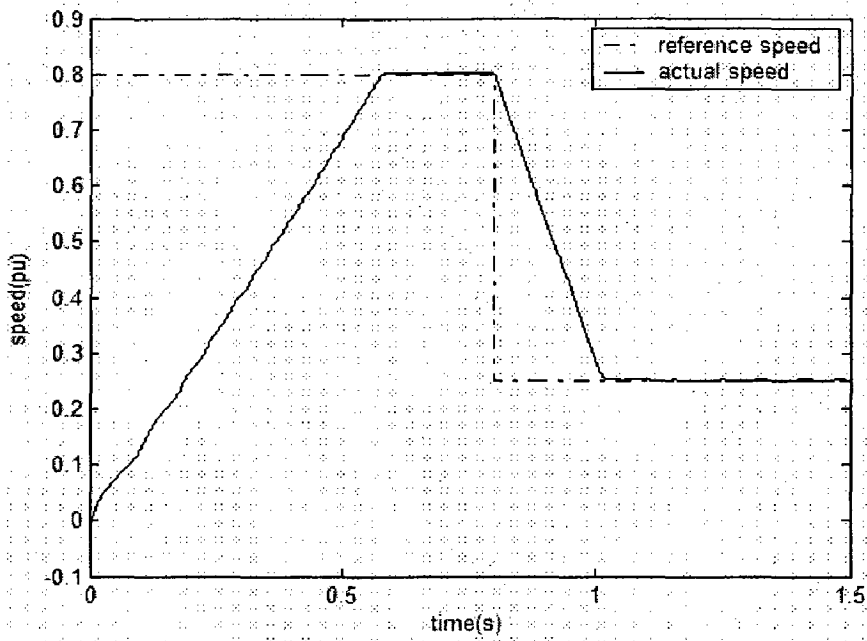


**Fig 3.8(b):** Speed response for step change in speed for direct torque controlled induction motor

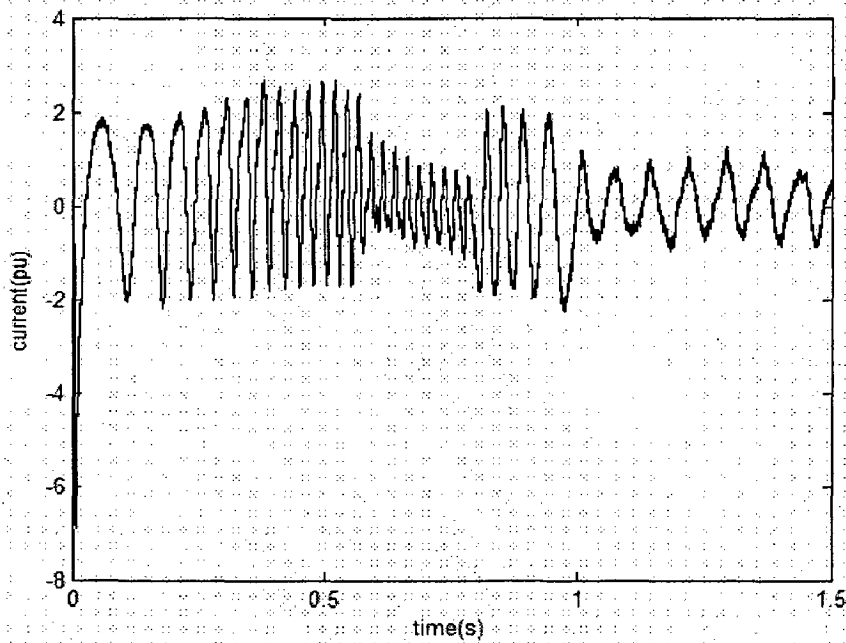


**Fig 3.8(c):** Phase current ( $I_{bs}$ ) response for step change in speed for direct torque controlled induction motor

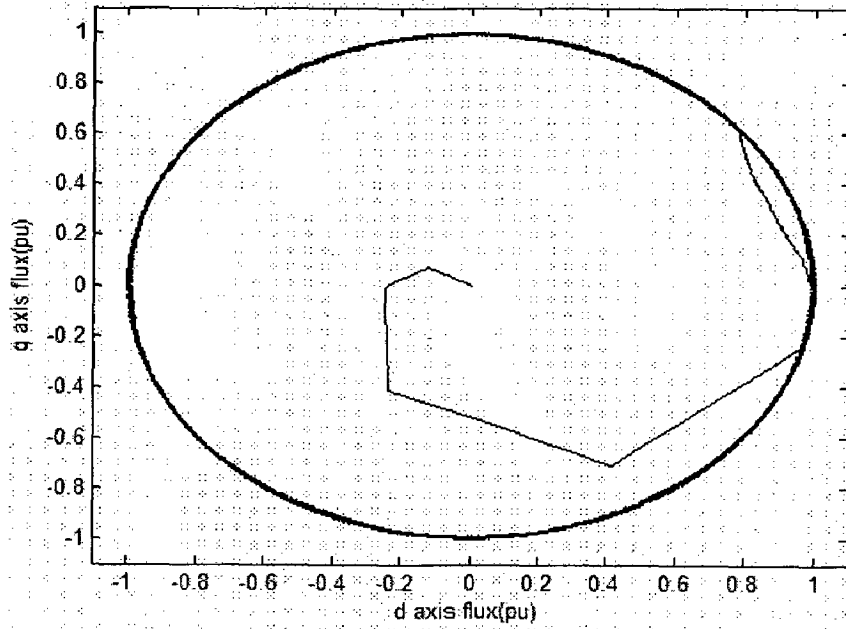


**Fig 3.8(d):** Stator d-q axis flux plot locus for step change in speed for direct torque controlled induction motor

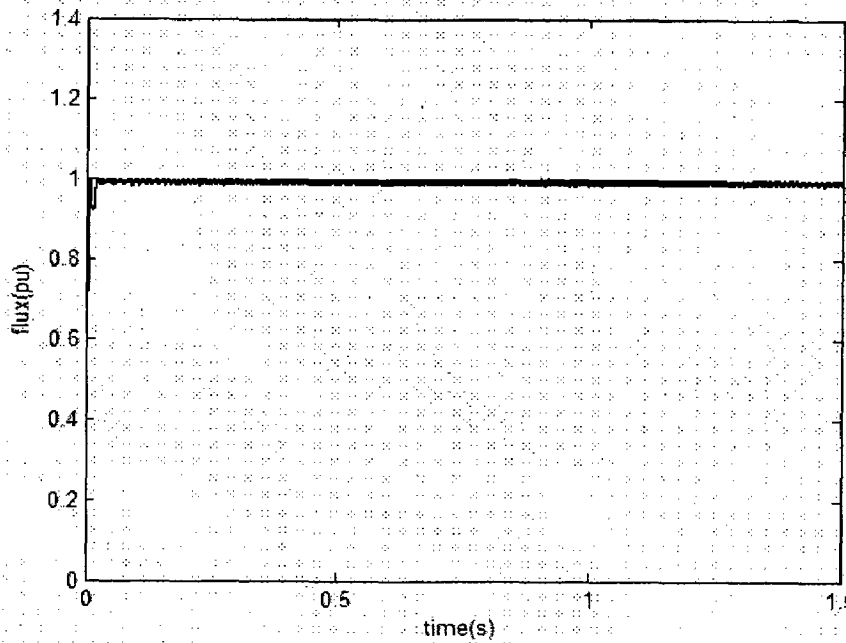


**Fig 3.8(e):** Stator flux magnitude plot for step change in speed for direct torque controlled induction motor

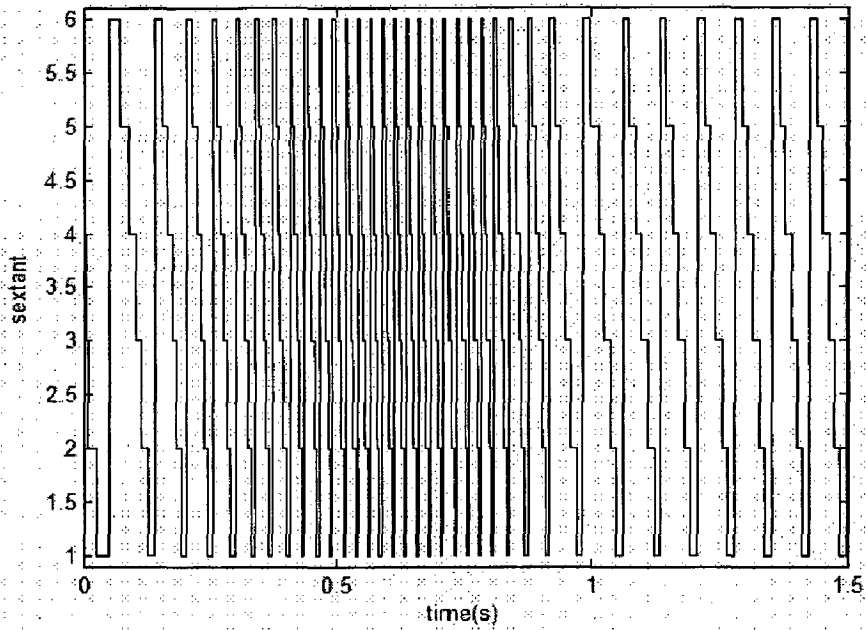


**Fig 3.8(f):** Sextant plot for step change in speed for direct torque controlled induction motor

### 3.7.2 Step change in load torque:

In this case load torque is changed from 0.25pu to 0.8pu at 0.8 sec with speed reference at 0.75pu. Results are shown in fig 3.9.

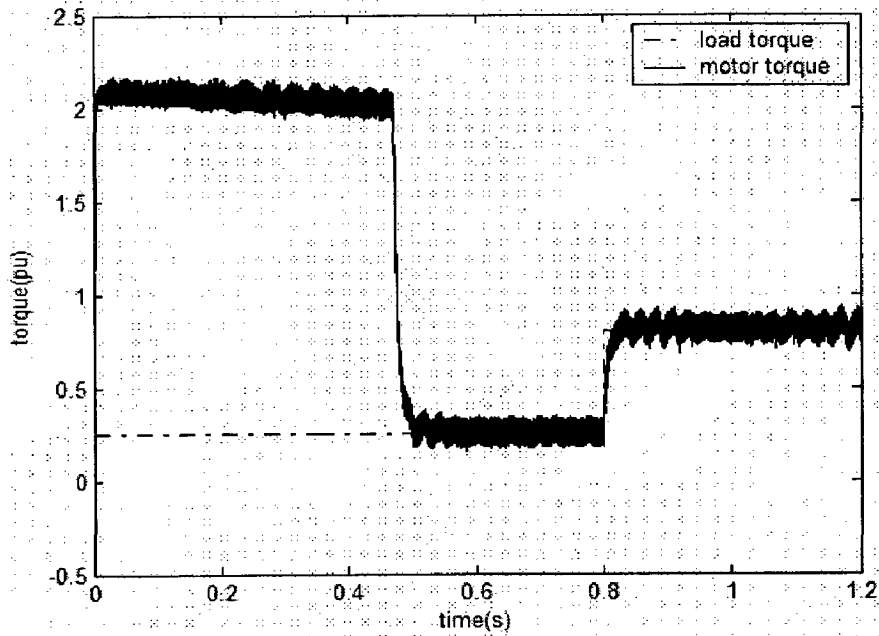


**Fig 3.9(a):** Torque response for step change in load torque for direct torque controlled induction motor

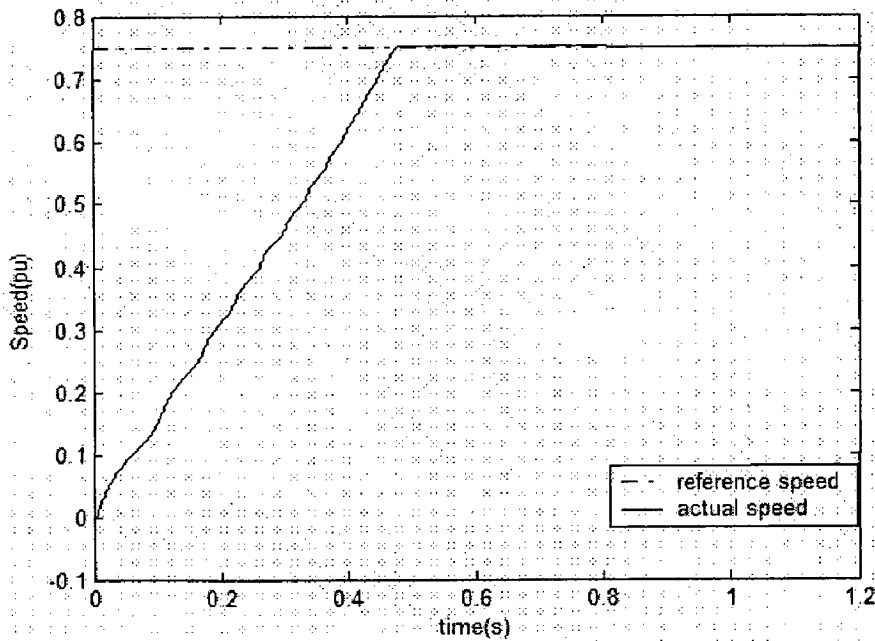


**Fig 3.9(b):** Speed response for step change in load torque for direct torque controlled induction motor

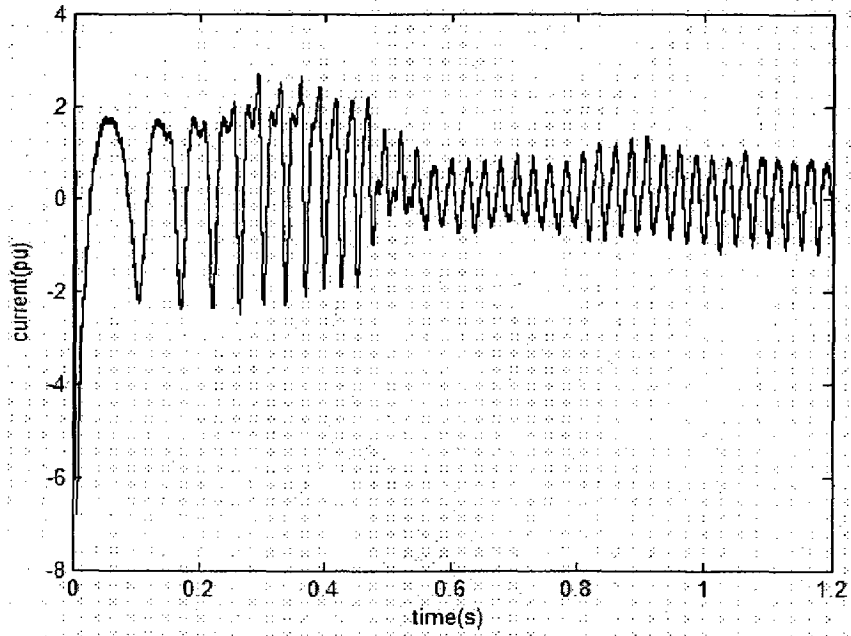


**Fig 3.9(c):** Phase current ( $I_{bs}$ ) response for step change in load torque for direct torque controlled induction motor

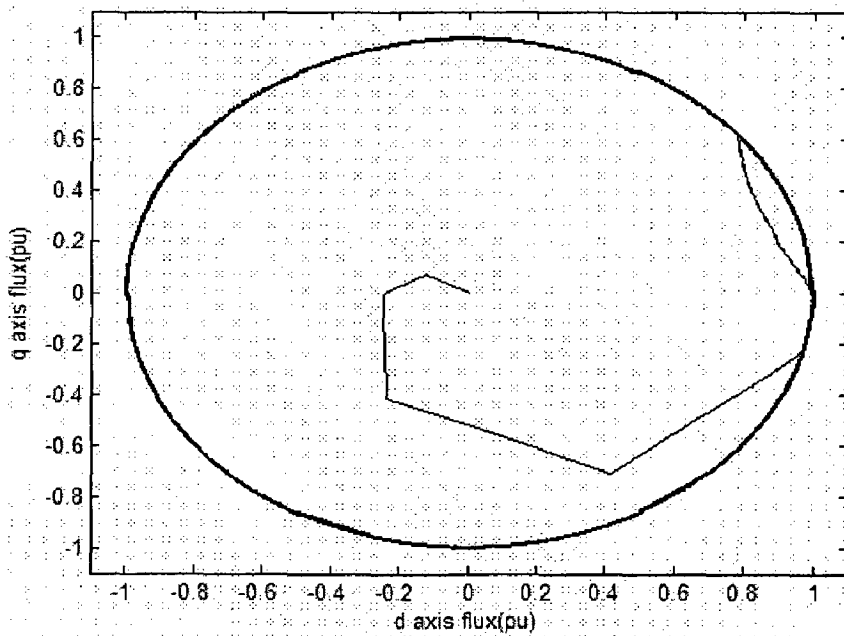


**Fig 3.9(d):** Stator d-q axis flux locus for step change in load torque for direct torque controlled induction motor



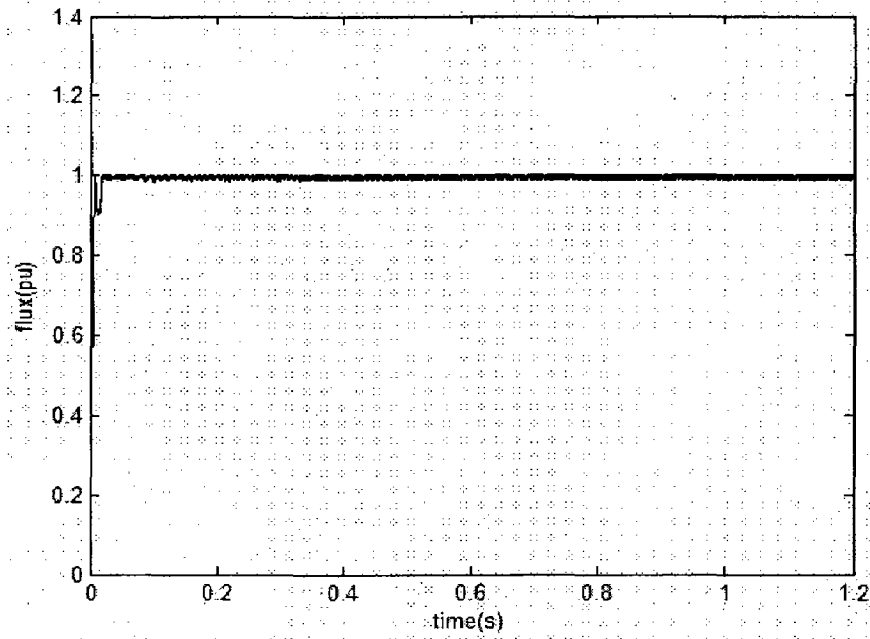


**Fig 3.9(e):** Stator flux magnitude for step change in load torque for direct torque controlled induction motor

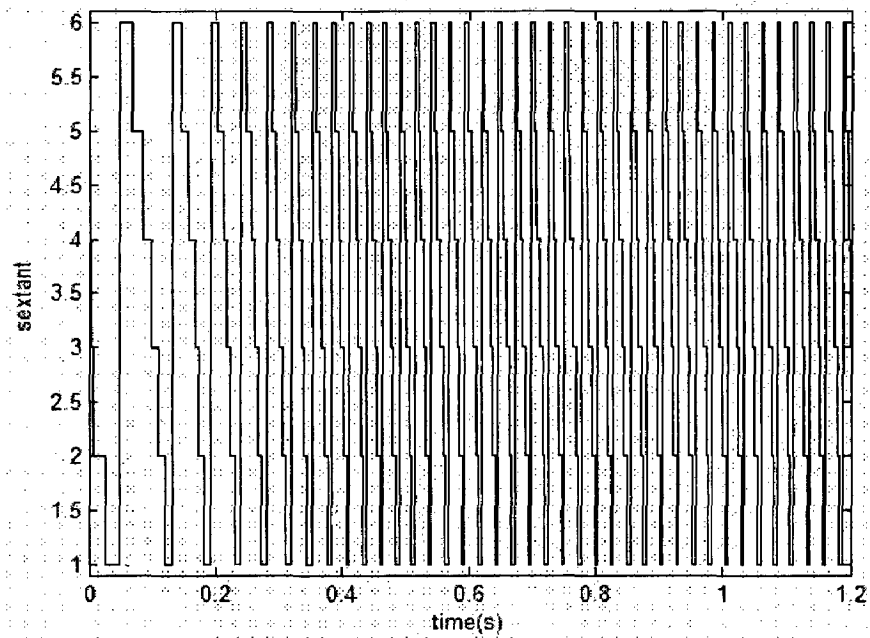


**Fig 3.9(f):** Sextant plot for step change in load torque for direct torque controlled induction motor

# **Sensorless Direct Torque Control of Induction Motor**

---

### **4.1 Introduction:**

A speed signal is required for closed loop operation of drive for speed and position signal. Speed signal can be obtained from a speed encoder or by speed estimation. Speed encoder is undesirable in a drive because it adds cost and reliability problems besides the need for a shaft extension and mounting arrangement. So the sensorless drives are gaining their popularity by playing vital role in reducing costs of high performance drive systems, by eliminating speed sensors and their interfaces [21]. Another reason is that a sensorless drive increases the motor versatility. Objectives of sensorless drive control are:

- Reduction of hardware complexity and cost
- Increased mechanical robustness
- Operation in hostile environments
- Higher reliability
- Increased noise immunity

Challenges imposed by speed estimation techniques are accuracy of speed estimation at low speeds particularly at zero speed, parameter variation problem.

### **4.2 Speed Estimation methods:**

The induction motor speed estimation techniques proposed in the literature [8] can generally be classified as follows:

1. Slip calculation
2. Direct synthesis from state equations
3. Model Referencing Adaptive Systems (MRAS)
4. Speed adaptive flux observer (Luenberger observer)
5. Extended Kalman filter (EKF)
6. Slot harmonics

## 7. Injection of auxiliary signal on salient rotor

Of the above mentioned speed estimation techniques 3, 4 and 5 methods are highly complicated, require more computing time, parameter sensitive and accuracy is poor at lower speeds. Method 6 requires a signal processing circuit to extract space harmonics from stator voltage which are generated by reluctance modulation provided by slots on the surface of the rotor. Thus this method depends on magnitude and frequency of harmonic voltages, which are very small at low speeds. Method 7 requires auxiliary signal generator and can be used only for salient rotor motor. Method 1 is more machine parameter dependent and gives poor estimation at low and near synchronous speeds. In the following section speed estimation by using direct synthesis from state equation is discussed.

### 4.3 Direct synthesis from state equations:

The d-q frame state equations of a machine can be manipulated to compute the speed signal directly [4]. The stator voltage equation for d axis voltage  $v_{ds}$  in d-q equivalent circuit can be written as:

$$v_{ds} = i_{ds} r_s + L_{ls} p i_{ds} + p \lambda_{dm} \quad \dots \dots \dots (4.1)$$

Flux linkage equation in d axis given by:

$$\lambda_{dr} = \frac{L'_r}{L_M} \lambda_{dm} - L'_{lr} i_{ds} \quad \dots \dots \dots (4.2)$$

Substituting equation (4.2) in (4.1) gives

$$v_{ds} = \frac{L_M}{L_r} p(\lambda_{dr}) + (r_s + \sigma L_s p) i_{ds} \quad \dots \dots \dots (4.3)$$

Where

$$\sigma = 1 - (L_M^2 / L_r L_s) \quad \dots \dots \dots (4.4)$$

Equation (4.3) can be rewritten as:

$$p \lambda_{dr} = \frac{L_r}{L_M} v_{ds} - \frac{L_r}{L_M} (r_s + \sigma L_s p) i_{ds} \quad \dots \dots \dots (4.5)$$

Similarly the  $\lambda_{dr}$  can be derived as

$$p\lambda_{qr} = \frac{L_r}{L_M} v_{qs} - \frac{L_r}{L_M} (r_s + \sigma L_s p) i_{qs} \quad \dots\dots\dots (4.6)$$

The rotor flux equations in d-q frame can be given as

$$p\lambda_{dr} = \frac{L_M}{T_r} i_{ds} - \omega_r \lambda_{qr} - \frac{1}{T_r} \lambda_{dr} \quad \dots\dots\dots (4.7)$$

$$p\lambda_{qr} = \frac{L_M}{T_r} i_{qs} + \omega_r \lambda_{dr} - \frac{1}{T_r} \lambda_{qr} \quad \dots\dots\dots (4.8)$$

Angle of rotor flux with respect to d axis can be written as

$$\theta_e = \tan^{-1} \left( \frac{\lambda_{qr}}{\lambda_{dr}} \right) \quad \dots\dots\dots (4.9)$$

Differentiating equation (4.9) we get

$$p\theta_e = \frac{\lambda_{dr} \dot{\lambda}_{qr} - \lambda_{qr} \dot{\lambda}_{dr}}{\lambda_r^2} \quad \dots\dots\dots (4.10)$$

Voltage equations for rotor circuit in d-q frame can be written as

$$p\lambda_{dr} + \frac{r_r}{L_r} i_{dr} + \omega_r \lambda_{qr} = 0 \quad \dots\dots\dots (4.11)$$

$$p\lambda_{qr} + \frac{r_r}{L_r} i_{qr} - \omega_r \lambda_{dr} = 0 \quad \dots\dots\dots (4.12)$$

Adding terms  $(L_M^r / L_r) i_{ds}$  and  $(L_M^r / L_r) i_{qs}$  respectively, on both sides of the above equations we get

$$p\lambda_{dr} + \frac{r_r}{L_r} (L_M^r i_{ds} + L_r i_{dr}) + \omega_r \lambda_{qr} = \frac{L_M^r}{L_r} i_{ds} \quad \dots\dots\dots (4.13)$$

$$p\lambda_{qr} + \frac{r_r}{L_r} (L_M^r i_{qs} + L_r i_{qr}) - \omega_r \lambda_{dr} = \frac{L_M^r}{L_r} i_{qs} \quad \dots\dots\dots (4.14)$$

Combining equations (4.13), (4.14) and (4.10) and simplifying, we get

$$\omega_r = p\theta_e - \frac{L_M}{T_r} \left[ \frac{\lambda_{dr} i_{qs} - \lambda_{qr} i_{ds}}{\lambda_r^2} \right] \quad \dots\dots\dots (4.15)$$

Or

$$\omega_r = \frac{1}{\lambda_r^2} \left[ \left( \lambda_{dr} \dot{\lambda}_{qr} - \lambda_{qr} \dot{\lambda}_{dr} \right) - \frac{L_M}{T_r} \left( \lambda_{dr} i_{qs} - \lambda_{qr} i_{ds} \right) \right] \dots \dots \dots (4.16)$$

Fig 4.1 gives a block diagram for speed estimation where the voltage model equations (4.5) and (4.6), have been used to estimate the rotor fluxes.

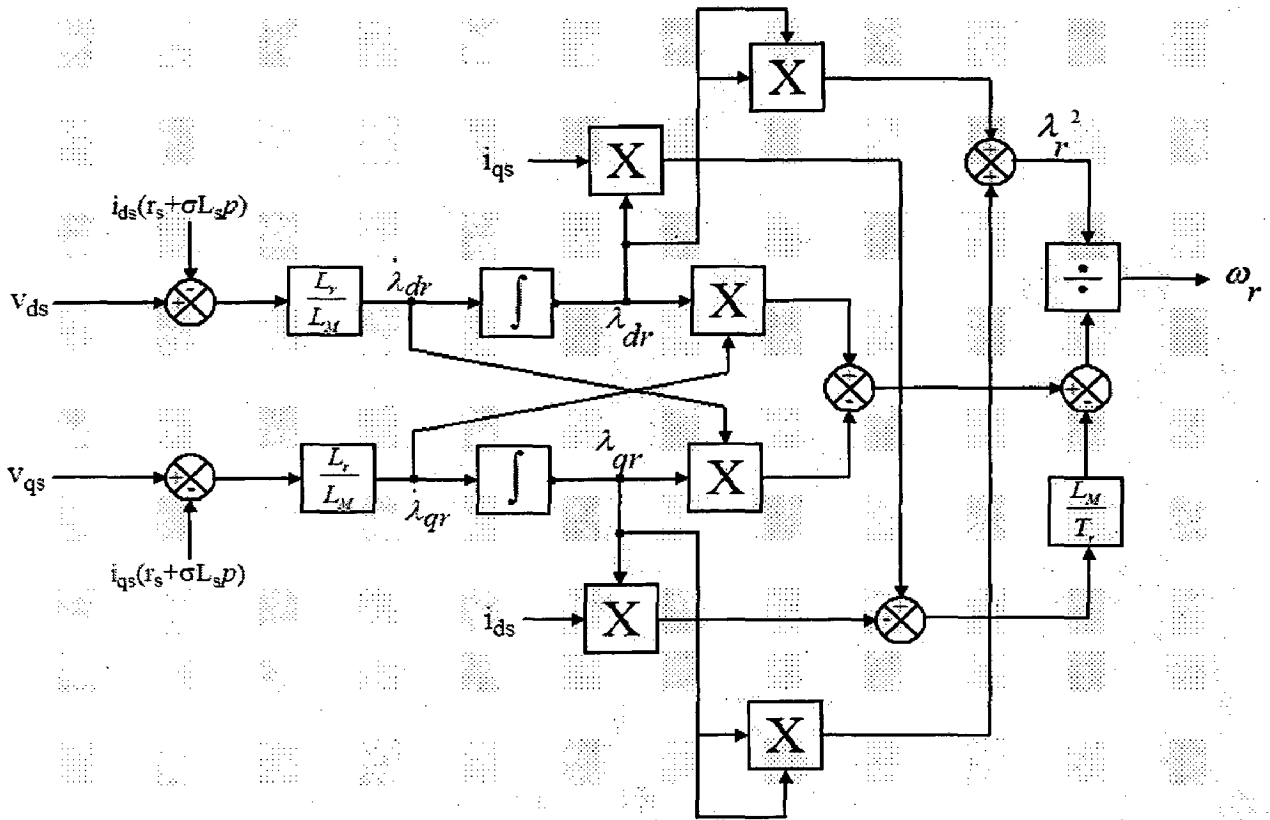


**Fig 4.1:** Speed estimation by direct synthesis from state equations

Sensorless implementation of direct torque control of induction motor is shown in fig 4.2

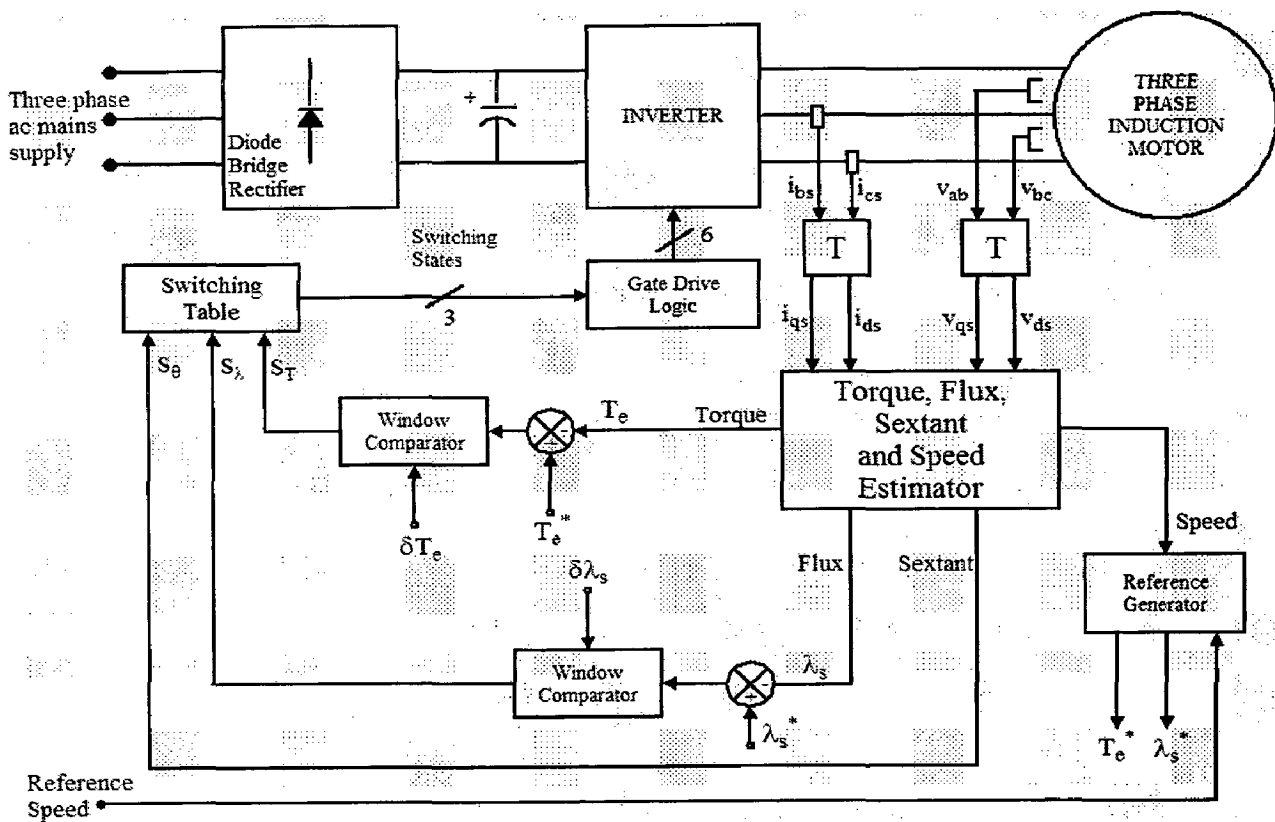


Fig 4.2: Block-diagram schematic of the sensorless direct torque induction motor drive

#### 4.4 Results:

Simulated block diagram of sensorless direct torque control of induction motor, implemented in MATLAB SIMULINK is shown in fig 4.3. In this case closed loop operation of the drive is done from speed signal from speed estimator. Performance of the drive for two different load conditions and speed references are presented here.

##### 4.4.1 Step change in speed reference:

In this case speed reference is changed from 0.8pu to 0.25pu at 0.8 sec with load torque at 0.5pu. Results are plotted and are shown in fig 4.4.



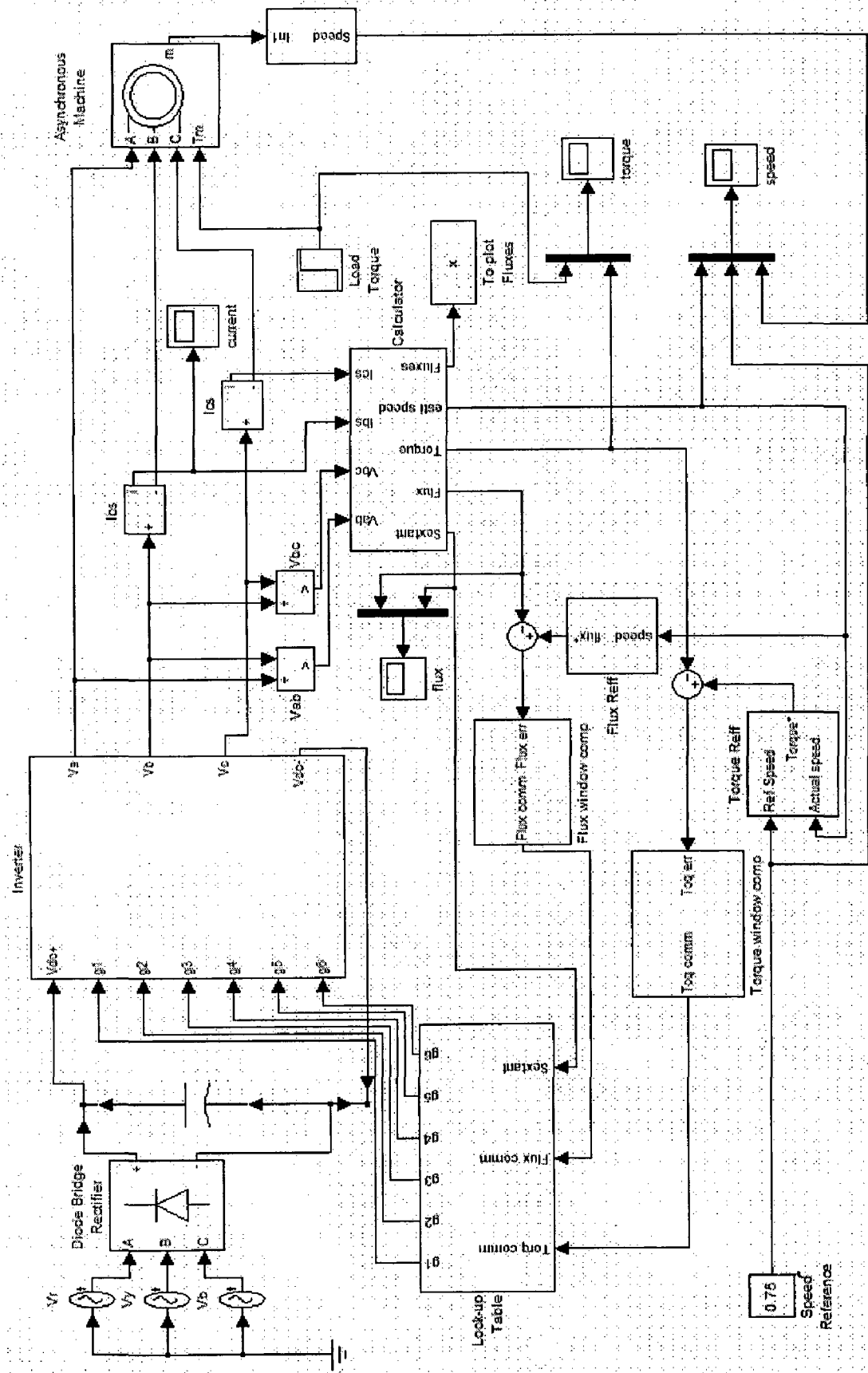
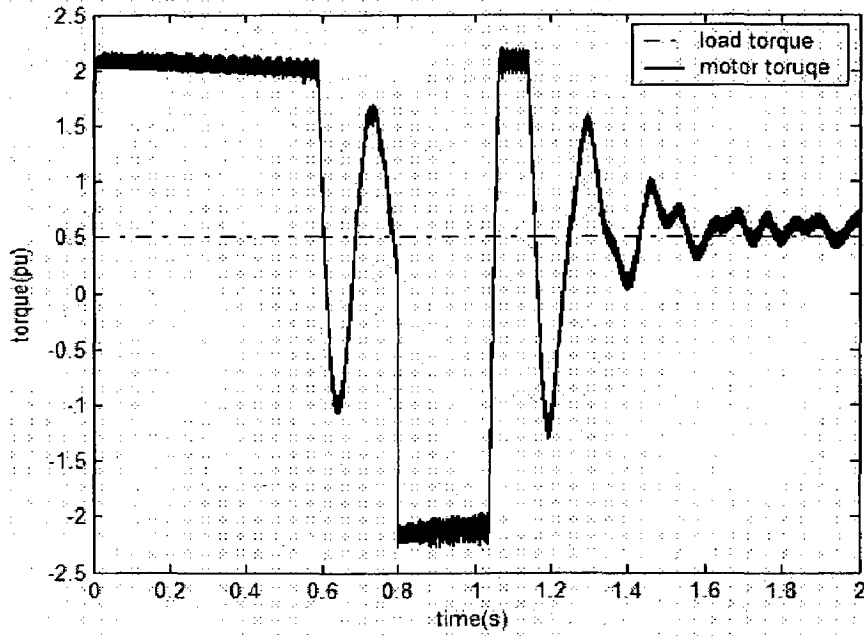
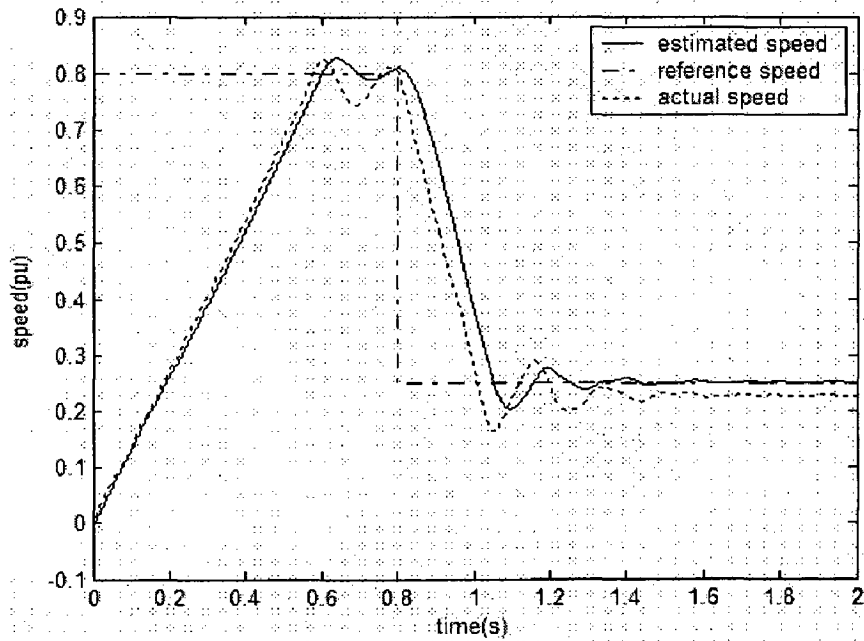


Fig 4.3: Block diagram model of sensorless direct torque control used for simulation in MATLAB SIMULINK



**Fig 4.4(a):** Torque response for step change in speed for sensorless direct torque controlled induction motor



**Fig 4.4(b):** Speed response for step change in speed for sensorless direct torque controlled induction motor



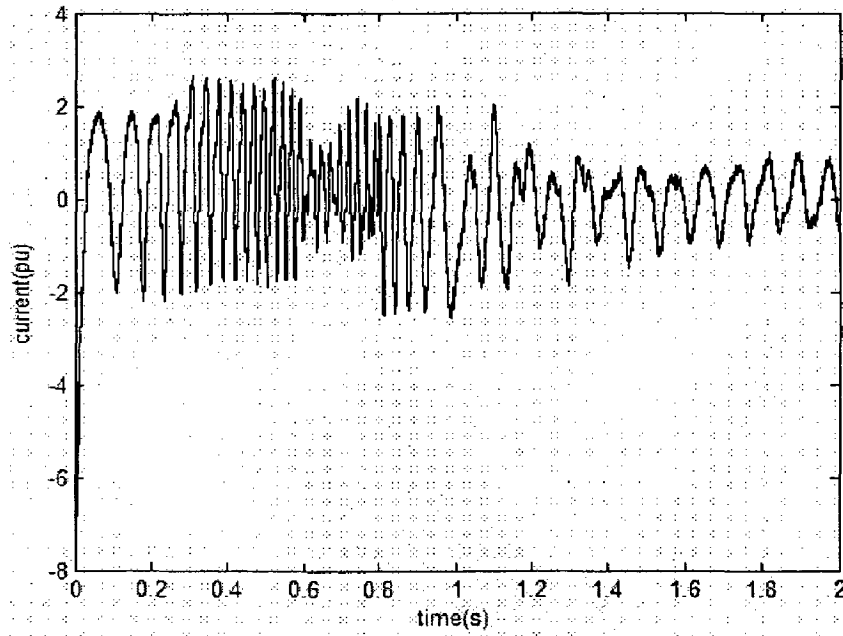


**Fig 4.4(c):** Phase current ( $I_{bs}$ ) response for step change in speed for sensorless direct torque controlled induction motor

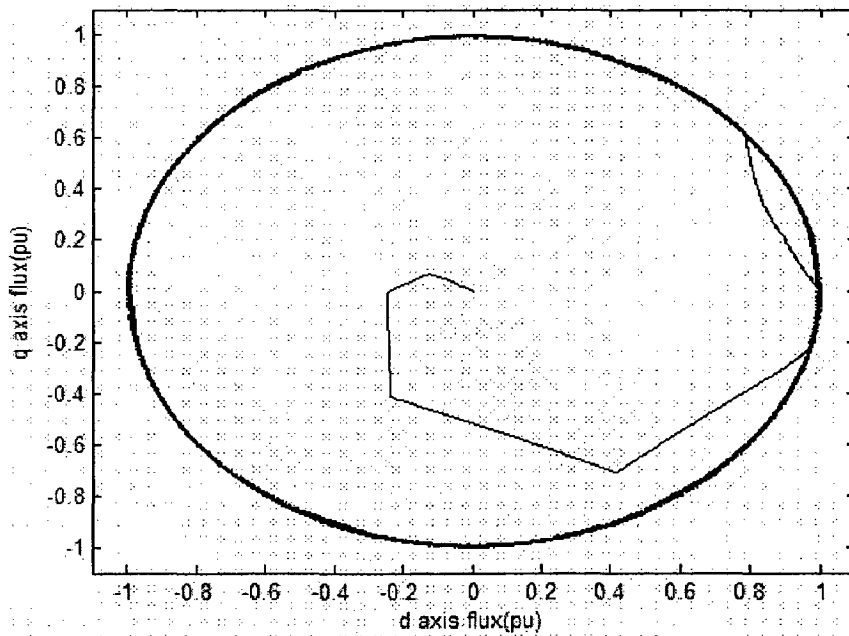


**Fig 4.4(d):** Stator d-q axis flux locus for step change in speed for sensorless direct torque controlled induction motor

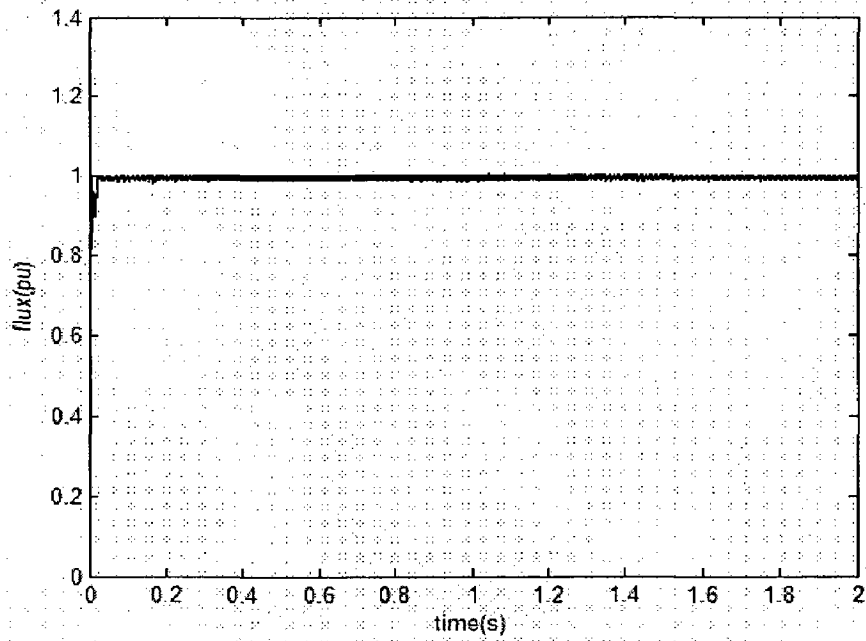


**Fig 4.4(e):** Stator flux magnitude for step change in speed for sensorless direct torque controlled induction motor

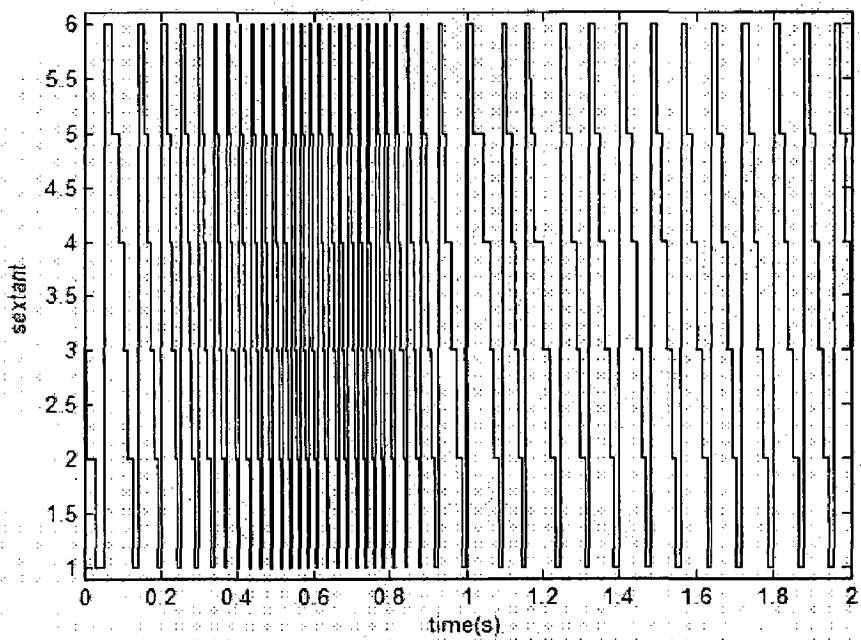


**Fig 4.4(f):** Sextant plot for step change in speed for sensorless direct torque controlled induction motor

#### 4.4.2 Step change in load torque:

In this case load torque is changed from 0.25pu to 0.8pu at 0.8 sec with speed reference at 0.75pu. Results are shown in fig 4.5.

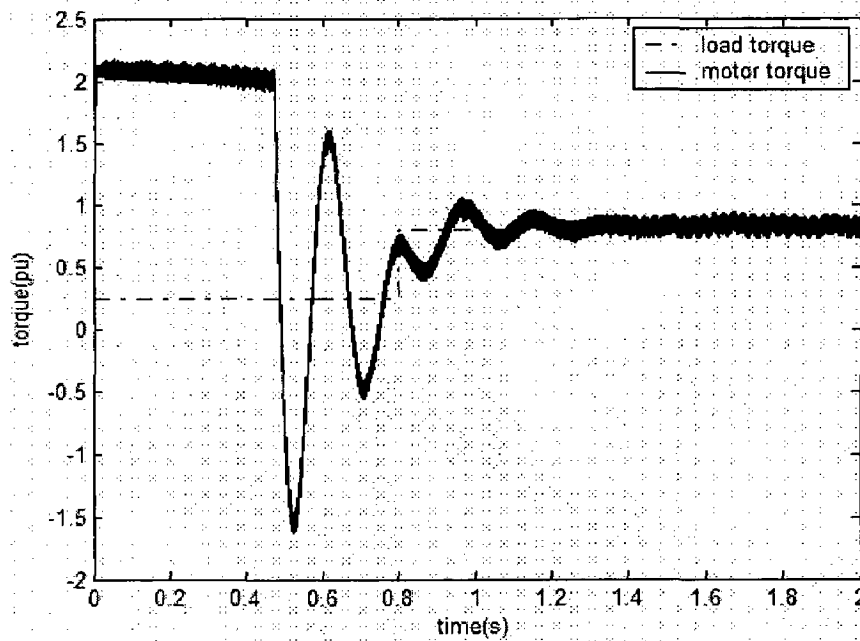


**Fig 4.5(a):** Torque response for step change in load torque for sensorless direct torque controlled induction motor

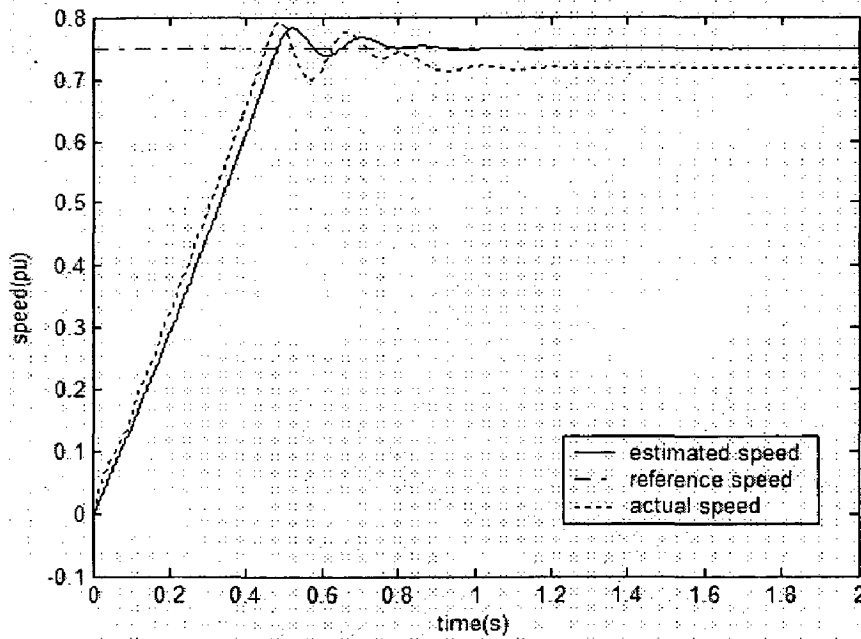


**Fig 4.5(b):** Speed response for step change in load torque for sensorless direct torque controlled induction motor

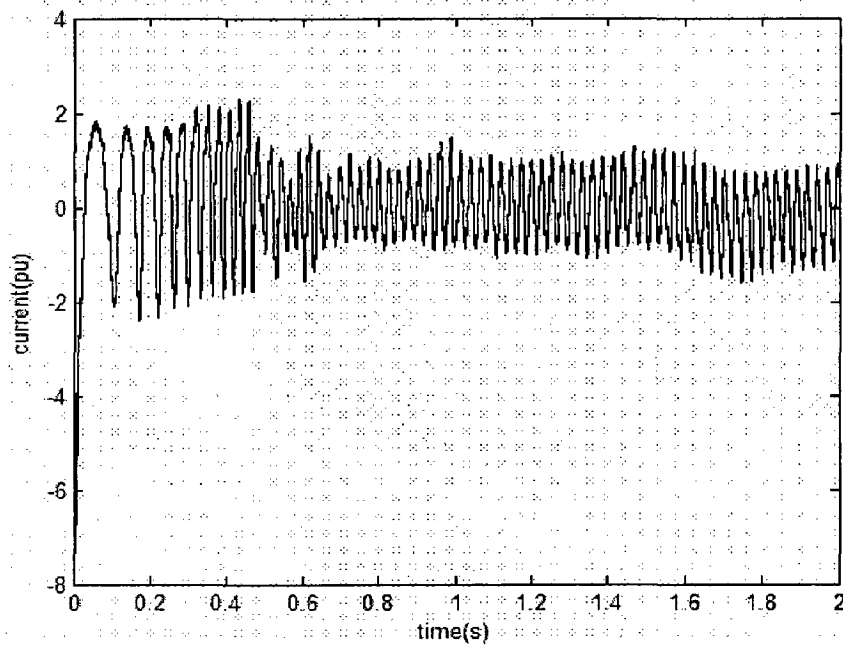


**Fig 4.5(c):** Phase current ( $I_{bs}$ ) response for step change in load torque for sensorless direct torque controlled induction motor

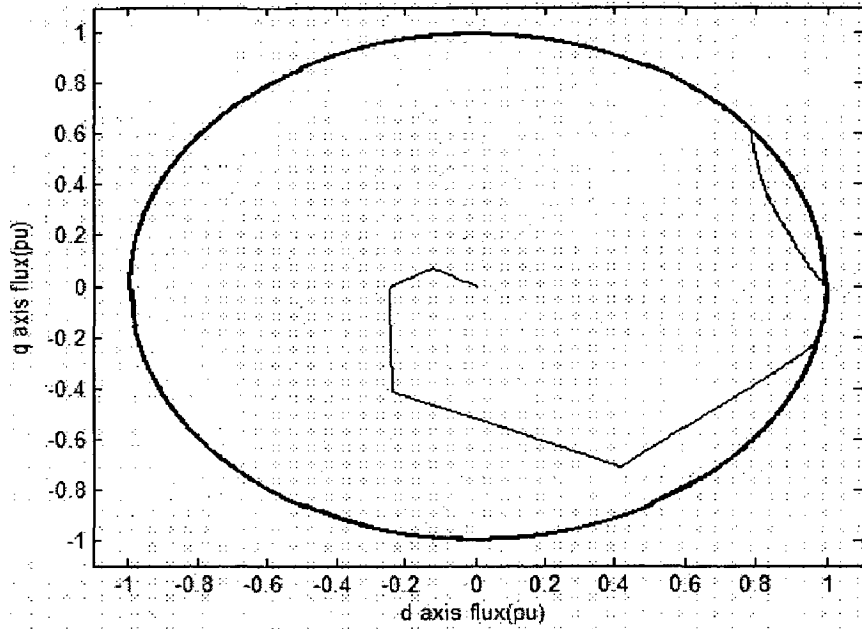


**Fig 4.5(d):** Stator d-q axis flux locus for step change in load torque for sensorless direct torque controlled induction motor

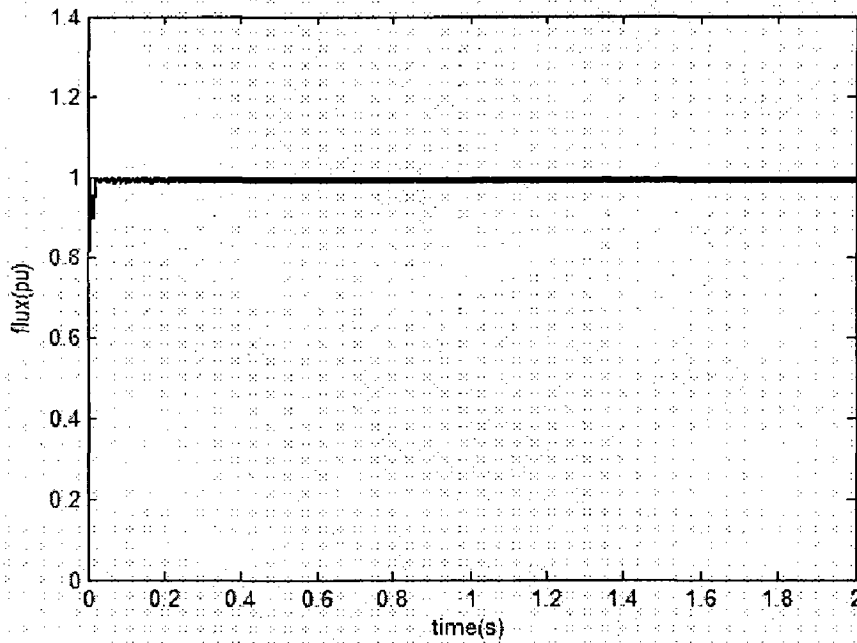


**Fig 4.5(e):** Stator flux magnitude for step change in load torque for sensorless direct torque controlled induction motor

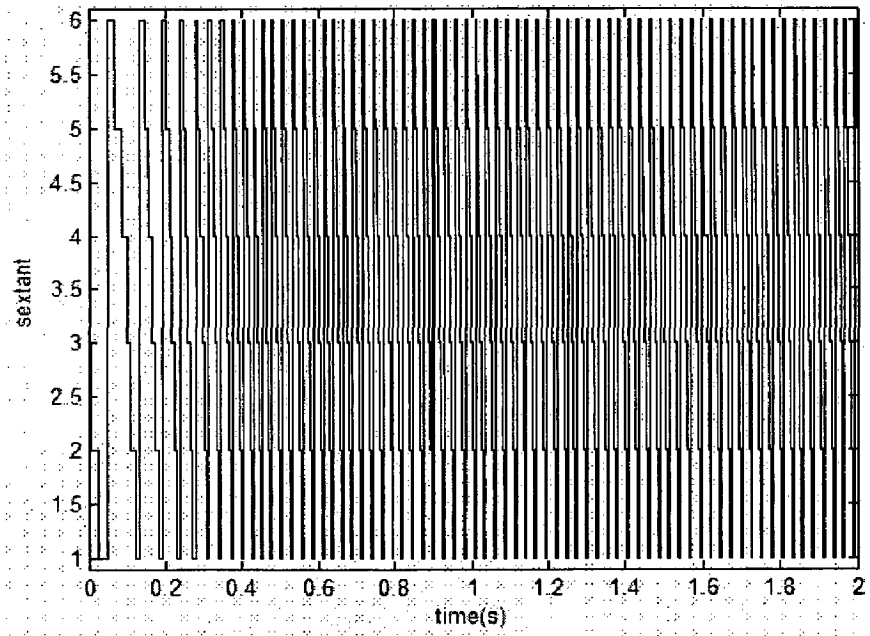


**Fig 4.5(f):** Sextant plot for step change in load torque for sensorless direct torque controlled induction motor

# **Improved Implementation Strategies for Direct Torque Control of Induction Motor**

---

### **5.1 Introduction:**

Direct torque control was introduced to give a fast and good dynamic torque response and can be considered as an alternative to the field oriented control technique [9, 14]. The direct torque control scheme is very simple; in its basic configuration it consists of direct torque controller, torque and flux calculator, and voltage source inverter. The configuration is much simpler than the FOC system due to the absence of frame transformer. It also does not need pulse width modulator and position encoder, which introduce delays and requires mechanical transducers respectively.

Drawback in direct torque control is that it produces flux and torque ripples, this is due to limited voltage vectors available from the voltage source inverter and their switching pattern. Two strategies to improve performance of direct torque control are discussed and are implemented in MATLAB SIMULINK software package.

### **5.2 Hybrid direct torque control:**

In this control strategy both PI control and fuzzy control are employed to generate torque reference from speed error, fuzzy controller in transient state and PI controller in steady state [12].

Fuzzy systems are being more widely used for control applications because of their efficient control and the mathematical modeling of the plant to be controlled is not required [4]. Instead it embeds the experience and the intuition of a human operator, and sometimes those of a designer and/or researcher of a plant. Fuzzy control is basically an adaptive and nonlinear control, which gives robust performance for a linear and nonlinear plant with parameter variation.

A fuzzy controller consists of the following five steps:

Step 1: Fuzzification of input variables.

Step 2: Application of fuzzy operator i.e. fuzzy rule base in IF-THEN format.

Step 3: Implication from rule base.

Step 4: Aggregation of all the fired rules.

Step 5: Defuzzification, conversion to a crisp value which is the control input to the plant.

Block diagram for implementing fuzzy control is shown in fig 5.1. Implementation of fuzzy control is mathematical and is time consuming. Performance and complexity increases with increase in membership functions.

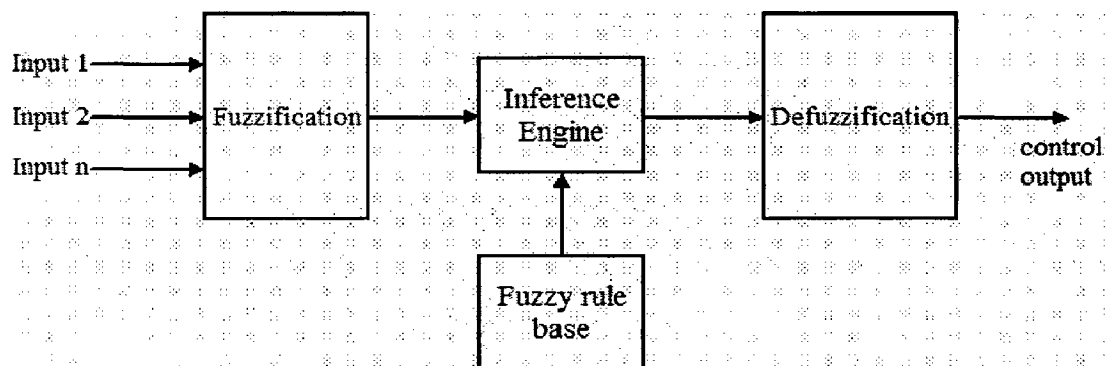


**Fig 5.1:** Block diagram of fuzzy controller

In the present control strategy fuzzy control is used for transient state to give better transient performance and PI controller in steady state to reduce mathematical computations. In this case PI controller was tuned to give good steady state response. Switching between the two controllers is done with help of a switch which uses speed error as control input. Speed error of 15rpm (1% of base speed) is chosen as switching point between the two controllers. If speed error is greater than 15rpm then fuzzy controller is used, else PI controller is chosen to generate reference torque. Block diagram of hybrid controller is shown in fig 5.2.



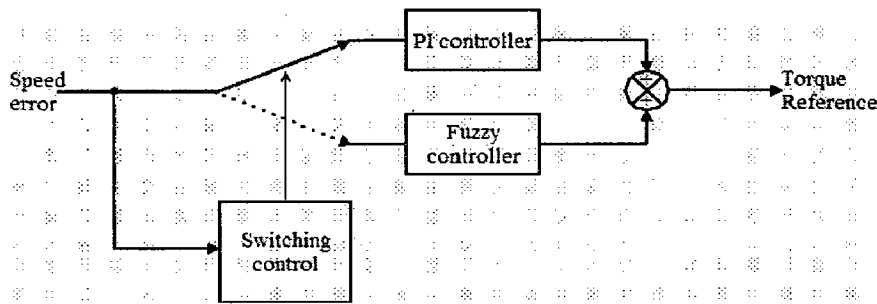


**Fig 5.2: Block diagram of hybrid controller**

Implementation of hybrid direct torque control of induction motor is similar to that of normal direct torque control except for torque reference generation. In this method both fuzzy and PI controllers are used for torque reference generation.

### **5.3 Split look-up table direct torque control:**

In normal direct torque control scheme motor is divided into six sectors called sextants, each  $60^\circ$ . These sextants range extends  $30^\circ$  to either direction of voltage vector corresponding to each sextant, i.e. sextant<1> extends  $30^\circ$  to either direction of voltage vector I.

From the look-up table for normal direct torque control given in chapter III (Table 3.5 on page 32) it can be noted that when stator flux vector is in sextant<1> and when increment in both flux and torque is required voltage vector  $V_{VI}$  is switched. When stator flux just enters into sextant<1> and voltage vector  $V_{VI}$  is applied, voltage vector is approximately  $90^\circ$  to stator flux vector which causes high increase in torque and no change to the flux. As hysteresis controller is employed to produce flux and torque commands, output from the controllers doesn't depend on magnitude of error. Thus, if only small increment in torque is required when stator flux just enters sextant<1>, application of voltage vector  $V_{VI}$  causes high increment in torque and dip in flux. This causes ripples in flux and torque. Same will be the case when stator flux is about to leave sextant <1>, and decrement in torque and increment in flux is required. In this case, application of voltage vector  $V_{II}$ , causes high decrement in torque and dip in flux. These two cases can be illustrated as in fig 5.3. This phenomenon can be explained when stator flux is in other sextants.

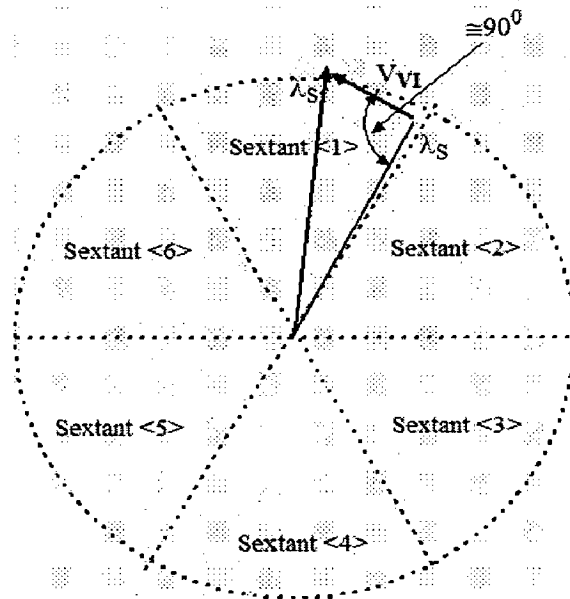


**Fig 5.3(a):** Stator flux vector just entered sextant<1> and increment in torque and flux is required.

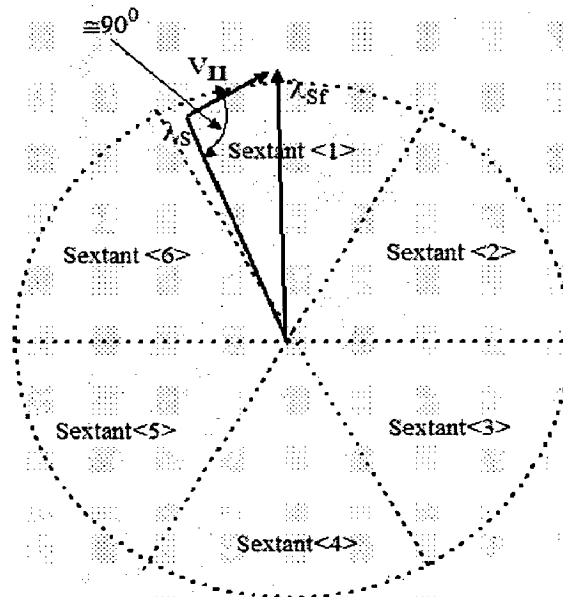


**Fig 5.3(b):** Stator flux vector is about to leave sextant<1> and decrement in torque and increment in flux is required.

Above two cases can be taken into account and ripple in flux and torque can be reduced by splitting the sextants into three segments which extends from  $0^0$  to  $\theta_1^0$ ,  $\theta_1^0$  to  $\theta_2^0$  and  $\theta_2^0$  to  $60^0$  of every sextant as show in fig 5.4. For the segment from  $\theta_1^0$  to  $\theta_2^0$  look-up table will be same as that of normal direct torque control. For the segment from  $0^0$  to  $\theta_1^0$  look-up table is modified for increment in torque case i.e. is  $S_T=1$ . For the

segment from  $\theta_2^0$  to  $60^0$ , look-up table is modified for decrement in torque case. Look-up table remains same as that of normal direct torque control for other case in segments  $0^0$  to  $\theta_1^0$  and  $\theta_2^0$  to  $60^0$ .

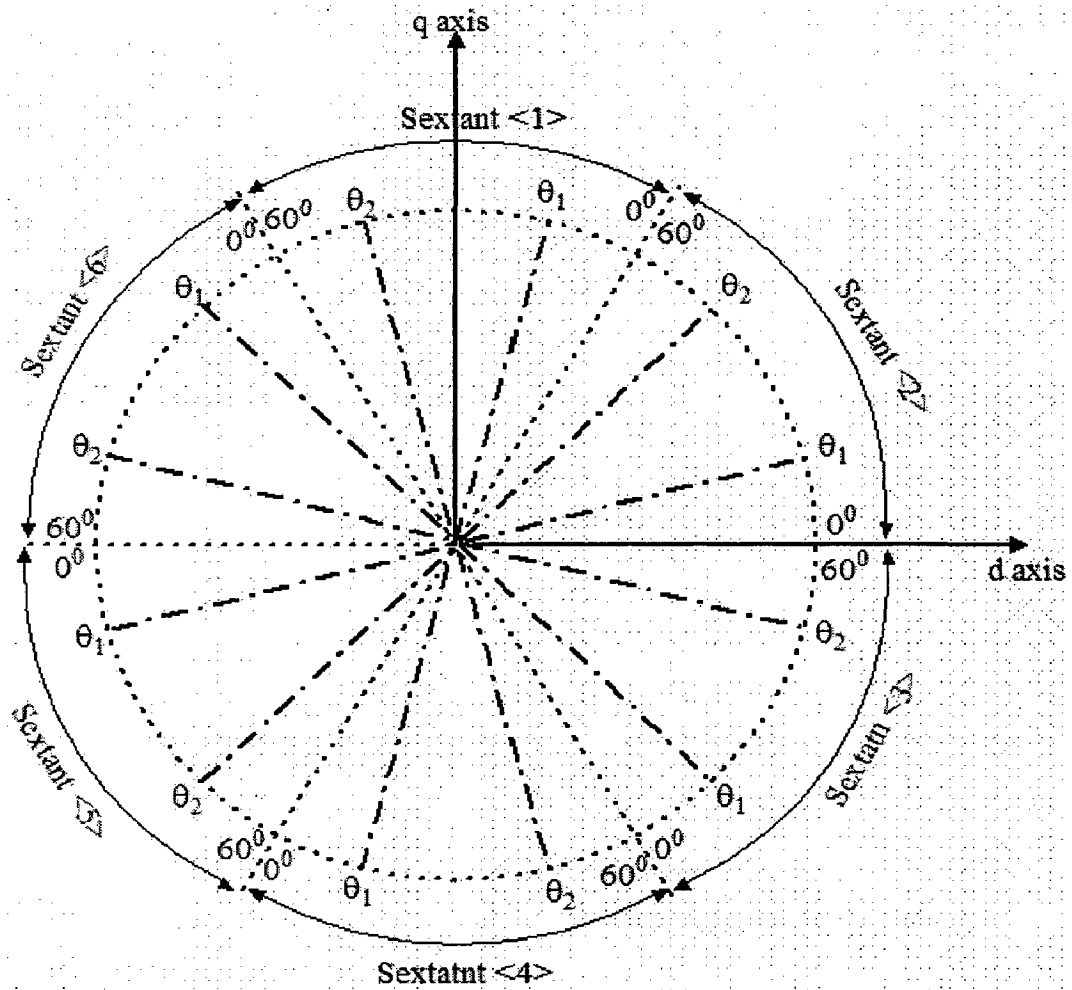


Fig 5.4: Segmentation of sextants

Modified look-up tables are given in table 5.1 Implementation of split look-up table is similar to that of normal direct torque control except for segment index calculation. Segment index decides which one of three look-up tables is to be selected. Block diagram for implementation is given in fig 5.5.

| Sextant     |       |      |      |      |      |      |      |
|-------------|-------|------|------|------|------|------|------|
| $S_\lambda$ | $S_T$ | <1>  | <2>  | <3>  | <4>  | <5>  | <6>  |
| 1           | +1    | I    | II   | III  | IV   | V    | VI   |
| 1           | 0     | VIII | VII  | VIII | VII  | VIII | VII  |
| 1           | -1    | II   | III  | IV   | V    | VI   | I    |
| 0           | +1    | VI   | I    | II   | III  | IV   | V    |
| 0           | 0     | VII  | VIII | VII  | VIII | VII  | VIII |
| 0           | -1    | III  | IV   | V    | VI   | I    | II   |

**Table 5.1(a):** Switching states for possible  $S_\lambda$ ,  $S_T$ , and  $S_\theta$  in segment 1

| Sextant     |       |      |      |      |      |      |      |
|-------------|-------|------|------|------|------|------|------|
| $S_\lambda$ | $S_T$ | <1>  | <2>  | <3>  | <4>  | <5>  | <6>  |
| 1           | +1    | VI   | I    | II   | III  | IV   | V    |
| 1           | 0     | VIII | VII  | VIII | VII  | VIII | VII  |
| 1           | -1    | II   | III  | IV   | V    | VI   | I    |
| 0           | +1    | V    | VI   | I    | II   | III  | IV   |
| 0           | 0     | VII  | VIII | VII  | VIII | VII  | VIII |
| 0           | -1    | III  | IV   | V    | VI   | I    | II   |

**Table 5.1(b):** Switching states for possible  $S_\lambda$ ,  $S_T$ , and  $S_\theta$  in segment 2

| Sextant     |       |      |      |      |      |      |      |
|-------------|-------|------|------|------|------|------|------|
| $S_\lambda$ | $S_T$ | <1>  | <2>  | <3>  | <4>  | <5>  | <6>  |
| 1           | +1    | VI   | I    | II   | III  | IV   | V    |
| 1           | 0     | VIII | VII  | VIII | VII  | VIII | VII  |
| 1           | -1    | I    | II   | III  | IV   | V    | VI   |
| 0           | +1    | V    | VI   | I    | II   | III  | IV   |
| 0           | 0     | VII  | VIII | VII  | VIII | VII  | VIII |
| 0           | -1    | II   | III  | IV   | V    | VI   | I    |

Table 5.1(c): Switching states for possible  $S_\lambda$ ,  $S_T$ , and  $S_\theta$  in segment 3

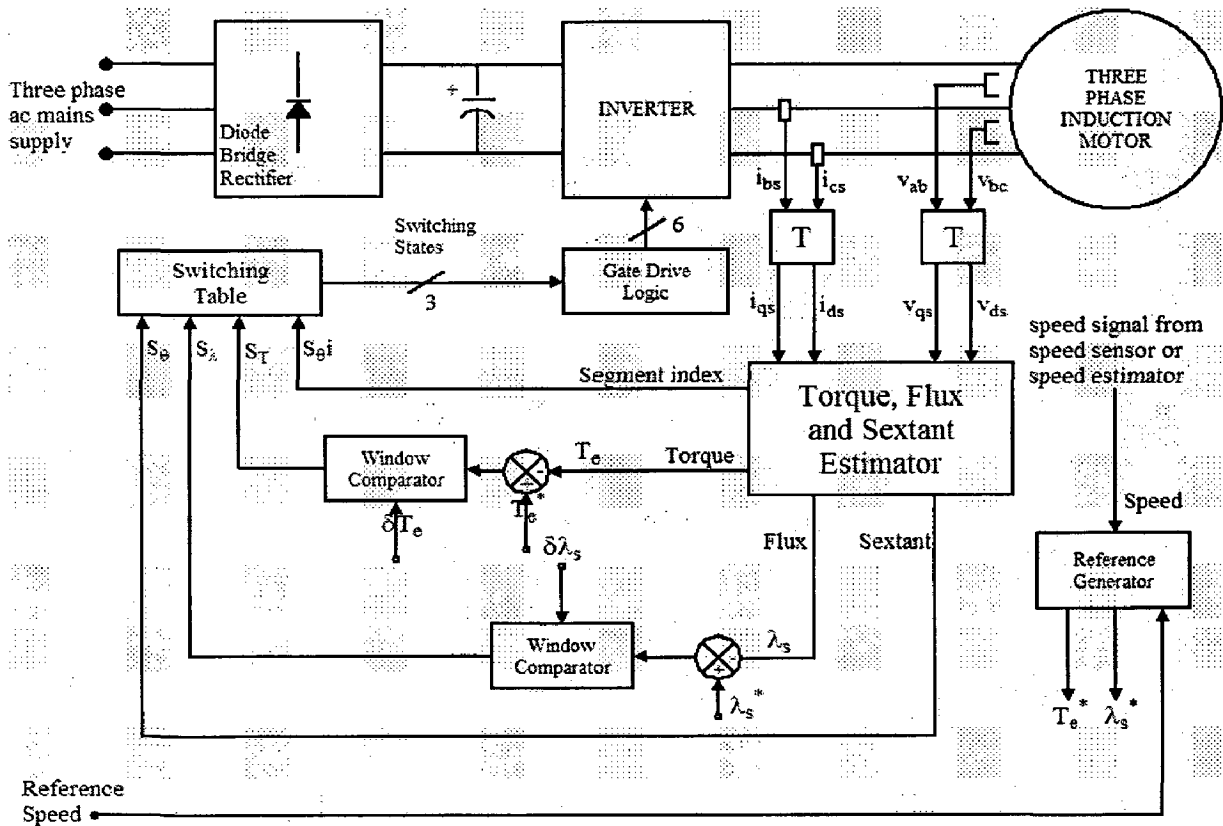


Fig 5.5: Block-diagram schematic of the split look-up table direct torque induction motor drive

## 5.4 Results:

Both the strategies proposed are simulated with and without speed sensors.

### 5.4.1 Hybrid direct torque control:

Simulated block diagram for hybrid direct torque control with speed sensor is shown in fig 5.6 and without speed sensor in fig 5.7.

#### 5.4.1.1 Step change in speed reference:

In this case speed reference is changed from 0.8pu to 0.25pu at 0.8 sec with load torque at 0.5pu. Results are show in fig 5.8 with speed sensor and in fig 5.9 for sensorless.

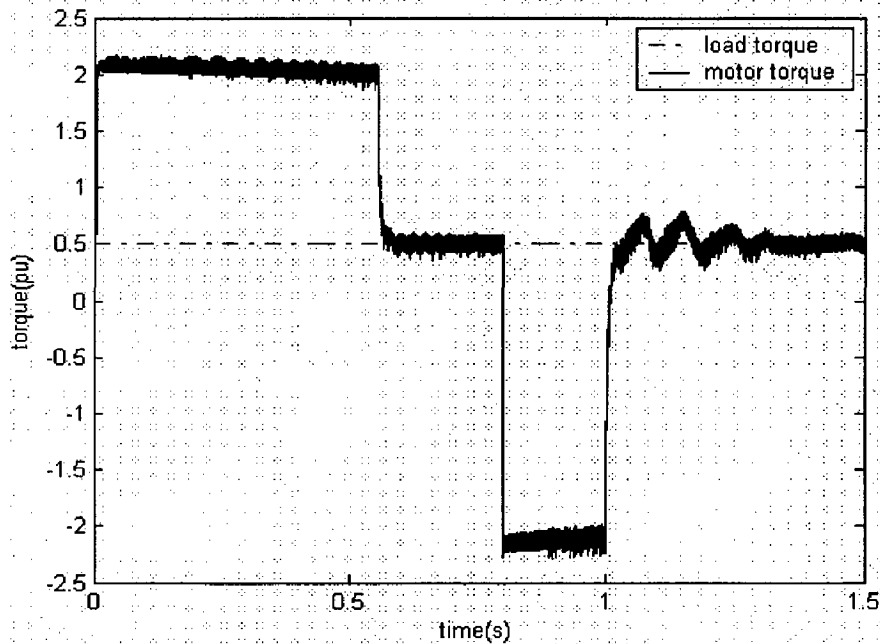


**Fig 5.8(a):** Torque response plot for step change in speed for hybrid direct torque controlled induction motor

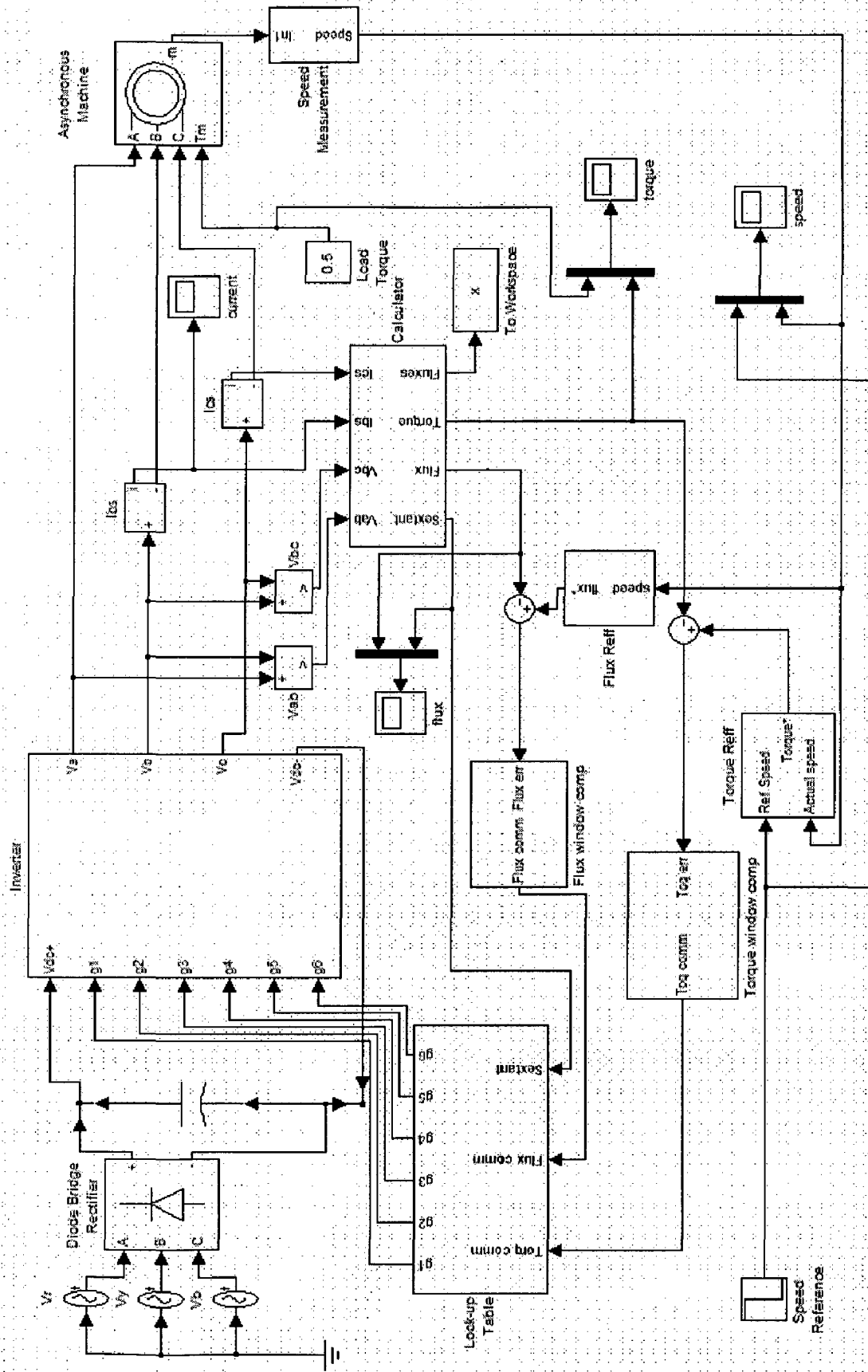


Fig 5.6: Block diagram model of hybrid direct torque control used for simulation in MATLAB SIMULINK

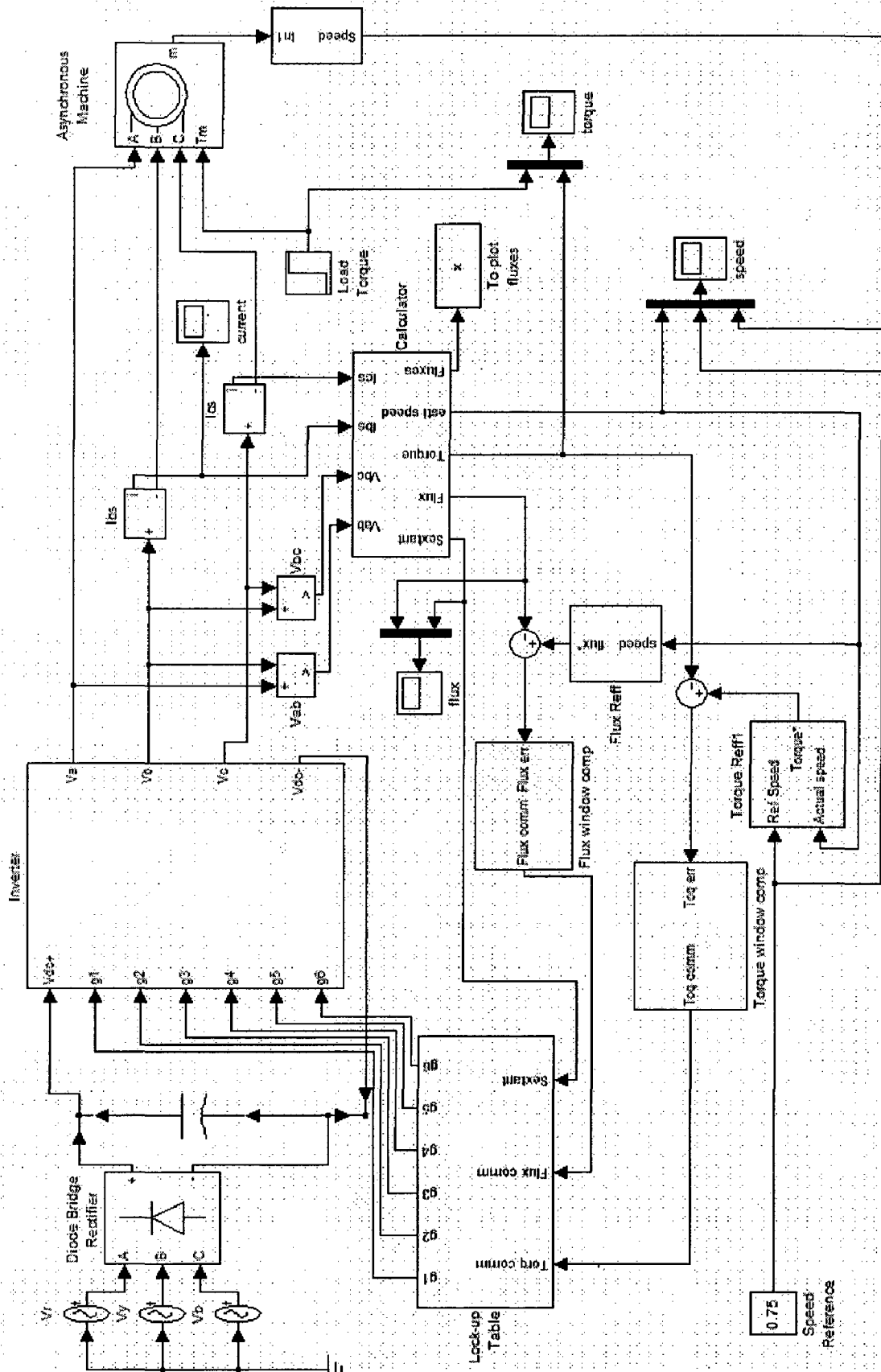
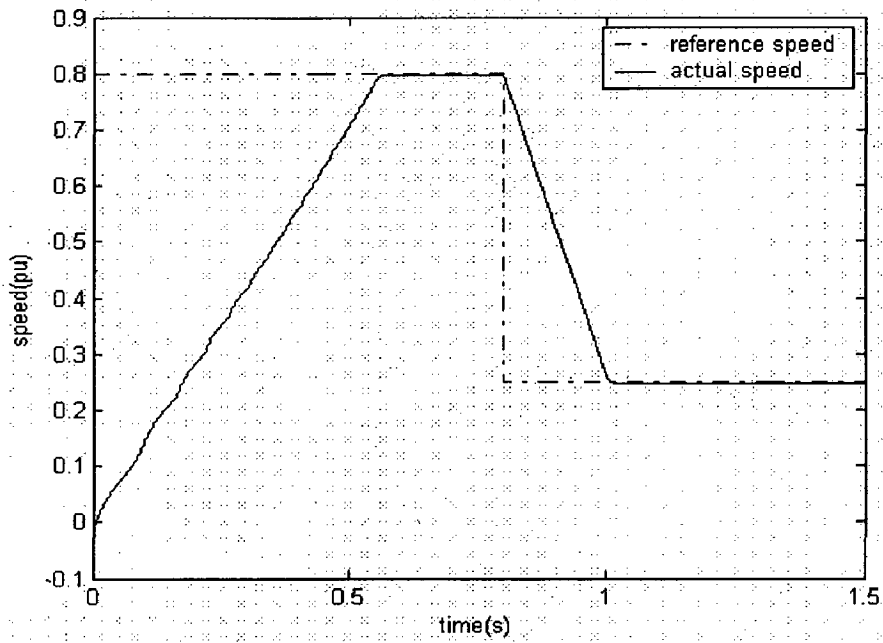
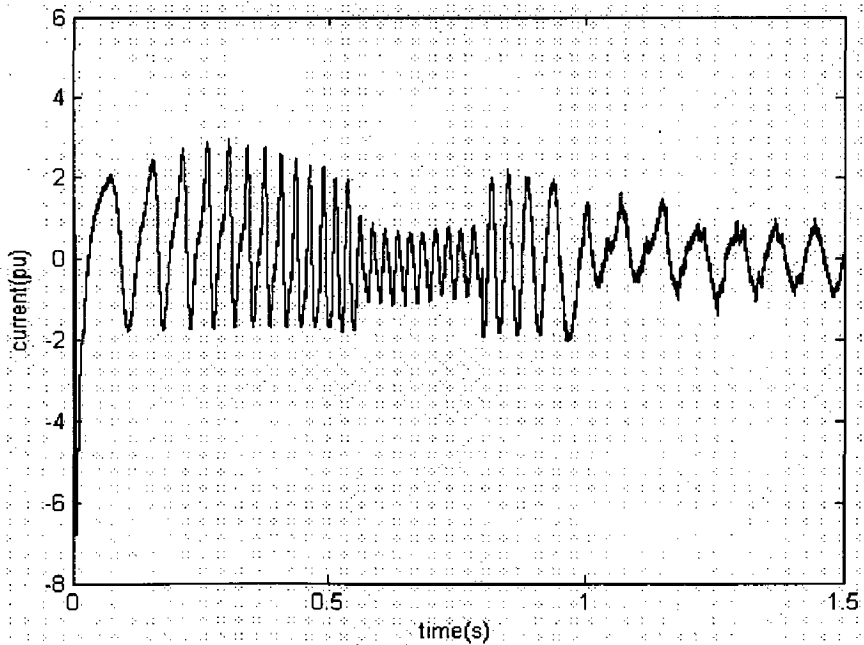


Fig 5.7: Block diagram model of sensorless hybrid direct torque control used for simulation in MATLAB SIMULINK





**Fig 5.8(b):** Speed response plot for step change in speed for hybrid direct torque controlled induction motor



**Fig 5.8(c):** Phase current ( $I_{bs}$ ) response plot for step change in speed for hybrid direct torque controlled induction motor

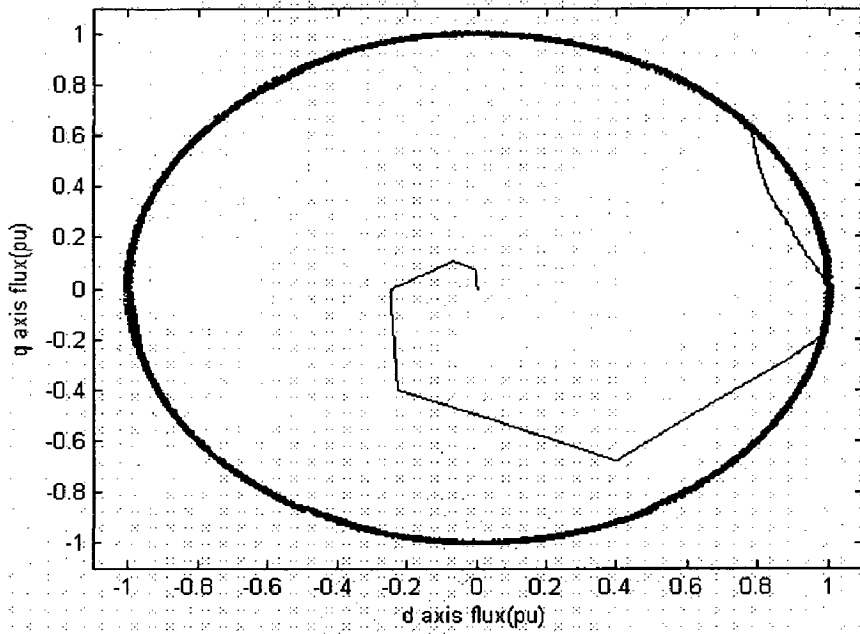


**Fig 5.8(d):** Stator d-q axis flux locus plot for step change in speed for hybrid direct torque controlled induction motor

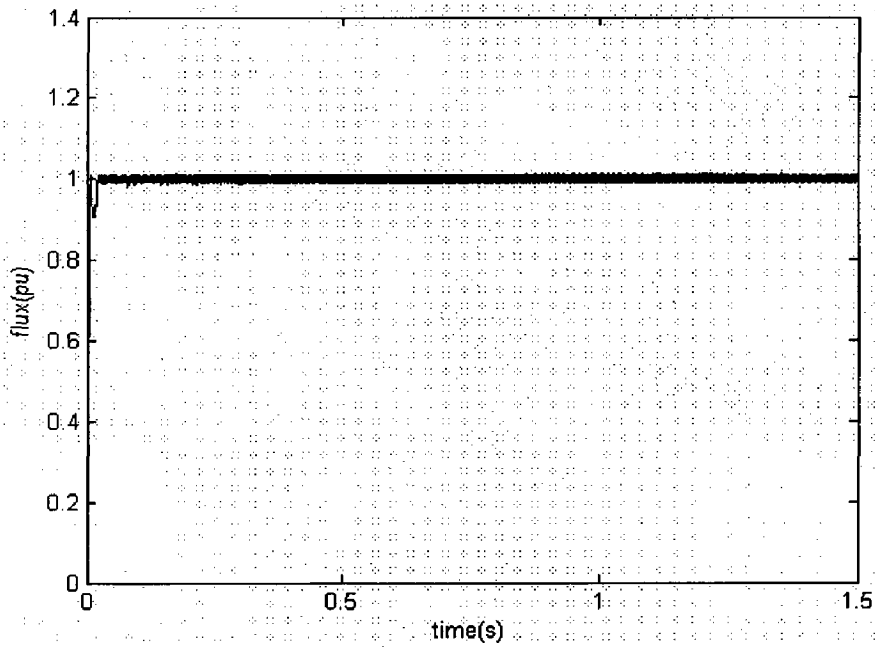


**Fig 5.8(e):** Stator flux magnitude plot for step change in speed for hybrid direct torque controlled induction motor

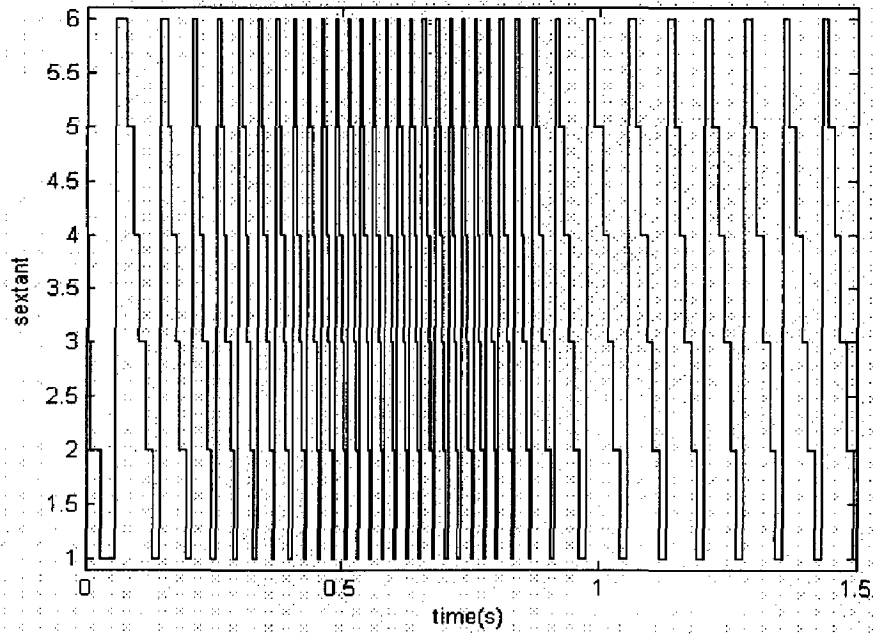


**Fig 5.8(f):** Sextant plot for step change in speed for hybrid direct torque controlled induction motor

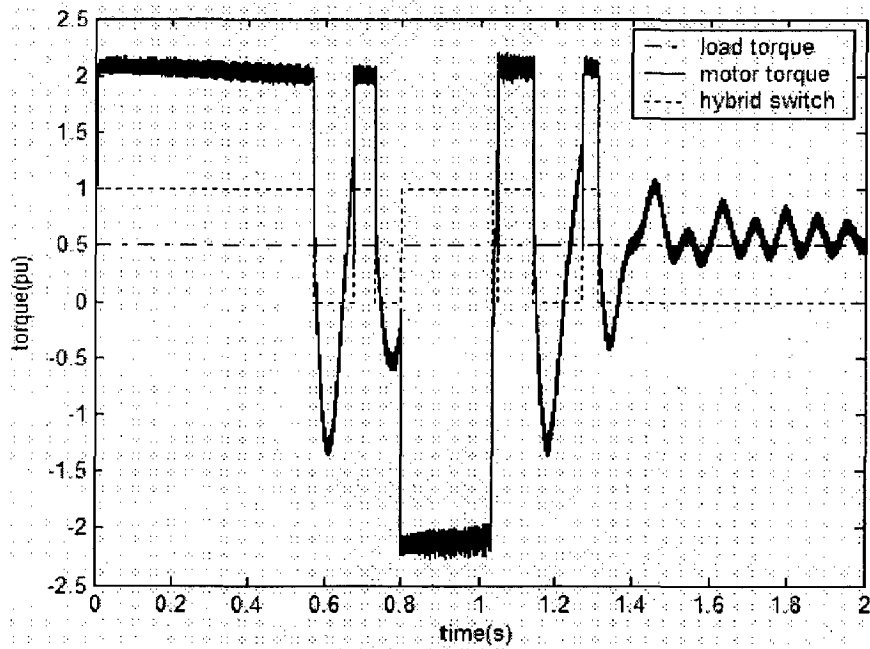


**Fig 5.9(a):** Torque response plot for step change in speed for sensorless hybrid direct torque controlled induction motor

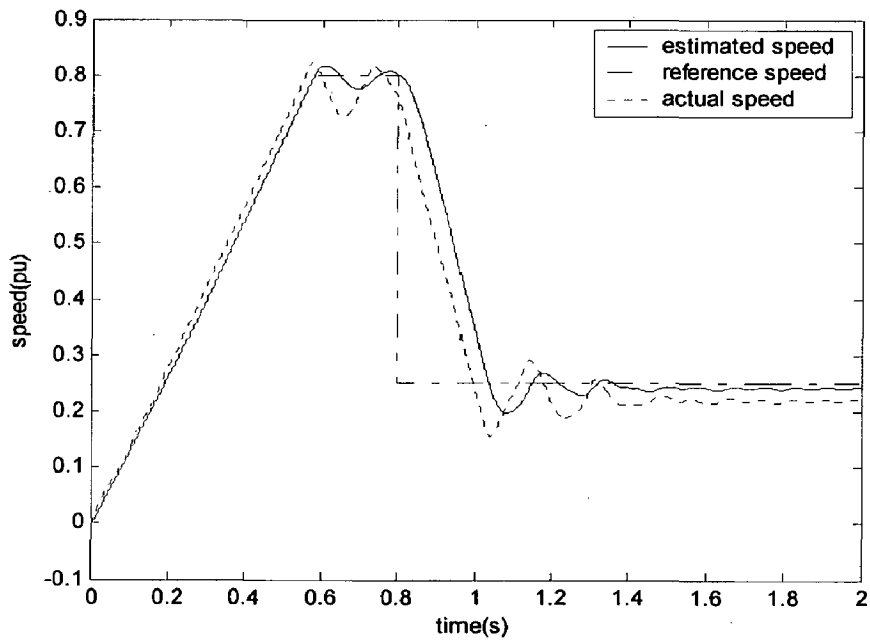


**Fig 5.9(b):** Speed response plot for step change in speed for sensorless hybrid direct torque controlled induction motor

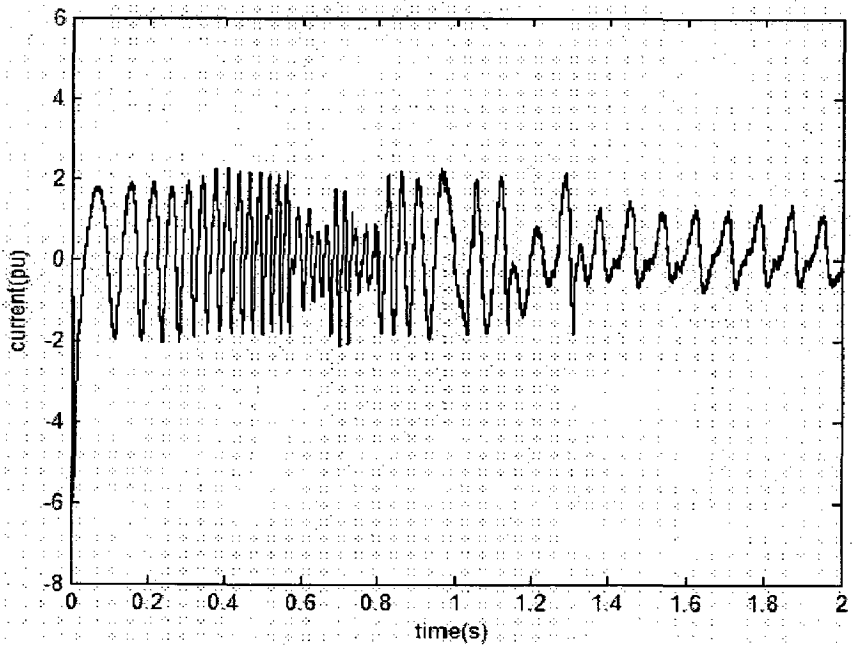


**Fig 5.9(c):** Phase current ( $I_{bs}$ ) response plot for step change in speed for sensorless hybrid direct torque controlled induction motor

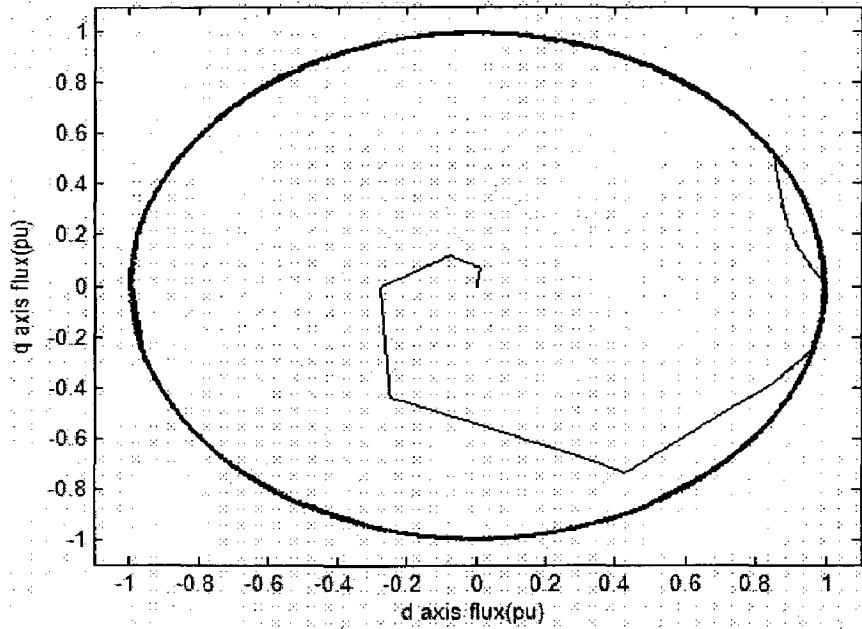


**Fig 5.9(d):** Stator d-q axis flux locus plot for step change in speed for sensorless hybrid direct torque controlled induction motor

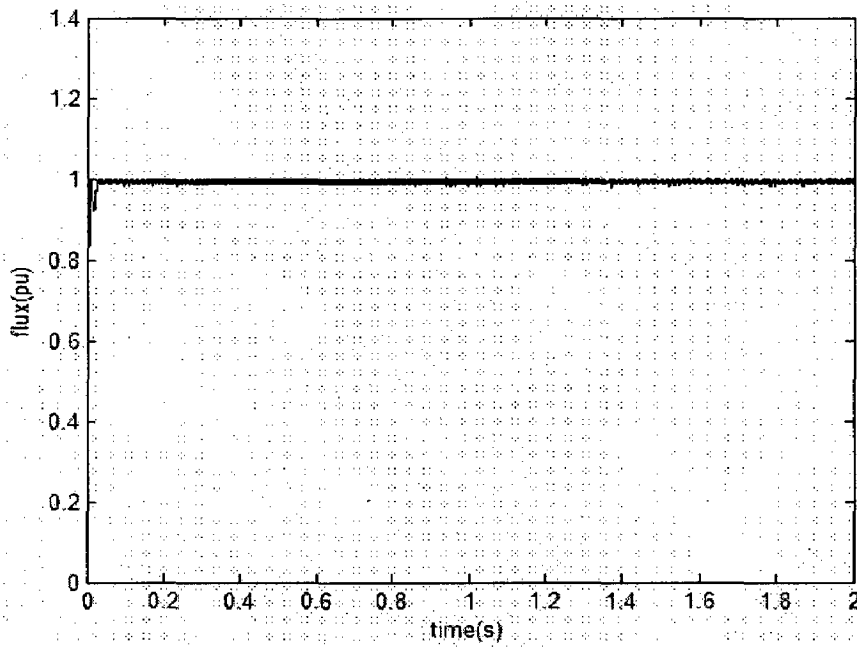


**Fig 5.9(e):** Stator flux magnitude plot for step change in speed for sensorless hybrid direct torque controlled induction motor

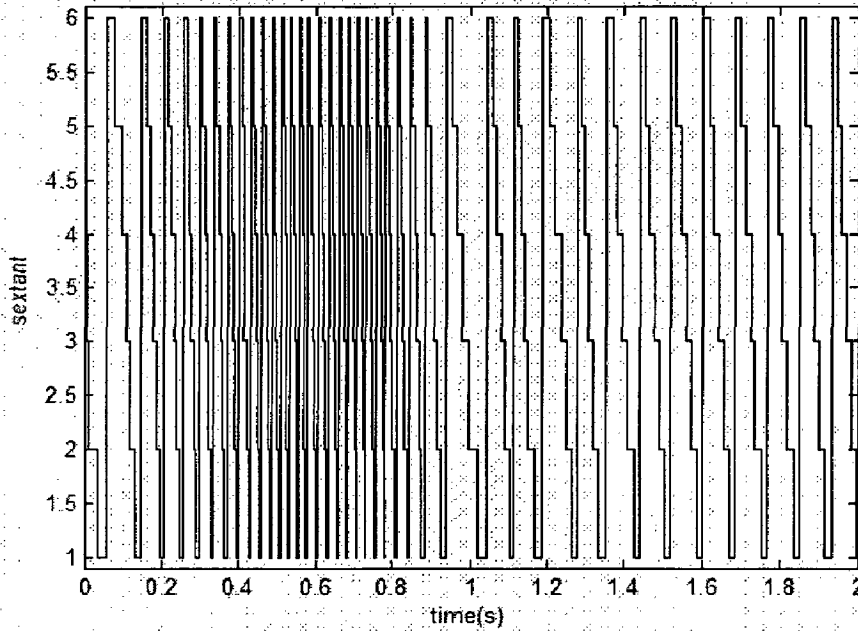


**Fig 5.9(f):** Sextant plot for step change in speed for sensorless hybrid direct torque controlled induction motor

#### 5.4.1.2 Step change in load torque;

In this case load torque is changed from 0.25pu to 0.8pu at 0.8 sec with speed reference speed at 0.75pu. Results are show in fig 5.10 with speed sensor and fig 5.11 without speed sensor.

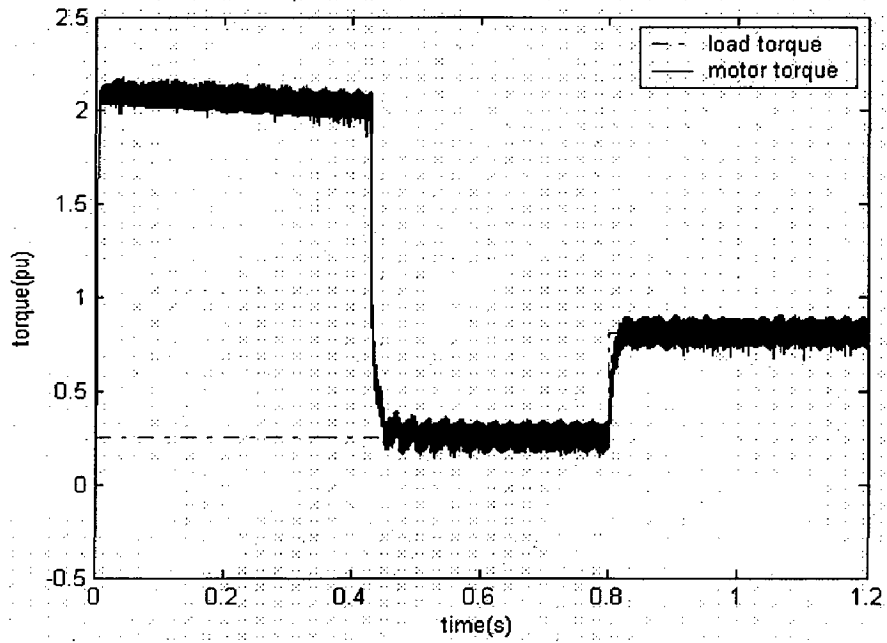


**Fig 5.10(a):** Torque response plot for step change in load torque for hybrid direct torque controlled induction motor

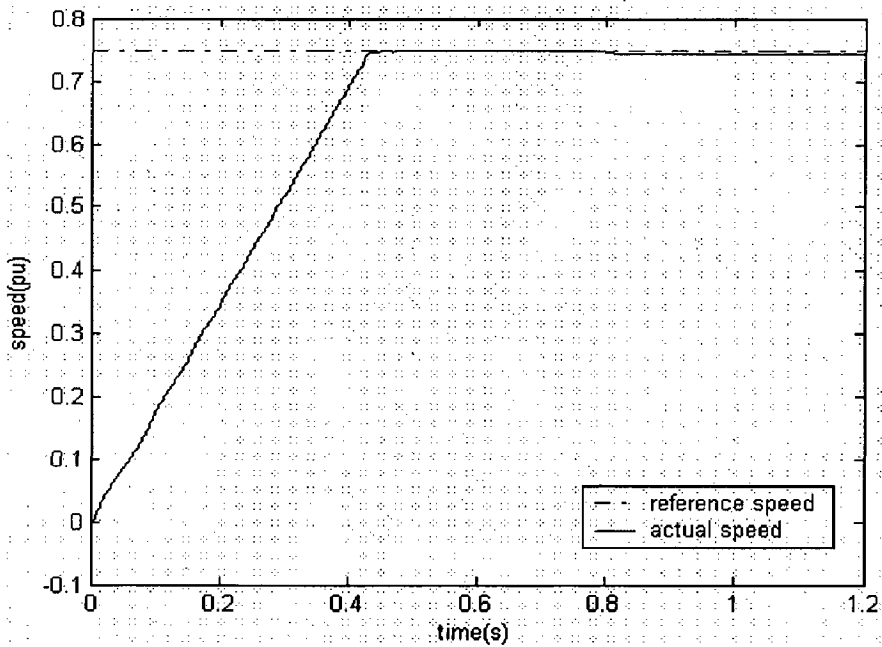


**Fig 5.10(b):** Speed response plot for step change in load torque for hybrid direct torque controlled induction motor

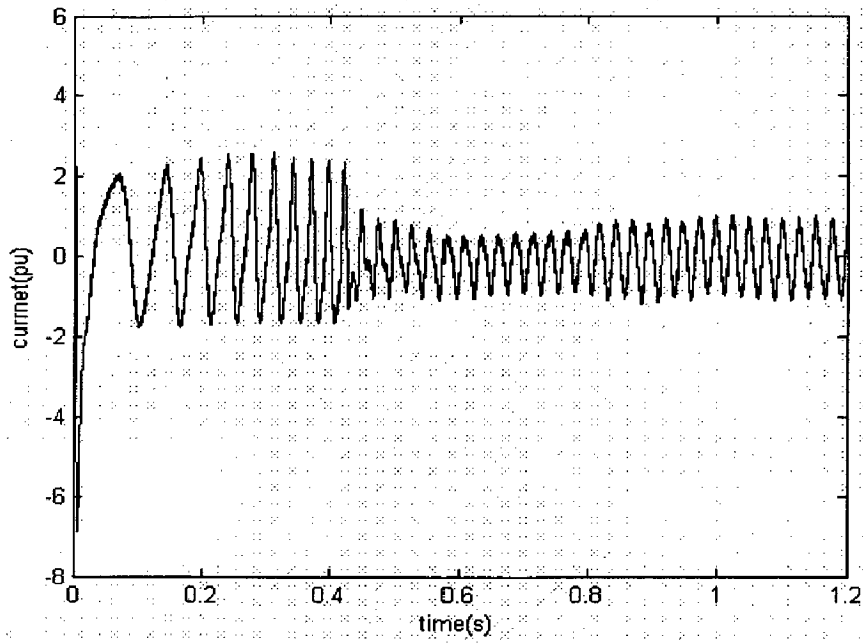


**Fig 5.10(c):** Phase current ( $I_{bs}$ ) response plot for step change in load torque for hybrid direct torque controlled induction motor

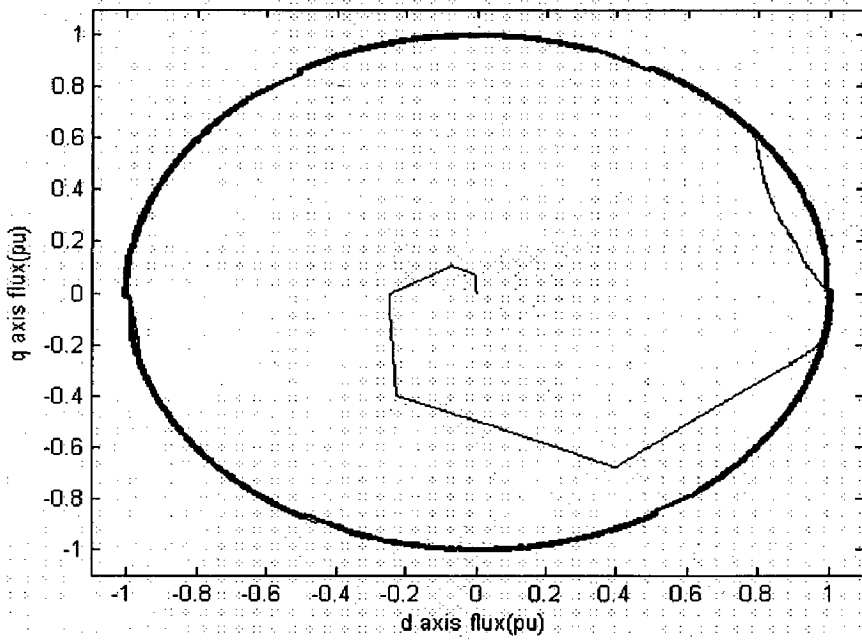


**Fig 5.10(d):** Stator d-q axis flux plot locus plot for step change in load torque for hybrid direct torque controlled induction motor



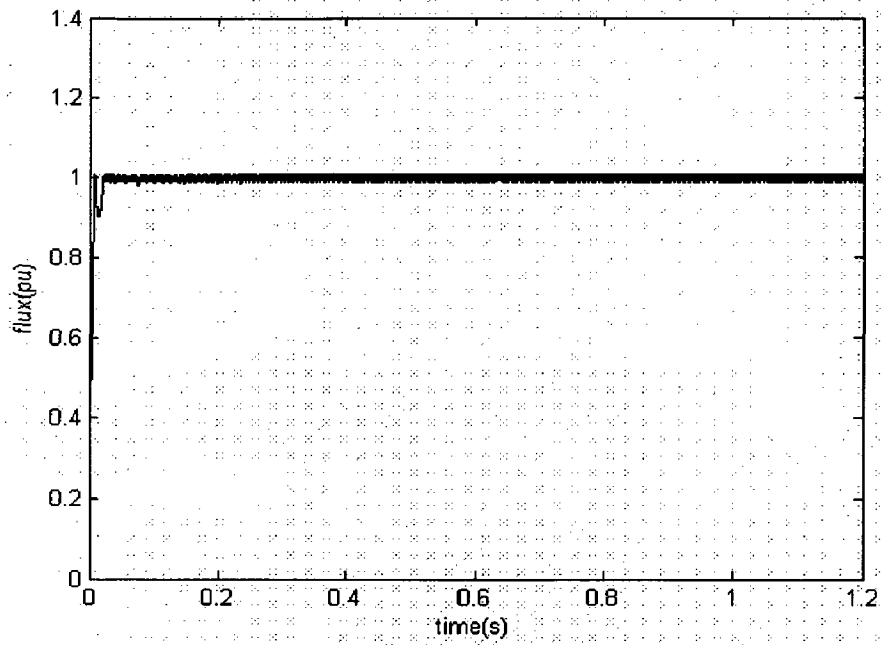


**Fig 5.10(e):** Stator flux magnitude plot for step change in load torque for hybrid direct torque controlled induction motor

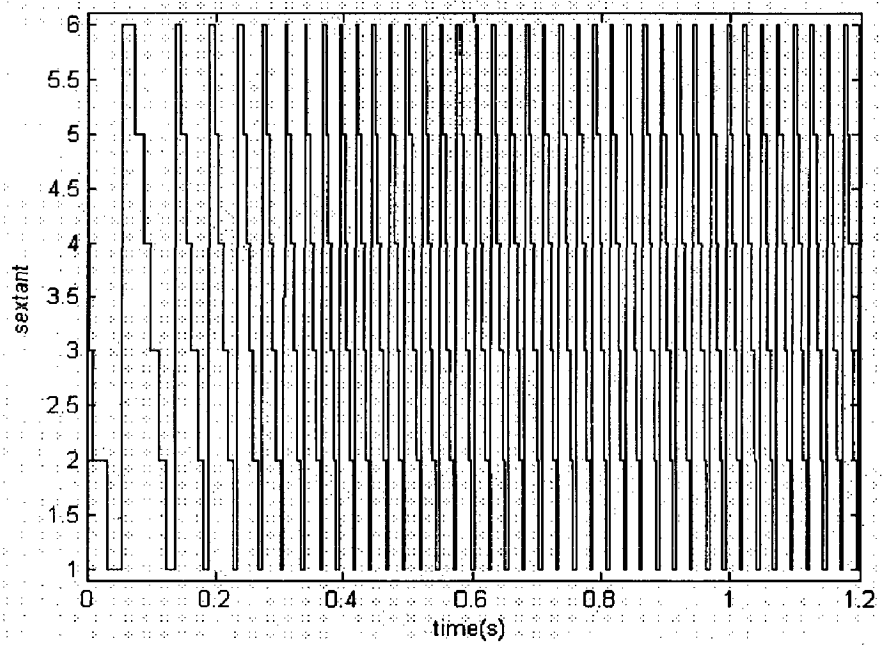


**Fig 5.10(f):** Sextant plot for step change in load torque for hybrid direct torque controlled induction motor

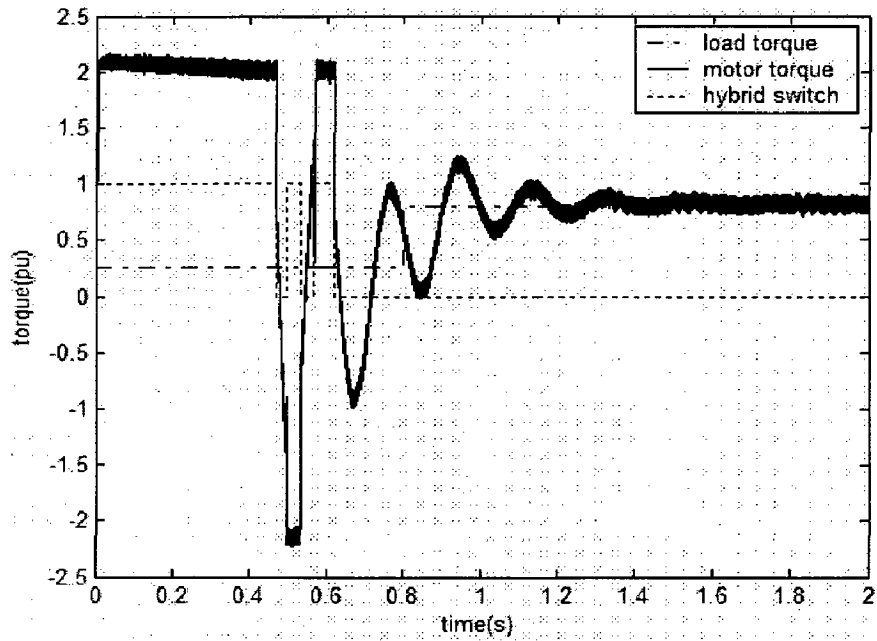


**Fig 5.11(a):** Torque response plot for step change in load torque for sensorless hybrid direct torque controlled induction motor

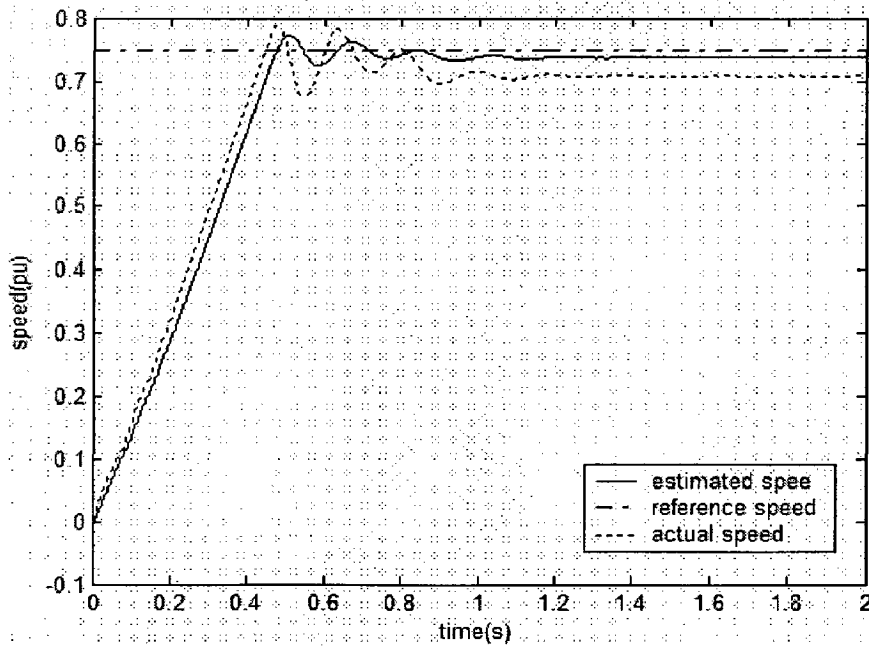


**Fig 5.11(b):** Speed response plot for step change in load torque for sensorless hybrid direct torque controlled induction motor

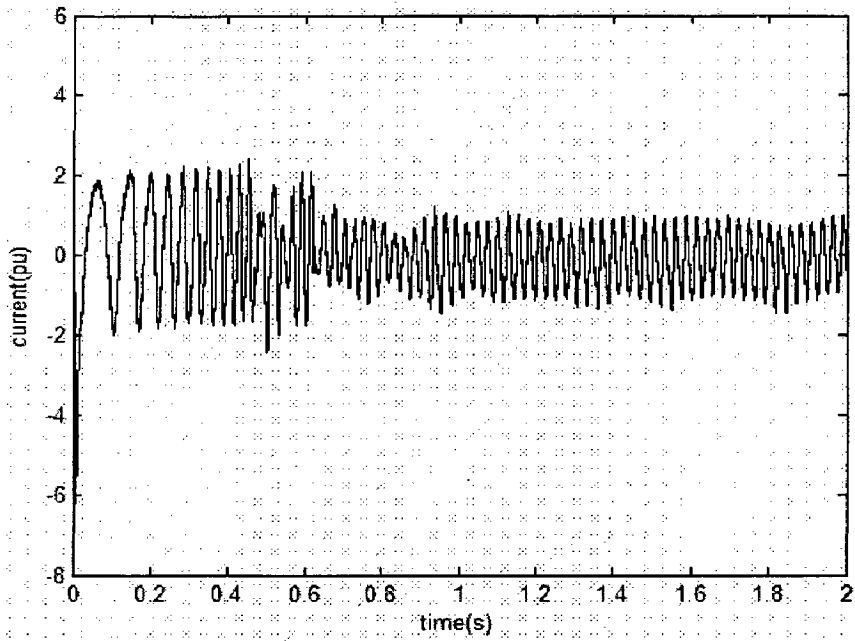


**Fig 5.11(c):** Phase current ( $I_{bs}$ ) response plot for step change in load torque for sensorless hybrid direct torque controlled induction motor

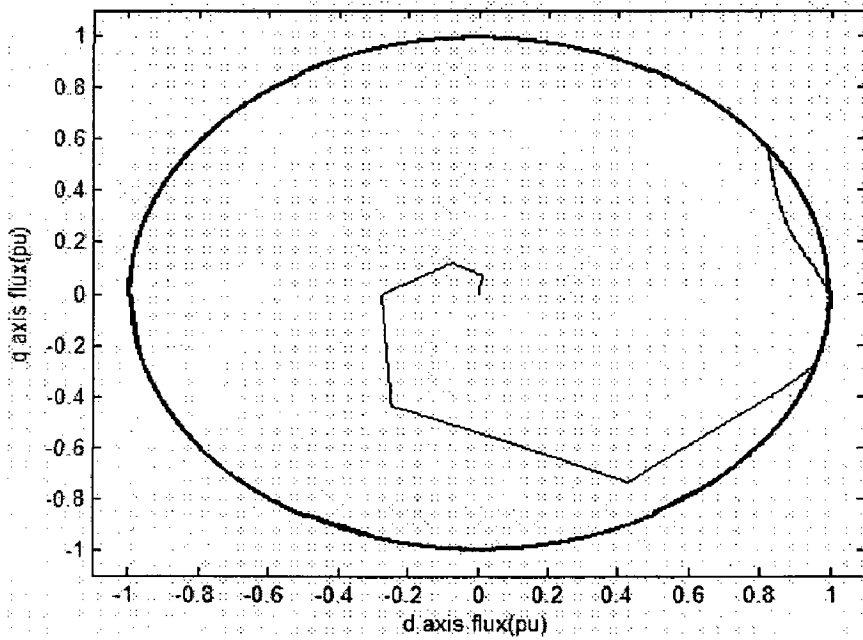


**Fig 5.11(d):** Stator d-q axis flux locus plot for step change in load torque for sensorless hybrid direct torque controlled induction motor

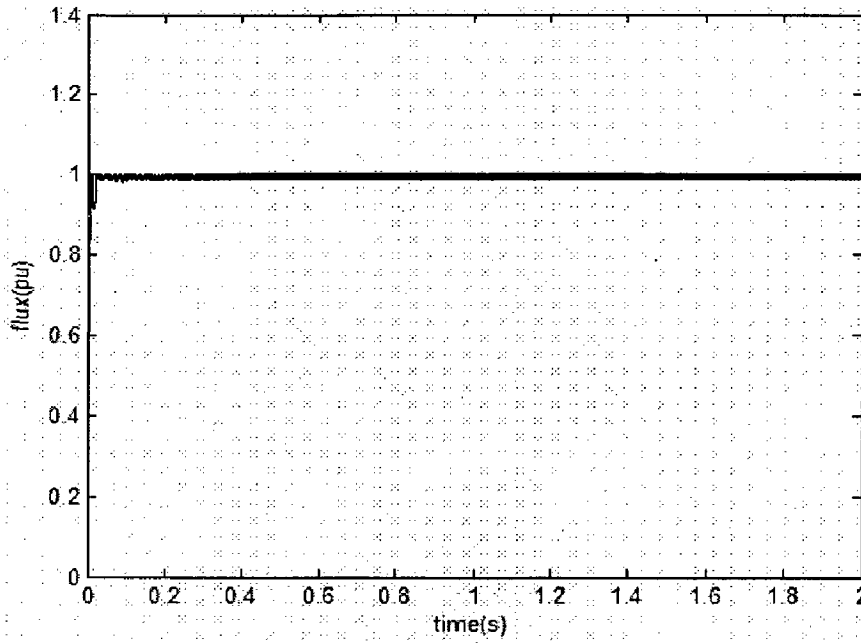


**Fig 5.11(e):** Stator flux magnitude plot for step change in load torque for sensorless hybrid direct torque controlled induction motor

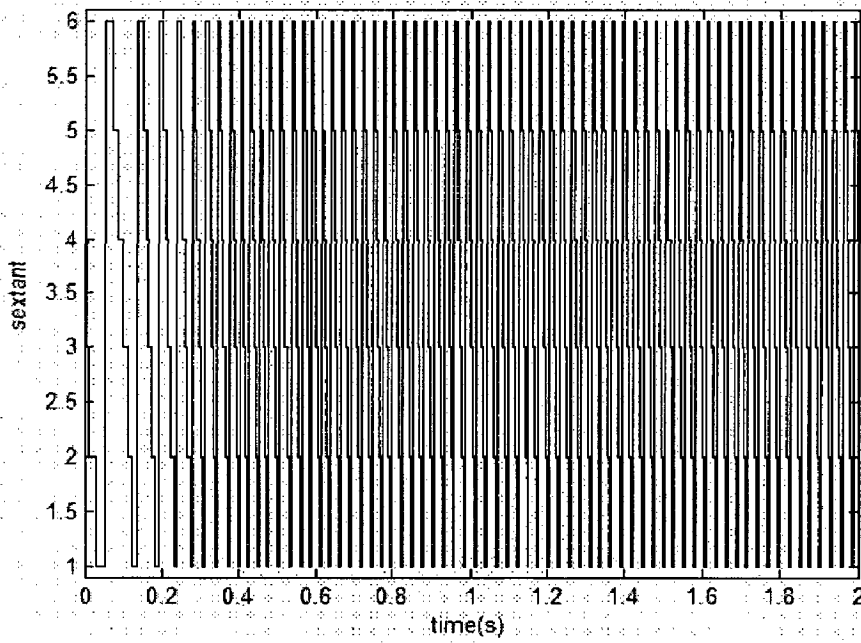


**Fig 5.11(f):** Sextant plot for step change in load torque for sensorless hybrid direct torque controlled induction motor

### 5.4.2 Split look-up table direct torque control:

Simulated block diagram for Split look-up table direct torque control with speed sensor is shown in fig 5.12 and without speed sensor in fig 5.13.

#### 5.4.2.1 Step change in speed reference:

In this case speed reference is changed from 0.8pu to 0.25pu at 0.8 sec with load torque at 0.5pu. Results are show in fig 5.14 with sensor and fig 5.15 for sensorless.

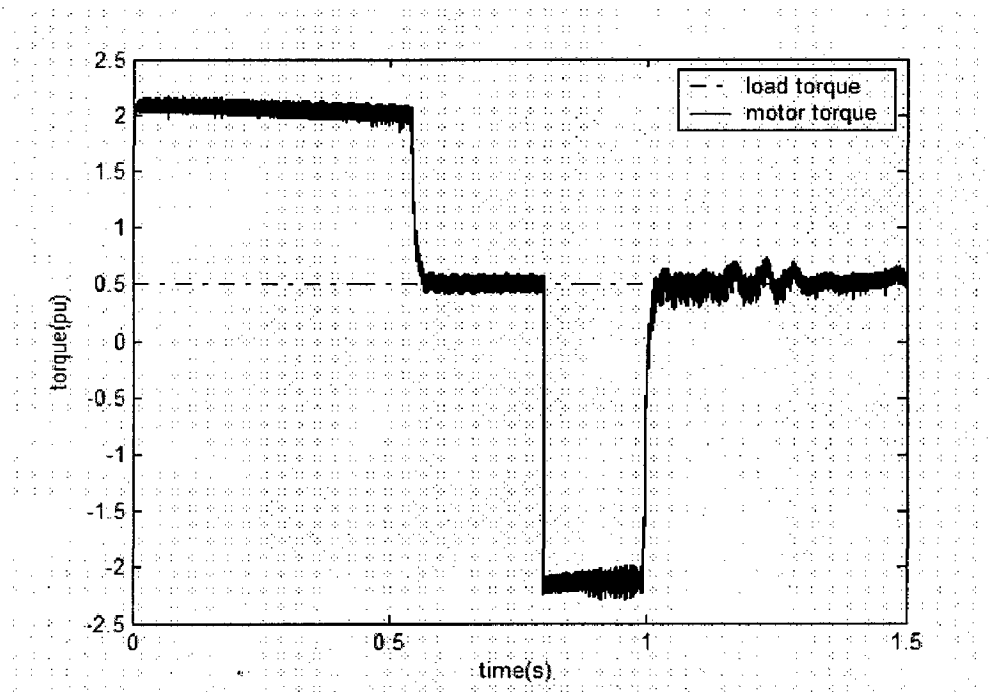


**Fig 5.14(a):** Torque response plot for step change in speed for split look-up table direct torque controlled induction motor



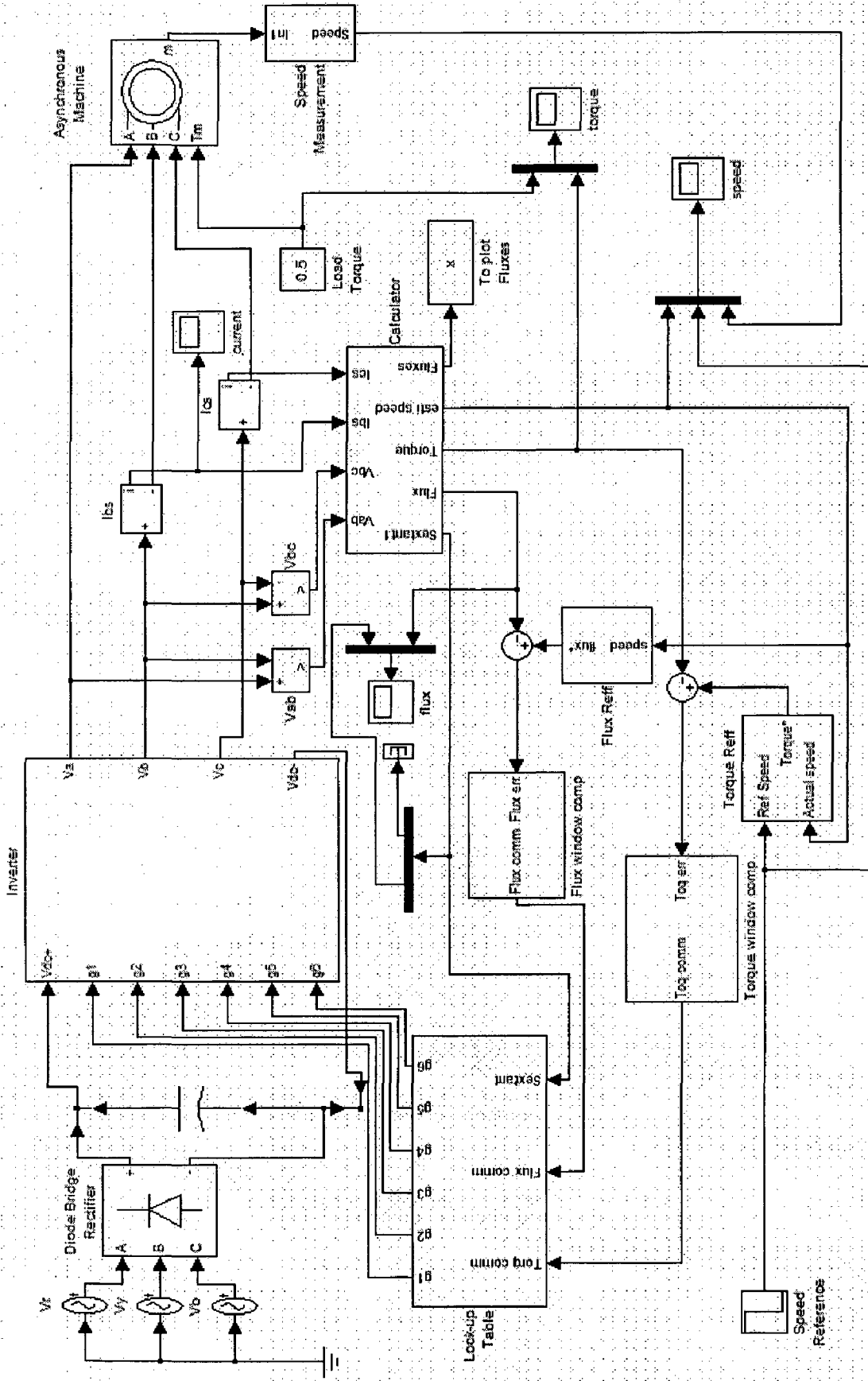
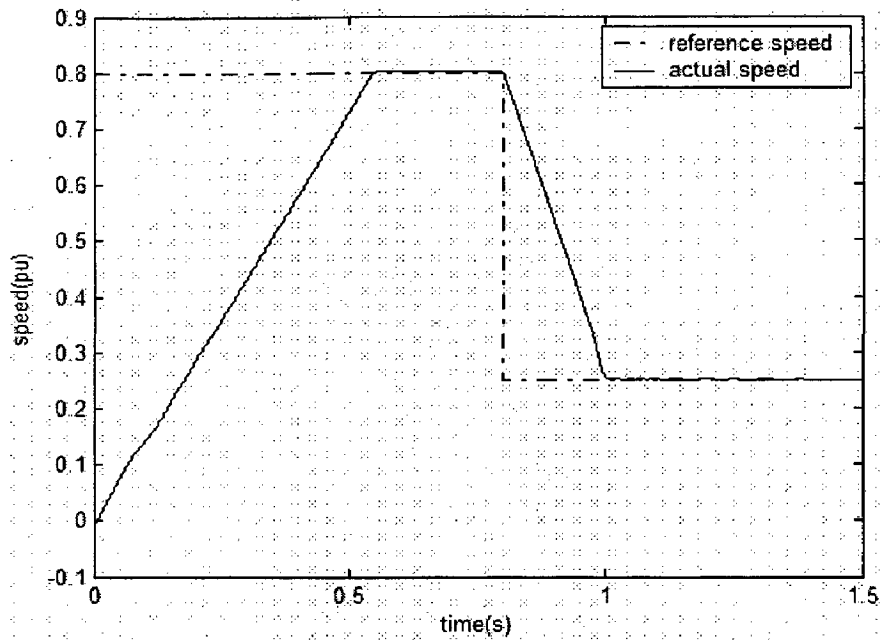
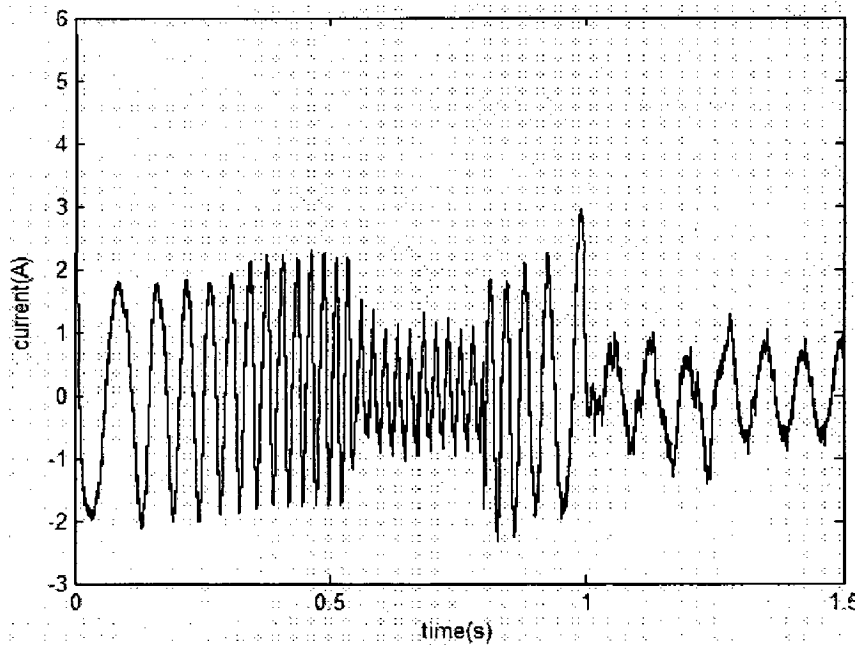


Fig 5.13: Block diagram model of sensorless split look-up table direct torque control used for simulation in MATLAB SIMULINK



**Fig 5.14(b):** Speed response plot for step change in speed for split look-up table direct torque controlled induction motor



**Fig 5.14(c):** Phase current ( $I_{bs}$ ) response plot for step change in speed for split look-up table direct torque controlled induction motor



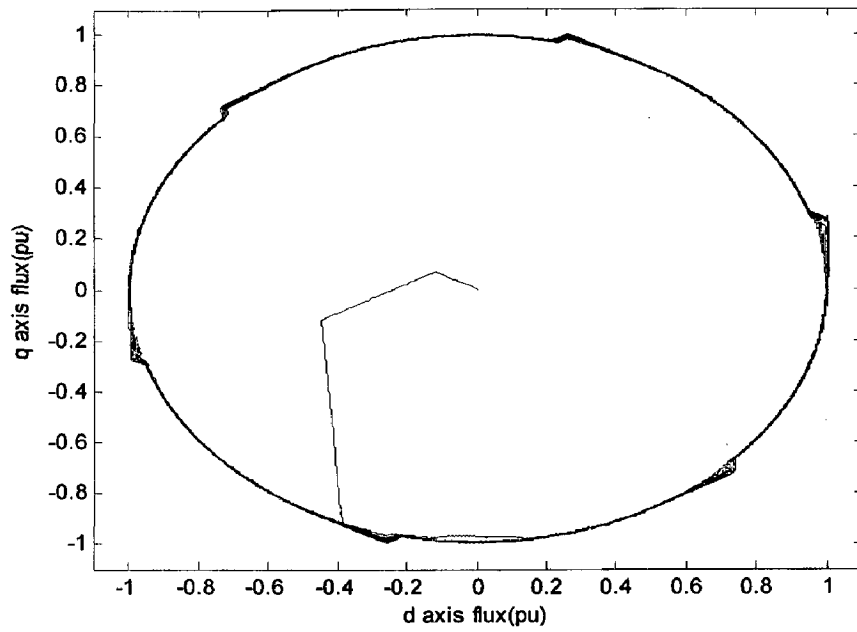


**Fig 5.14(d):** Stator d-q axis flux locus plot for step change in speed for split look-up table direct torque controlled induction motor

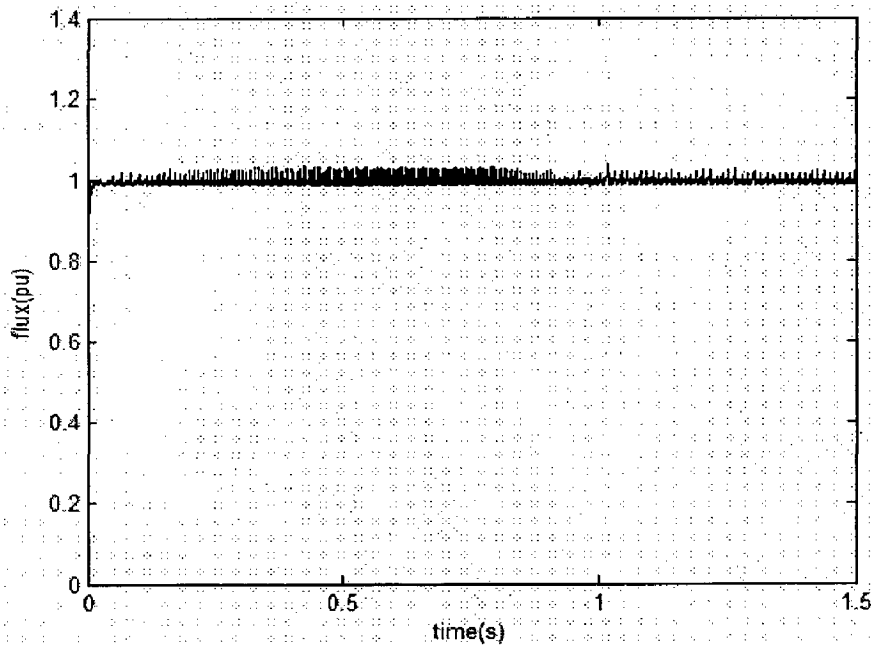


**Fig 5.14(e):** Stator flux magnitude plot for step change in speed for split look-up table direct torque controlled induction motor

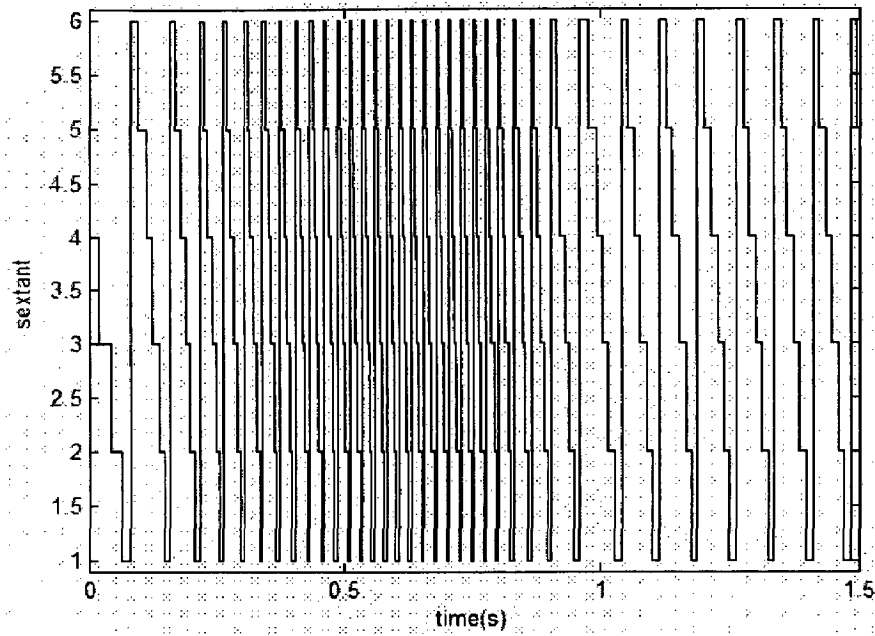


**Fig 5.14(f):** Sextant plot for step change in speed for split look-up table direct torque controlled induction motor

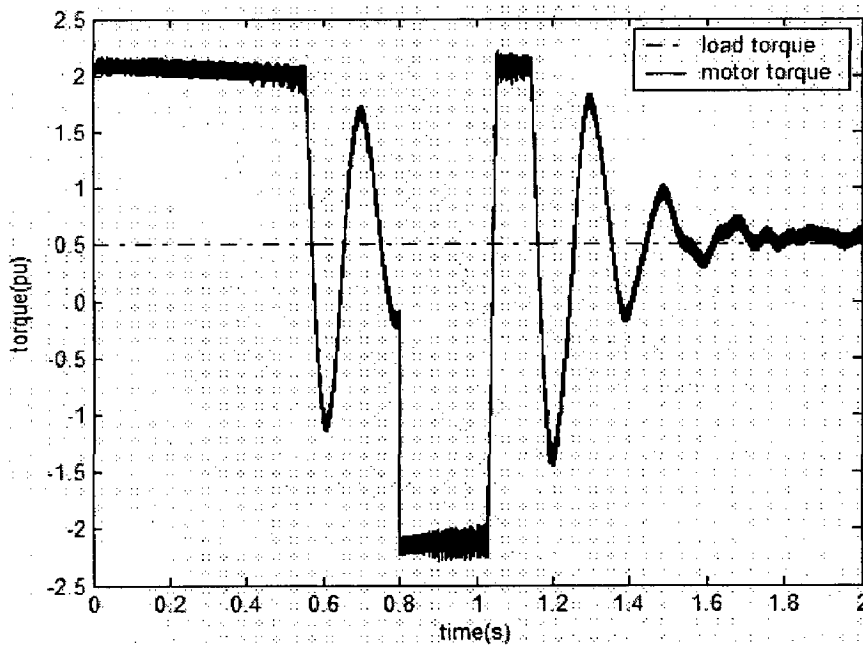


**Fig 5.15(a):** Torque response plot for step change in speed for sensorless split look-up table direct torque controlled induction motor

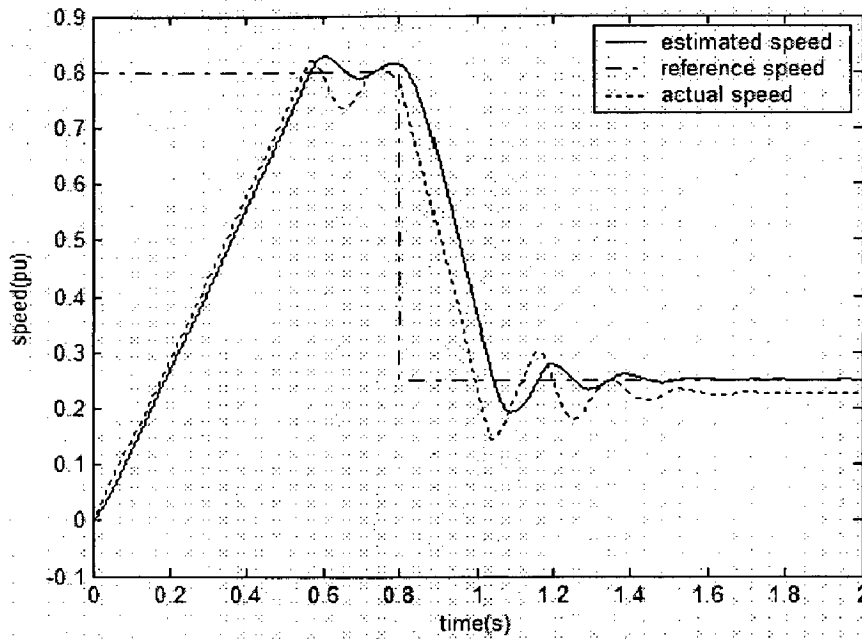


**Fig 5.15(b):** Speed response plot for step change in speed for sensorless split look-up table direct torque controlled induction motor

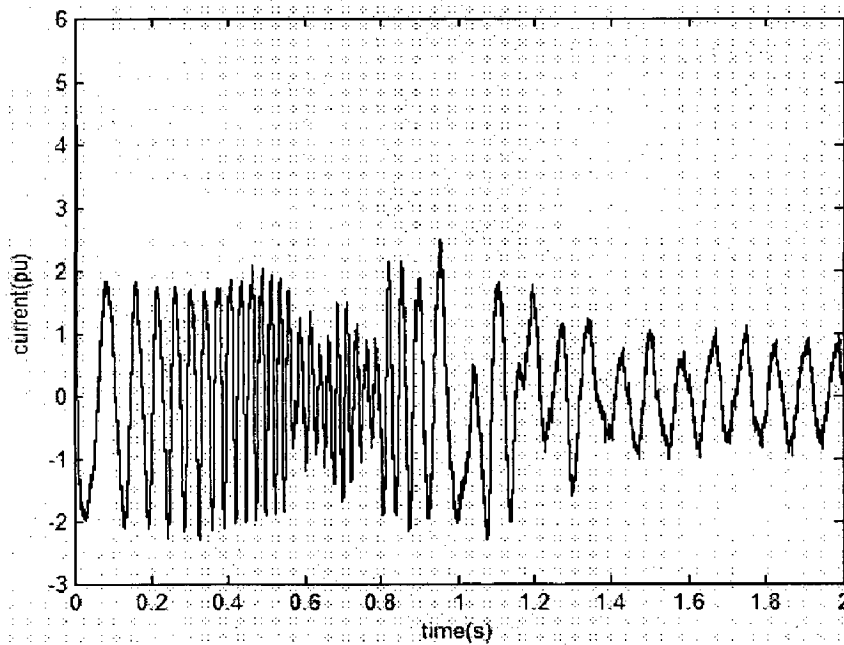


**Fig 5.15(c):** Phase current ( $I_{bs}$ ) response plot for step change in speed for sensorless split look-up table direct torque controlled induction motor

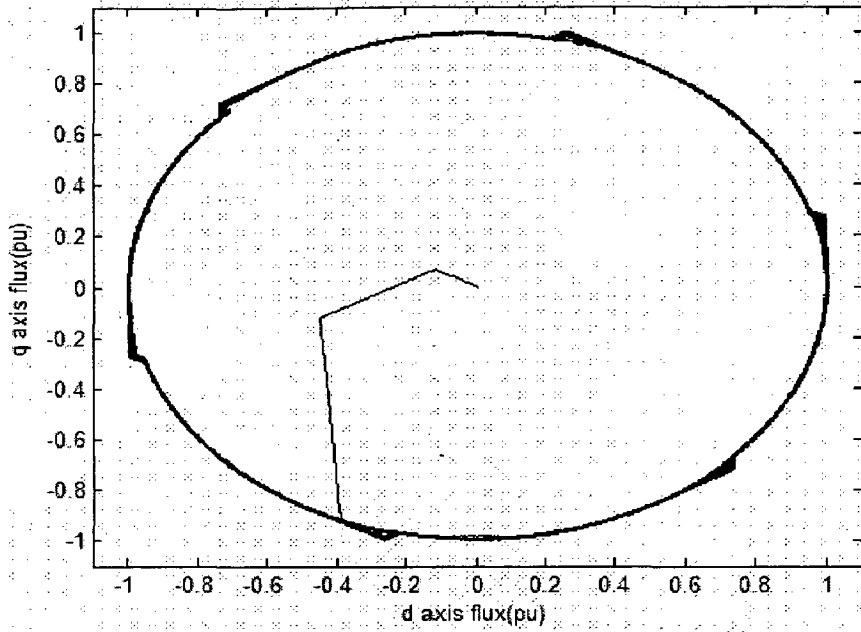


**Fig 5.15(d):** Stator d-q axis flux locus plot for step change in speed for sensorless split look-up table direct torque controlled induction motor

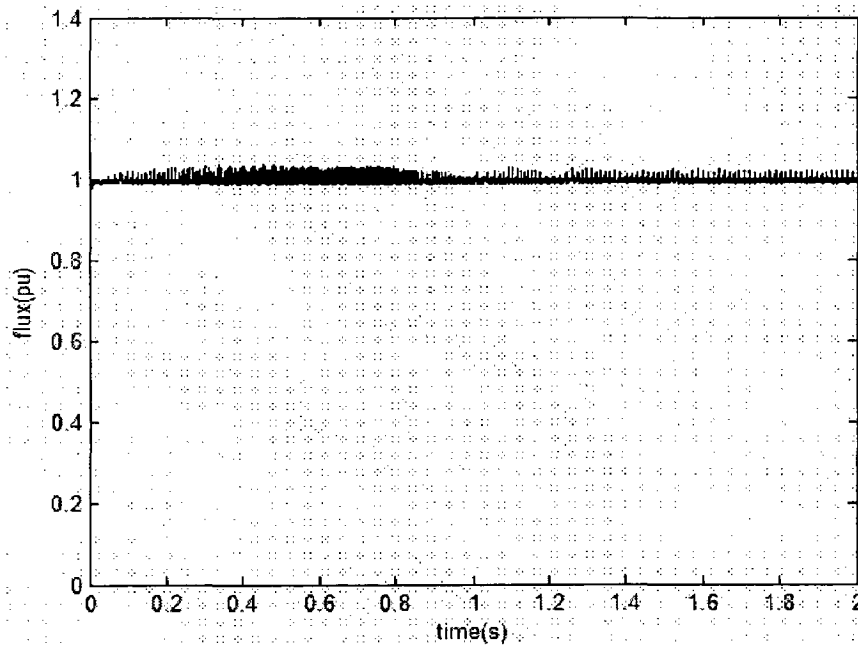


**Fig 5.15(e):** Stator flux magnitude plot for step change in speed for sensorless split look-up table direct torque controlled induction motor

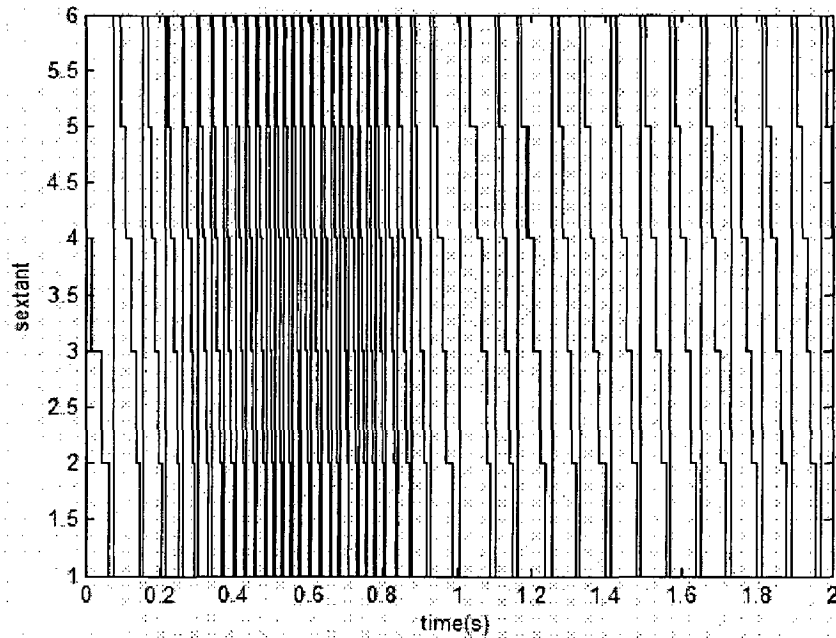


**Fig 5.15(f):** Sextant plot for step change in speed for sensorless split look-up table direct torque controlled induction motor

#### 5.4.2.2 Step change in load torque;

In this case load torque is changed from 0.25pu to 0.8pu at 0.8 sec with speed reference speed at 0.75pu. Results are show in fig 5.16 with speed sensor and fig 5.17 for sensorless.

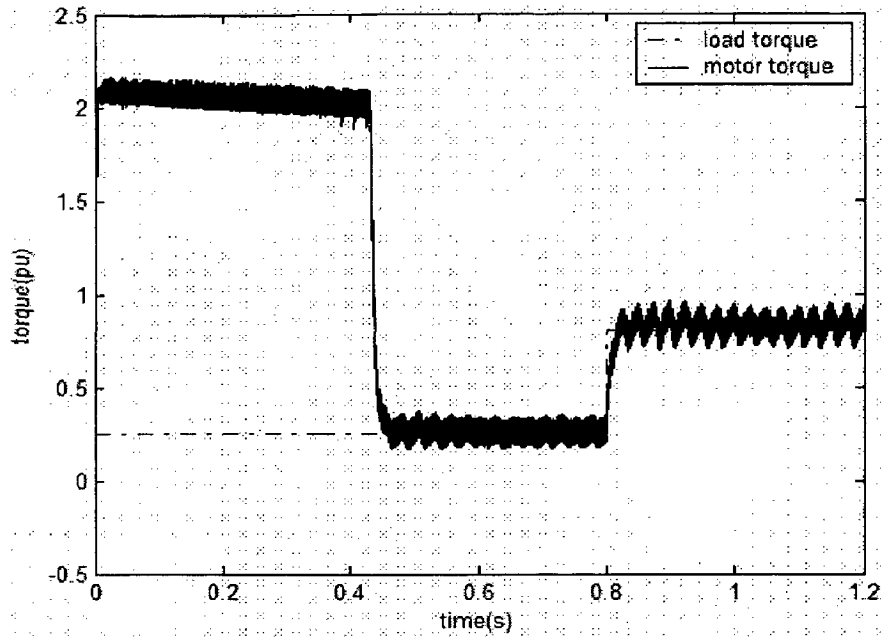


**Fig 5.16(a):** Torque response plot for step change in load torque for split look-up table direct torque controlled induction motor

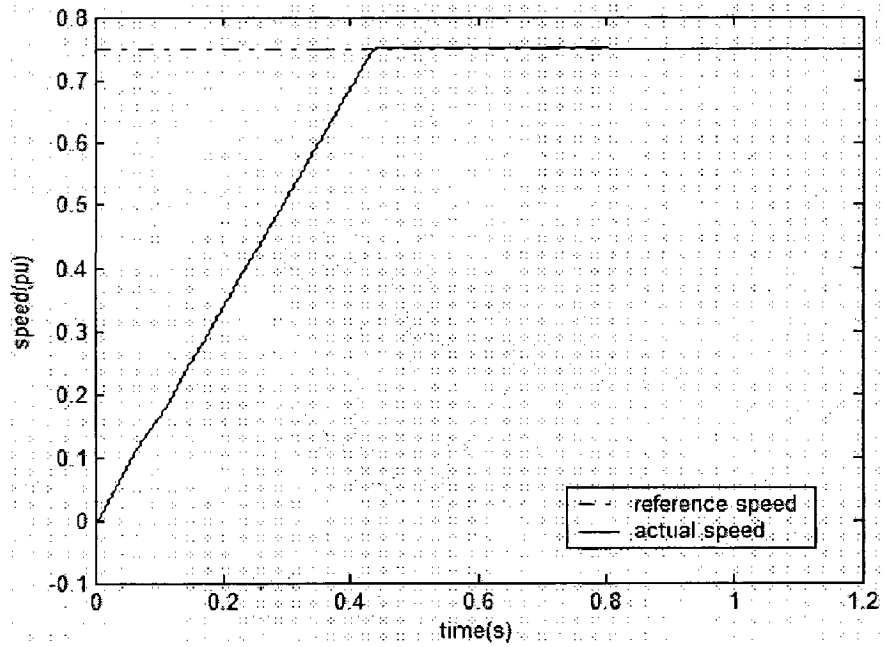


**Fig 5.16(b):** Speed response plot for step change in load torque for split look-up table direct torque controlled induction motor

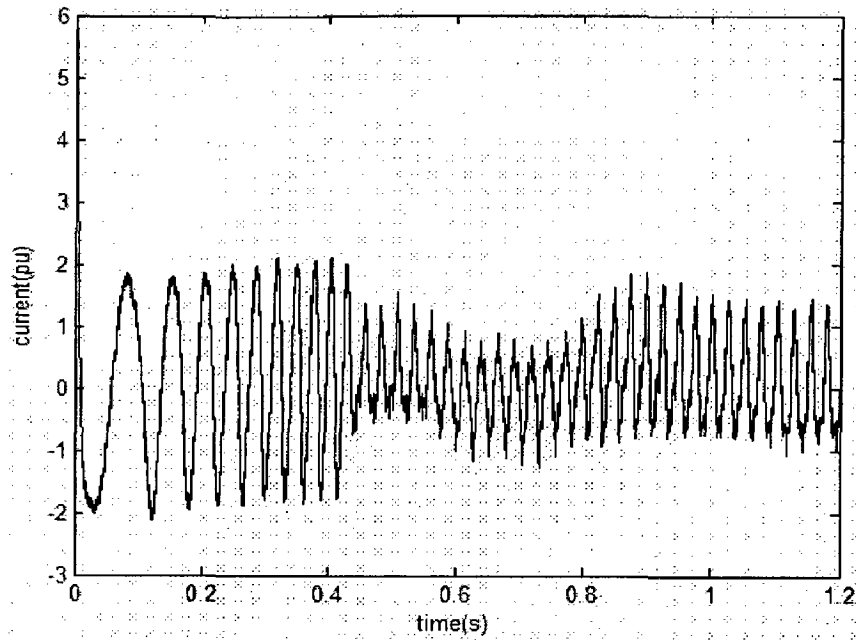


**Fig 5.16(c):** Phase current ( $I_{bs}$ ) response plot for step change in load torque for split look-up table direct torque controlled induction motor

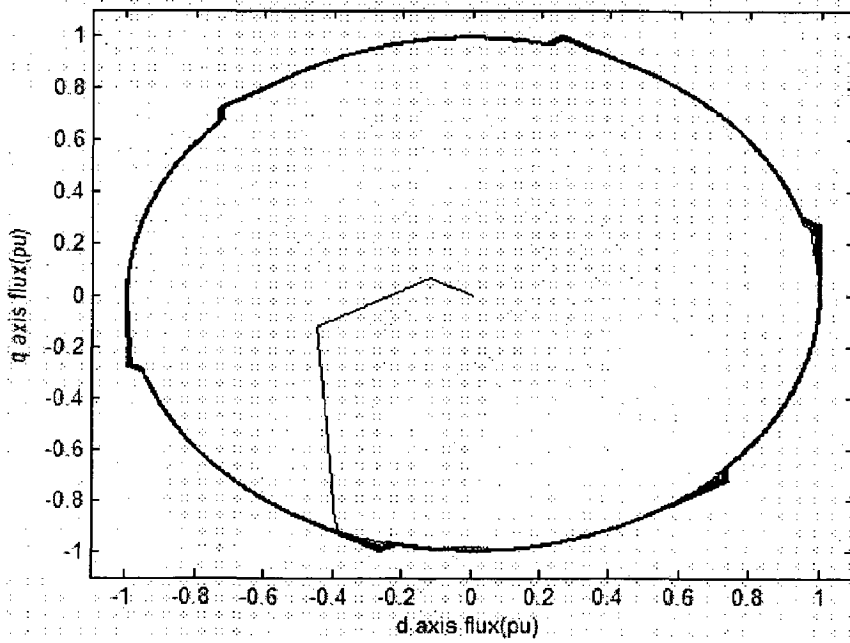


**Fig 5.16(d):** Stator d-q axis flux locus plot for step change in load torque for split look-up table direct torque controlled induction motor

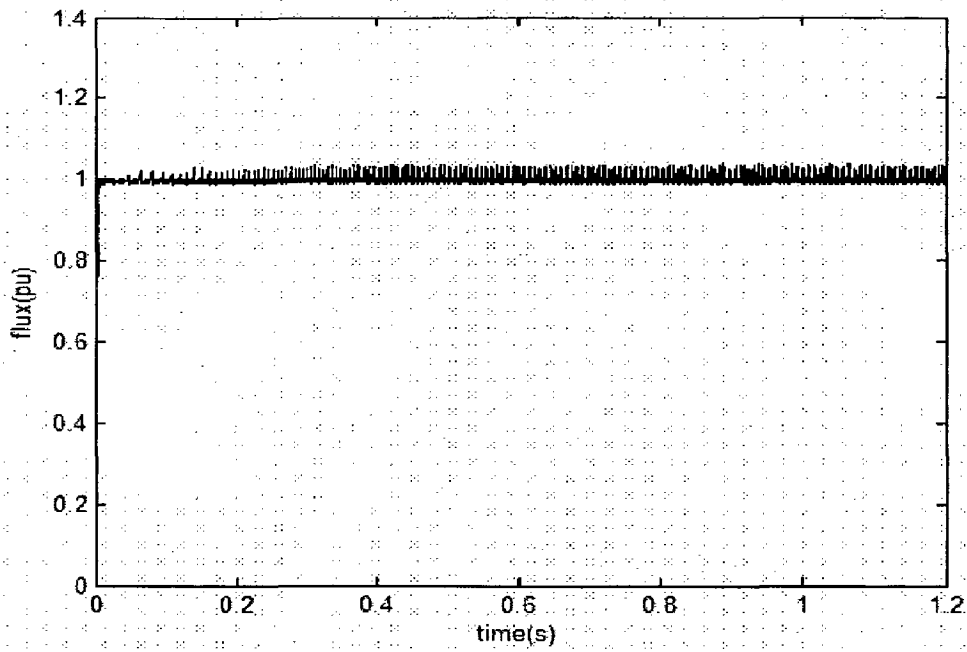


**Fig 5.16(e):** Stator flux magnitude plot for step change in load torque for split look-up table direct torque controlled induction motor

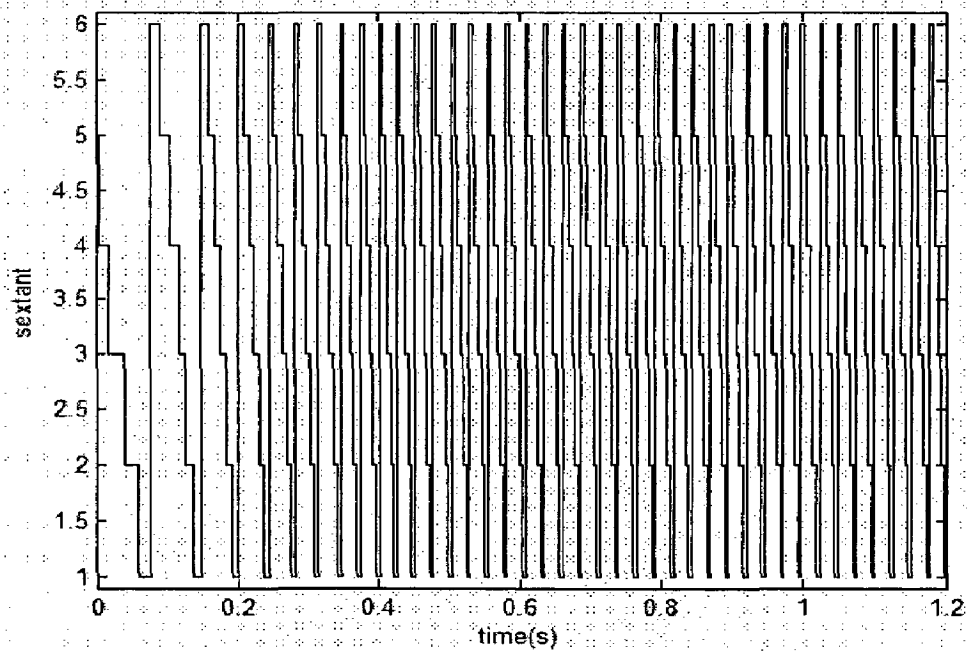


**Fig 5.16(f):** Sextant plot for step change in load torque for split look-up table direct torque controlled induction motor



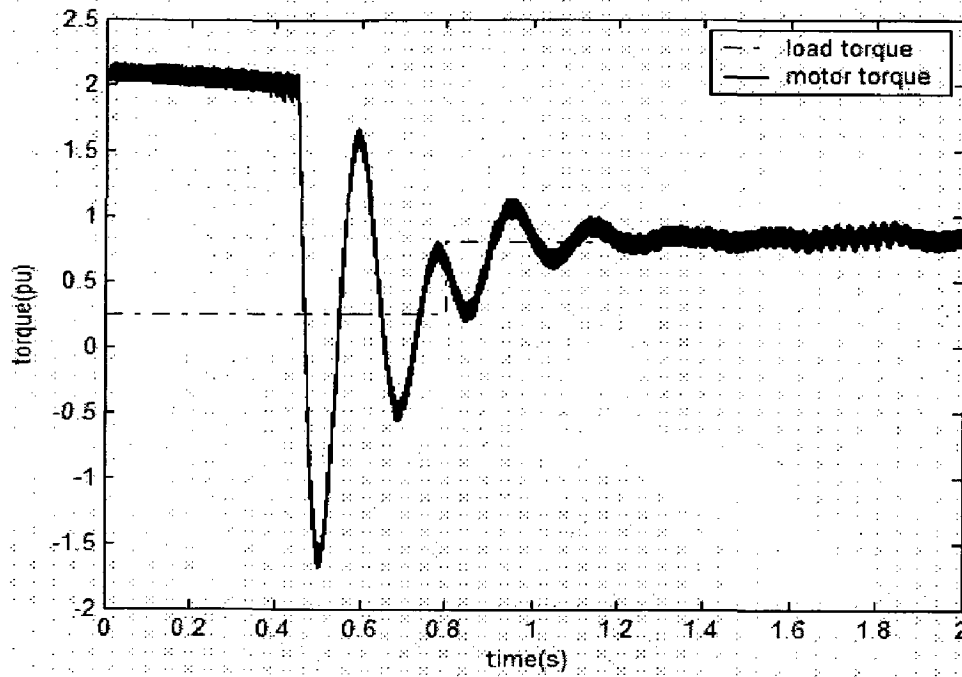


**Fig 5.17(a):** Torque response plot for step change in load torque for sensorless split look-up table direct torque controlled induction motor

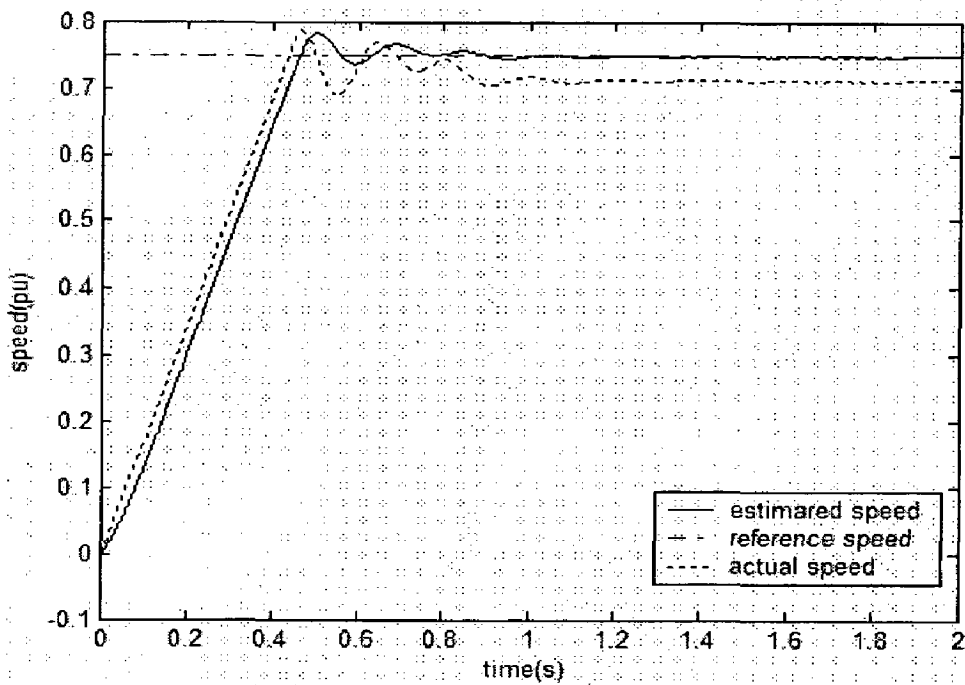


**Fig 5.17(b):** Speed response plot for step change in load torque for sensorless split look-up table direct torque controlled induction motor

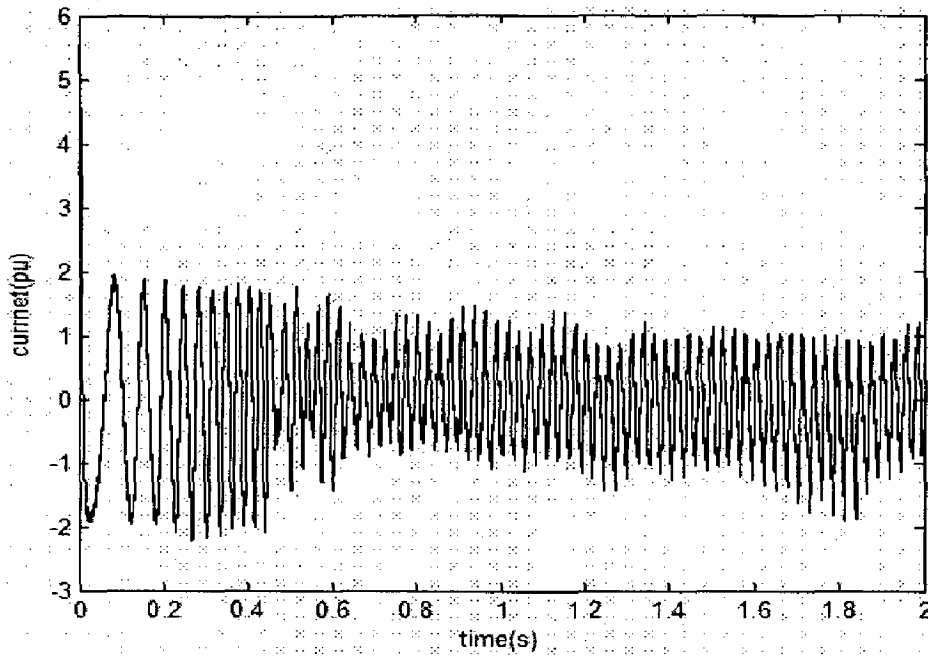


**Fig 5.17(c):** Phase current ( $I_{bs}$ ) response plot for step change in load torque for sensorless split look-up table direct torque controlled induction motor

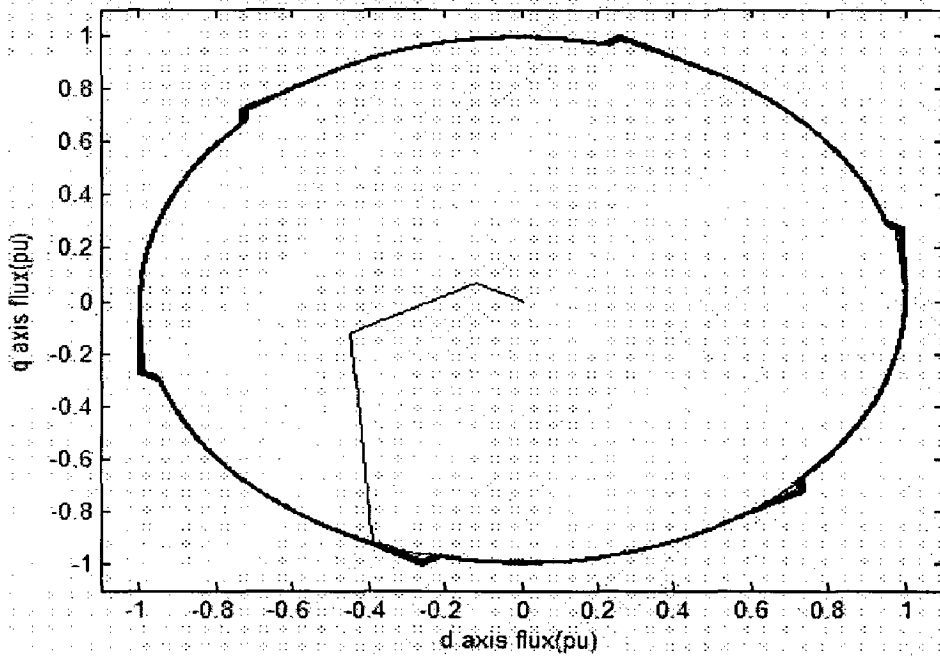


**Fig 5.17(d):** Stator d-q axis flux locus plot for step change in load torque for sensorless split look-up table direct torque controlled induction motor

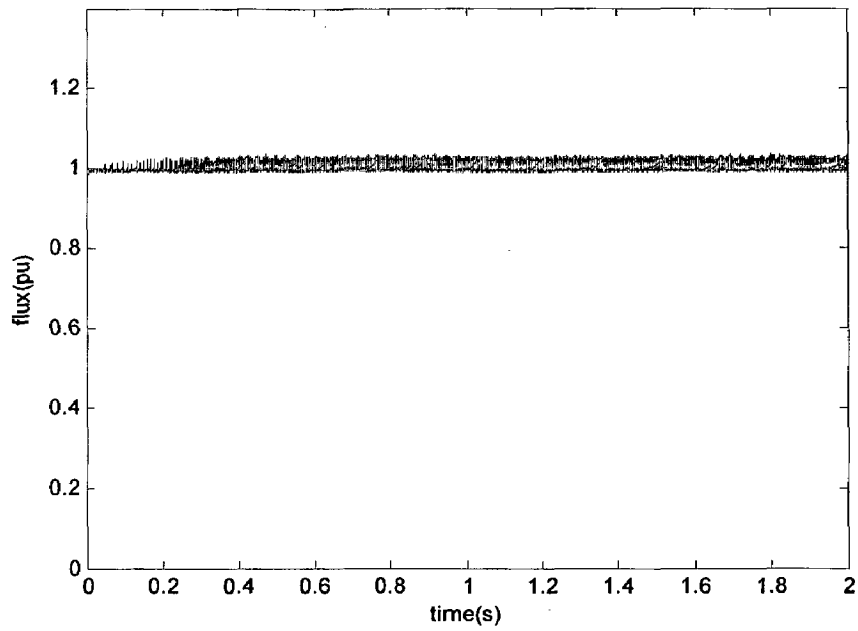


**Fig 5.17(e):** Stator flux magnitude plot for step change in load torque for sensorless split look-up table direct torque controlled induction motor

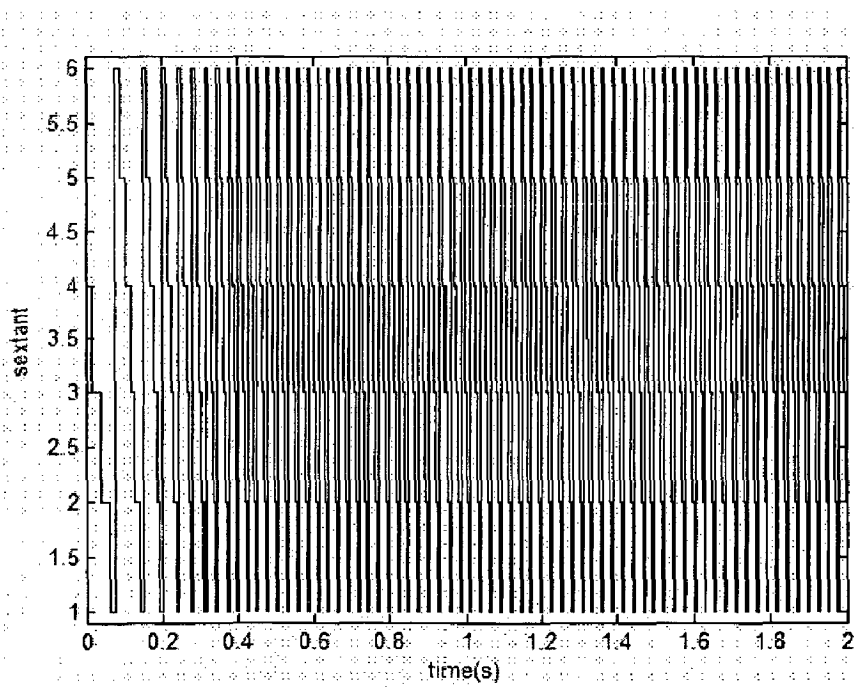


**Fig 5.17(f):** Sextant plot for step change in load torque for sensorless split look-up table direct torque controlled induction motor

# Conclusions and Future Scope

---

### 6.1 Conclusions:

In the present work, direct torque control of induction motor using three control strategies is presented. The three control strategies are normal direct torque control, hybrid direct torque control, split look-up table direct torque control.

The drive was fed from a voltage source inverter, which is used to generate six non-zero and two zero voltage vectors. Two line to line voltages and two phase currents are sensed and are converted to  $dq$  stationary reference frame, which are used to estimate flux and torque of the motor. Stator flux position (sextant) was obtained from  $d$  and  $q$  component fluxes. Torque and flux references were generated from speed error and motor speed respectively. Torque reference was obtained using PI controller in case of normal and split look-up table direct torque control. In case of hybrid direct torque control fuzzy and PI controllers are used for transient and steady states respectively. Flux reference was 1pu for speeds below base speed, and is inversely proportional to speed for above base speeds. Flux and torque commands were generated from flux and torque errors, from flux and torque hysteresis controllers. From these two commands and sextant in which stator flux phasor is presented, voltage vector to be switched was decided from look-up table in case of normal and hybrid direct torque control, from split look-up table in case of split look-up table direct torque control.

All the three strategies were simulated in MATLAB SIMULINK for both with and without speed sensor. Speed signal was obtained from speed sensor in case of normal drive and from speed estimator in case of sensorless drive. All the models developed were analyzed for different load conditions and speed references and were presented. It was observed that hybrid direct torque control has shown better performance in transient condition. Split look-up table direct torque control has shown better performance at low speeds.

## **6.2 Future Scope:**

The following list contains some proposals for further extensions to the work presented here.

1. Hardware implementation can be done for all the strategies, with and without speed sensor.
2. The split look-up table method can be combined with other methods to achieve better performance for whole speed range.
3. Sensorless drives with better speed estimation techniques can be implemented using DSP based processors.

## **References:**

---

- [1] "Direct Torque Control of Induction Motors", I.Ludtke, Dr. M.G. Jayne, University of Glamorgan.
- [2] Domenico Casadei, Francesco Profumo, Giovanni Serra, Angelo Tani, "FOC and DTC: Two Viable Schemes for Induction Motors Torque Control", IEEE Transactions on Power Electronics, Vol 17, No.5, September 2002.
- [3] "High Performance Motion Control of AC Motors Drives", Gerd Terorde, Ronnie Belmans.
- [5] Petar R. Matic, Branko D. Blanusa, Slobodan N. Vukosavic, "A Novel Direct Torque and Flux Control Algorithm for the Induction Motor Drive".
- [6] Nik Rumzi Nik Idris , Abdul Halim Mohd Yatim, "Modeling of a New Torque Controller for Direct Torque Control of Induction Machines".
- [7] Mihai Comanescu, "Flux and Speed Estimation Techniques for Sensorless Control of Induction Motors" A dissertation report.
- [8] "Methods for Speed Sensorless Control of AC Drives", Joachim Holtz, University of Wuppertal-Germany.
- [9] N.R.N. Idris, "Improved direct torque control of induction machines", PhD Thesis, University Technology Malaysia, 2000.
- [10] Joachin Holtz, "Sensorless Control of Induction Motor Drives", Proceedings of the IEEE, Vol. 90, No. 8, Aug 2002.
- [11] Salmon Chavez Velazquez, Ruben Alejos Palomares, Alfredo Nava Segura. University of the Americas, Puebla, "Speed Estimation for an Induction Motor using Extended Kalman Filter".
- [12] yen-Shin Lai, Juo-Chiun Lin, "New Hybrid Fuzzy Controller for Direct Torque Control Induction Motor Drives". IEEE Transaction on Power Electronics, Vol. 18. No. 5, Sept 2003.
- [13] Lus Romeral, Antoni Arias, Emiliano Aldabas, Marcel G. Jayne, "Novel Direct Torque Control(DTC) Scheme with Fuzzy Adaptive Torque-ripple Reduction". IEEE Transaction on Industrial Electronics, Vol. 50, No. 3, June 2003.

- [14] "A Comparison of Direct Torque Control Methodologies for Induction Motor", P. Marino, M.D'Incecco and Visciano.
- [15] "Design of Fuzzy Controllers", Jan Jantzen.
- [16] Fatiha Zidani, Rachid Nait Said, "Direct Torque Control of Induction Motor with Fuzzy Minimization Torque Ripple", Journal of Electrical Engineering, Vol. 56, No. 7-8, 2005.
- [17] "Fuzzy Logic Direct Torque Control", A. Arias, J.L. Romeral, E. Aldabas, M.G. Jayne.
- [18] "Direct Torque Control of Induction Motors using Fuzzy Variable Switching Sectors", Ji-Su Ryu, In-Sic Yoon, Kee-Sang Lee and Soon-Chan Hong.
- [19] Pawel Z. Grabowski, Marian P. Kazmierkowski, Bimal K. Bose and Frede Blaabjerg, "A Simple Direct-Torque Neuro-Fuzzy Control of PWM-Inverter-Fed Induction Motor Drive", IEEE Transactions on Industrial Electronics, Vol. 47, No. 4, August 2000.
- [20] R.Krishnan, "Electric Motor Drives - Modeling, Analysis and Control" Pearson Education (Singapore) Pte. Ltd., Indian Branch, Delhi, 2003(Book).
- [21] Ion Boldea, S.A. Nasar, "Electric drives", CRC Press, Taylor and Francis Group, 2006 print(Book).
- [22] Mohan, Undeland , Robbins. "Power Elëctronics". John Wiley & Sons Third edition.2003(Book).
- [23] Paul C. Krause, Oleg Wasynczuk, Scott D. Sudhoff, "Analysis of Electric Machinery and Drive Systems", Wiley Interscience 2004(Book).

## Machine Parameters

---

Specifications of the Induction Motor selected for simulation:

|                           |                 |
|---------------------------|-----------------|
| Rotor type                | : Squirrel cage |
| Power rating              | : 3 H.P.        |
| Line-to-line voltage      | : 415V          |
| Phase                     | : 3             |
| Frequency                 | : 50Hz          |
| Stator resistance (in pu) | : 0.0201        |
| Rotor resistance (in pu)  | : 0.0377        |
| Stator inductance (in pu) | : 0.0349        |
| Rotor inductance (in pu)  | : 0.0349        |
| Mutual inductance (in pu) | : 1.2082        |
| Inertia constant          | : 0.4906s       |
| Number of poles           | : 4             |